Conditions Affecting Ergothioneine Levels in *Mycobacterium smegmatis* & The Attempted Isolation of α-*N*, *N*, *N*-Histidine Methyltransferase, the First Enzyme in Ergothioneine Biosynthesis.

Monique J. Williams

Thesis Presented for the Degree of
DOCTOR OF PHILOSOPHY

Department of Clinical Laboratory Sciences
UNIVERSITY OF CAPE TOWN

May 2007

Declaration

I, Monique Williams, hereby declare that the work on which this dissertation is based on my original work (*except where acknowledgements indicate otherwise*) and that neither the whole work nor any part of it has been, is being, or is to be submitted for another degree in this or any other university.

I empower the university to reproduce for the purposes of research either the whole or any portion of the contents in any manner whatsoever.

Signature:.....

Date: 16 - 10 - 2007

Acknowledgements:

I would like to express my heartfelt appreciation to the following people, who played an invaluable role in this journey:

My supervisors, Prof. Lafras Steyn & Assoc. Prof. Daan Steenkamp, for their guidance and assistance throughout this project.

Prof. PD van Helden from the Department of Biomedical Sciences at the University of Stellenbosch, for his advice in the compilation of this thesis.

The staff and students of the Divisions of Medical Microbiology and Chemical Pathology for a pleasant learning environment, in particular Vuyo, Jackson and Gabriel, for their assistance and friendship.

Dr. Ros Chapman and Ryan Vogt for their willingness to share their knowledge and experience.

Dr. S. Burton & Caryn Vengadajellum from the UCT Chemical engineering department for supplying the *Neurospora crassa* used in this study and for technical assistance.

Dr. M. Stander from the University of Stellenbosch Mass Spectrometry Unit for LC-MS/MS analysis and her assistance with protein identification.

My family, both natural and spiritual, their encouragement and prayers. My parents for their support in pursuing my dreams and my brother Chris for inspiring my love for science.

To the many people who I have met along the way and who I am privileged to call my friends – there are too many to mention, but I know I am richer for having you in my life.

Jacky and Michelle for being there through the ups and downs.

Edwin K. Murungi for the comparative modelling of HP-GlcPU, assistance with the structural aspects of this project and above all for his friendship and support.

I am grateful for financial assistance provided by the National Research Foundation of SA, Medical Research Council of SA and UCT Postgraduate Funding and their donors.

Finally, I would like to acknowledge my Lord and Saviour Jesus Christ, for His grace, provision and strength, without which none of this would have been possible.

Abstract:

Ergothioneine and mycothiol are the two major low molecular weight thiols present in mycobacteria. The generation of mycothiol-deficient mutants has demonstrated its role in protecting *M. tuberculosis* against oxidative and nitrosative stress. To date, no ergothioneine-deficient mutants have been identified and the role of ergothioneine in mycobacteria remains unknown. The work in this thesis was performed with the aim of better understanding the function of ergothioneine in mycobacteria, by studying its biosynthesis and the conditions affecting its production.

Firstly, an attempt was made to purify the first enzyme in ergothioneine biosynthesis from *Neurospora crassa*, with the intention of identifying the equivalent enzyme in mycobacteria. A number of purification methods were investigated including gel filtration, hydroxyapatite, cation exchange, affinity and dye-ligand chromatography, which did not prove to be useful. Good purification factors were obtained for anion exchange chromatography utilising DEAE cellulose and a HPLC DEAE column, zinc immobilised metal ion affinity chromatography (IMAC), chromatofocusing and ammonium sulphate fractionation and these methods were optimized for use in a large-scale purification. The large-scale purification utilising these methods was performed on approximately 1kg of frozen mycelium and yielded a number of candidate proteins. None of these proteins were annotated as probable methyltransferases, but one of the candidate proteins was identified as a member of the transferase superfamily of enzymes and was therefore investigated further. Sequence and structural analysis however supported its annotation as a "probable glucose-1-phosphate uridylyltransferase" and ruled it out as the first enzyme in ergothioneine biosynthesis. It was therefore concluded that the scale on which the purification was performed was too small to obtain sufficient amounts of the α-N, N, N-histidine methyltransferase to identify it by mass spectrometry.

Secondly *M. smegmatis* was used as a model organism to identify conditions which affect ergothioneine production in mycobacteria. Oxidative and nitrosative stress did not result in the induction of ergothioneine or mycothiol in *M. smegmatis*. Ergothioneine levels were shown to increase dramatically as *M. smegmatis* entered stationary phase and also accumulated in the media. Ergothioneine was therefore investigated as an autoinducer, but was found to have no effect on growth of *M. smegmatis.* It is not understood why *M. smegmatis* releases ergothioneine into the media, but in a pathogen like *M. tuberculosis* it could play an anti-inflammatory role.

Abbreviations:

µl	microlitre
AIDS	acquired immunodeficiency syndrome
ADP	adenosine diphosphate
AMP	adenosine monophosphate
ATP	adenosine triphosphate
BAN	2'-bromoacetonaphthone
BCG	Bacille Calmette-Guérin
BLAST	Basic Local Alignment Search Tool
CHAPS	3-[(3-chloramidopropyl)-dimethylammonio]-1-propanesulphonate
Ci	Curie
cm	centimetre
cpm	counts per minute
CTP	cytosine triphosphate
Da	dalton(s)
DMH	dimethylhistidine
DMNQ	dimethoxy-1, 4-naphthoquinone
DNA	dideoxynucleic acid
DTT	dithiothreitol
DE52	diethylaminoethyl cellulose 52
DEAE	diethylaminoethyl
EDC	1-ethyl-3-(3-dimethylaminopropyl)-carbodiamide
ESH	ergothioneine
ESSE	ergothioneine disulphide / oxidized ergothioneine
g	gram(s)
GDH	glycine dehydrogenase
Grxs	glutaredoxins
GSH	glutathione
GSNO	s-nitrosoglutathione
GSSG	glutathione disulphide / oxidized glutathione
Hb	hemoglobin
HEPES	*N*-2-hydroxyethylpiperazine-*N*'ethanesulphonic acid
HIV	human immunodeficiency virus

HILIC	hydrophilic interaction chromatography
HP-GlcPU	hypothetical protein containing glucose-1-phosphate uridylyltransferase conserved domain from *N. crassa*
HPLC	high performance liquid chromatography
ICTM	isoprenylcysteine carboxyl methytansferase
IDA	iminodiacetic acid agarose
IFN-γ	interferon-γ
IMAC	immobilised metal ion affinity chromatography
IMP	inosine monophosphate
INH	isoniazid
kDa	kilodalton
LC	liquid chromatography
LLO	listeriolysin O
ManLAM	phosphatidylinositol lipoarabinomannan
Mb	myoglobin
MDR	multi-drug resistant
MES	acetate-2-(N-morpholino)ethanesulphonic acid
MIC	minimum inhibiting concentration
mA	milliamperes
ml	millilitre
mm	millimetre
mM	millimolar
MOPS	morpholinopropanesulphonic acid
MS	mass spectrometry
MSH	mycothiol
MSSM	mycothiol disulphide / oxidized mycothiol
MTase	methyltransferase
MTB	*Mycobacterium tuberculosis* (*M. tuberculosis*)
MW	molecular weight marker
$NADP^+$	nicotinamide adenine dinucleotide phosphate
NADPH	reduced nicotinamide adenine dinucleotide phosphate
NHS	*N*-hydroxysuccinimide
NFκβ	nuclear factor κβ
nm	nanometre(s)

NMDA	*N*-methyl-D-aspartate
NO	nitric oxide
NRP	non-replicating Phase
PAGE	polyacrylamide gel electrophoresis
PAS	p-aminosalicylic acid
PCR	polymerase chain reaction
Pi	phosphate
PI3P	phosphotidylinositol 3-phosphate
Pkn G	protein kinase G
PMSF	phenylmethylsulphonyl fluoride
PZA	pyrazinamide
RIF	rifampicin
RNA	ribonucleic acid
RNI	reactive nitrogen intermediates
ROI	reactive oxygen intermediates
rpm	revolutions per minute
SAH	S-adenosylhomocysteine
SAM	S-adenosylmethioneine
SDS	sodium dodecyl sulphate
SET	Su(var), Enhancer of zeste, Trithorax
TACO	tryptophan aspartate-containing coat protein
TB	tuberculosis
TCA	trichloroacetic acid
TEMED	N, N, N', N'-tetramethyl ethylene diamine
TFA	trifluoroacetic acid
TNF	tumour neucrosis factor
TPCK	N-tosyl-phenylalanine chloromethyl ketone
TLCK	N-tosyl-L-leucine chloromethyl ketone
Tris	2-amino-2-(hydroxymethyl)-1,3-propandiol
Trxs	thioredoxin
UV	ultraviolet
w/v	weight per volume
XDR	extremely / extensively drug resistant

List of Figures:

List of Tables:

BRIEF CONTENTS:

DETAILED CONTENTS

CHAPTER 1: GENERAL INTRODUCTION

Part A:

The Attempted Isolation of α-*N, N, N*-Histidine Methyltransferase, the First Enzyme in Ergothioneine Biosynthesis.

CHAPTER 2: INTRODUCTION

CHAPTER 3: MATERIALS & METHODS

Part B:
Conditions Affecting Ergothioneine Levels in *M. smegmatis*

CHAPTER 5: INTRODUCTION

CHAPTER 6: MATERIALS & METHODS

CHAPTER 7: RESULTS & DISCUSSION

CHAPTER 1: GENERAL INTRODUCTION

1.1. A HISTORY OF TUBERCULOSIS

1.1.1 The Origins of Human Tuberculosis

It has been widely speculated that *Mycobacterium tuberculosis* (*M. tuberculosis)* has evolved from *Mycobacterium bovis* (*M. bovis*), the agent of bovine tuberculosis, through specific adaptation of an animal pathogen to the human host. Brosch *et al.* (2002) however showed that *M. bovis* has undergone numerous deletions relative to *M. tuberculosis* and it is proposed that the *Mycobacterium Africanum* → *M. bovis* lineage branched from the progenitor of *M. tuberculosis* isolates. The host specificity of ancestral *M. tuberculosis* strains and of *Mycobacterium carnetti*, which is thought to have diverged before *M. tuberculosis*, suggests that the progenitor of *M. tuberculosis* was a human pathogen (Brosch *et al.*, 2002).

Skeletal hunchback deformities, which are suggestive of tuberculosis (TB), have been found in a skeleton which dates back to about 5000BC. This evidence is however not conclusive as the deformity could have resulted from several other causes including other bacterial or fungal infections, trauma, bone tumors and arthritis. The earliest definitive evidence of tuberculosis is from an Egyptian mummy, which dates back to about 3400BC, in which acid-fast bacilli were visualized in the vertebral bone (Zimmerman, 1979).

1.1.2 Historical Epidemiology of Tuberculosis

The discovery of *Mycobacterium tuberculosis* as the causative organism of tuberculosis is attributed to Robert Koch. Although this breakthrough was made in 1882, it took about a decade before it was accepted in Britain. The absence of data is a major difficulty in determining the historical epidemiology of tuberculosis and estimates of tuberculosis incidence have only become available in the twentieth century as a result of the introduction of compulsory notification of tuberculosis.

When a new infection is introduced into a susceptible population, the mortality and morbidity rates follow a predictable curve. This curve is characterized by a sharp rise to a peak followed by a more gradual decent as the number of susceptible people in the

population declines. For tuberculosis the epidemiological curve is thought to run its course in 300 years, with mortality and morbidity peaking after 50 and 100 years respectively (Dutt & Stead, 1999). In most developed countries mortality due to tuberculosis peaked during rapid industrialization, as a result of the overcrowding and poor living conditions caused by rapid urbanization. In Britain, where reliable tuberculosis statistics have been available since 1838, the epidemic has since shown a decline in mortality. Factors contributing to this decline were improved living and working conditions, pasteurization to eliminate milk as a source of infection, the introduction of dispensaries for diagnosis and education in environmental hygiene and the establishment of sanatoriums for treatment of tuberculosis. Tuberculosis mortality was already at a low level in Britain when chemotherapy and BCG vaccination were introduced. European colonization and the establishment of sanatoriums in America, Australia and Africa resulted in the spread of tuberculosis to these regions (Metcalf, 1991).

1.1.3 The History of Tuberculosis in South Africa

Tuberculosis was not common in indigenous people in southern Africa before European colonisation and the initial spread of the disease was closely related to their degree of contact with the Europeans. South Africa was promoted as a health resort in the nineteenth century due its favorable climate. Consequently, the influx of infected individuals caused the mortality rates of towns that had sanatoria to increase. The mining industry also played a key role in the spread of tuberculosis in southern Africa. Poor living and working conditions of mine workers favoured the spread of infection and resulted in high incidences of tuberculosis among these workers. The use of migrant labour both from within South Africa and from neighboring countries resulted in the disease spreading to the rural areas. The discovery of diamonds and gold led to rapid industrial development and urbanization in the late nineteenth century, and saw an increase in the prevalence of tuberculosis in urban areas. Segregation and forced population removals during the apartheid era created areas of high tuberculosis incidence and mortality rates due to poverty, overcrowding and poor healthcare in township areas. Although the introduction of anti-tuberculosis drugs in the 1950's resulted in a sharp decline in tuberculosis mortality rates, incidence rates continued to increase (Metcalf, 1991). South Africa currently has one of the worst tuberculosis epidemics in the world, and in 1997 the Medical Research Council of South

Africa estimated that the incidence of the disease was 419 cases per 100 000 of the total population. This incidence is up to 60 times higher than those currently seen in the United States of America and Europe (Fourie, 1991-2003).

1.1.4 Tuberculosis and the HIV/AIDS Epidemic

In 2005 it was estimated that 40.3 million people were living with HIV of which 25.8 million were in Sub-Sahara-Africa and that AIDS had caused the death of 3.1million people in that year (UNAIDS AIDS epidemic update 2005). The relationship between the HIV and TB epidemics is a complex one as each contributes to the prevalence and mortality of the other (Collins *et al.,* 2002). Although a number of factors have been implicated in the increase in the TB incidence in the United States between 1985 and 1992, a large percentage of these cases can be attributed to HIV infection (Bloom & Murray, 1992). In Africa TB is the leading cause of death in people infected with HIV (Tuberculosis and AIDS: UNAIDS point of view, 1997).

The risk of developing active tuberculosis from new *M. tuberculosis* infection is 20 times greater in HIV infected individuals, while the rate of reactivation of latent tuberculosis and the frequency of extra-pulmonary TB in these individuals is also higher. In HIV positive individuals the immune response in the lung is ineffective and is characterized by the recruitment of fewer lymphocytes to the site of infection and the less efficient activation of macrophages (Collins *et al.,* 2002). Co-infection with tuberculosis results in a more rapid progression to AIDS and increased mortality in HIV positive individuals. *M. tuberculosis* contributes to disease progression by increasing viral replication, improving the efficiency of HIV transmission to T-cells, and increasing HIV genome diversification (Collins *et al.,* 2002; Lawn, 2004).

1.2. TB INFECTION AND DISEASE PROGRESSION

Tubercle bacilli enter the body via the respiratory route and approximately 30% of exposed people become infected (Parrish *et al.*, 1998). The development of clinical TB occurs in approximately 40% of infected individuals and this primary disease develops within 1 or 2 years after infection. Post-primary TB can develop after a number of years and is caused either by reactivation of bacteria which remain after the initial infection or by exogenous reinfection (Stewart *et al.*, 2003). In the past it was assumed that post-primary TB is typically caused by reactivation. However, more recent studies have revealed that exogenous reinfection is a major cause of post-primary TB in areas with a high disease incidence (Sonnenberg *et al.*, 2001; van Rie *et al.*, 1999) and the risk of reinfection is further elevated in HIV-positive individuals (Sonnenberg *et al.*, 2001).

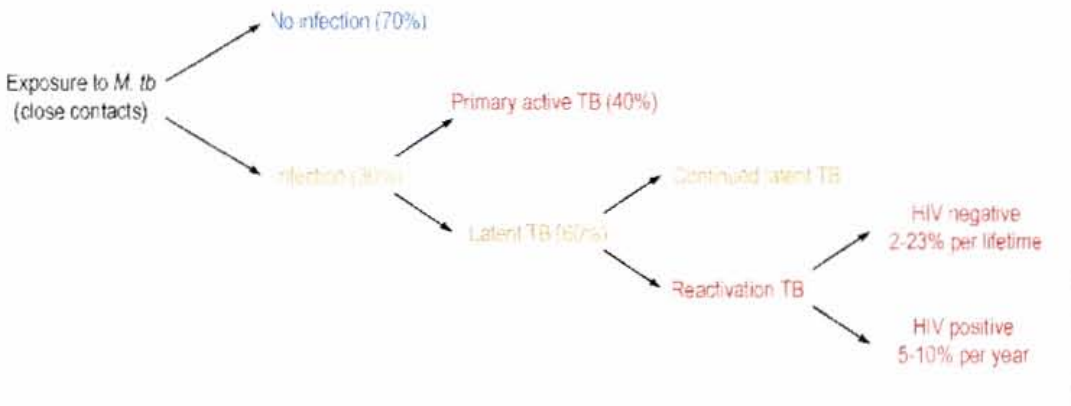

Figure 1.1: Outcomes associated with exposure to *Mycobacterium tuberculosis*
(modified from Parrish *et al.* 1998)

During the initial stages of infection, the host immune response may be inadequate resulting in the escape of tubercle bacilli from macrophages and transient bacteremia (Parrish *et al.*, 1998). In most immuno-competent individuals cell mediated immunity develops within 2-4 weeks and there is an influx of lymphocytes and activated macrophages to the site of infection. Infiltrating cells form granulomas, resulting in the containment of the infection and the killing of most of the bacilli (Raja, 2004). In individuals that are able to contain the infection active disease does not develop, but some bacilli persist and are able to remain dormant for several years. In 10% of these individuals, TB will develop into full-blown disease in response to stresses or if the

immune system becomes compromised. Several features may influence the development of active disease. HIV infection, malnutrition, drug use, cancer, diabetes, chronic renal insufficiency and immunosuppressive drug therapy are thought to increase the risk of reactivation (Parrish et al., 1998)

1.2.1 Survival of Mycobacteria in Macrophages

For infection to be established inhaled tubercle bacilli must be ingested by phagocytic alveolar macrophages. Once internalized the bacilli are able to multiply within the phagosomal compartment of non-activated macrophages (Parrish *et al.,* 1998). Phagocytosed material is normally transported along the phagosomal and endocytic pathway to lysosomes for degradation. However, phagosomes containing living mycobacteria are able to resist delivery to the lysosome. This is due to a process exerted by the mycobacteria, and involves both host and mycobacterial processes.

Coronin 1, also known as tryptophan aspartate-containing coat protein (TACO) is a host protein which belongs to a family of tryptophan aspartate-repeat actin binding proteins. In murine macrophages coronin 1 is retained on the membrane of phagosomes containing live mycobacteria. This is an active process since coronin 1 dissociates from phagosomes containing dead mycobacteria, resulting in their delivery to the lysosome (Ferrari *et al.,* 1999). Phosphotidylinositol 3-phosphate (PI3P) is a lipid, which controls intracellular trafficking and signal transduction. It affects the localization and function of proteins containing FYVE, PH or PX domains, including proteins which may be involved in phagosome maturation. The formation of PIP3 on the surface of the maturing phagosome is inhibited by mycobacteria and this is thought to occur by the calmodulin dependant regulation of PI3P (Chua and Deretic, 2004).

Phosphatidylinositol lipoarabinomannan (ManLAM), a lipid produced by *M. tuberculosis*, resembles PI3P. Latex beads coated with glycosylated ManLAM were shown to block phagosome maturation by blocking the delivery of lysosomal components from the trans golgi network. This block in trafficking results in the exclusion of cathepsin D, Mannose 6-phosphate receptor (M6PR) and H^+-ATPase from the mycobacterial phagosome (Fratti *et al.,* 2003). Protein kinase G (Pkn G) is a eukaryotic-like protein kinase which is actively secreted by pathogenic mycobacteria. The kinase is present in the phagosomal lumen and cytosol of infected macrophages where it interferes with lysosome delivery. The deletion of

pknG in *M. bovis* resulted in its transfer to the lysosome and the mutant was unable to survive in macrophages. Infection of macrophages with BCG or *M.* tuberculosis in the presence of a Pkn G inhibitor also resulted in delivery to the lysosome and killing of the mycobacteria (Walburger *et al.,* 2004). The activation of macrophages by interferon-γ (IFN-γ) reduces the ability of mycobacteria to replicate. Although the molecular mechanism of this suppression is not fully understood, the generation of nitric oxide is thought to play an important role.

1.2.2 Latency and Persistence

Latency in tuberculosis has been defined as "the presence of any tuberculosis lesion which fails to produce symptoms of its presence" (Amberson, 1938). The ability of *M. tuberculosis* to persist in the lungs of latently infected individuals is central to its success as a pathogen. Direct evidence of this persistence is the detection of viable bacteria in tissue from asymptomatic individuals. Early studies on lung tissue removed at autopsy revealed the presence of *M. tuberculosis* in the lungs of individuals that had died from causes unrelated to TB. This was shown either by direct culture or by the infection of guinea pigs (Stewart *et al.,* 2003). Interestingly, microscopic examination of infective tissue was sometimes unable to identify the presence of acid-fast bacilli. The two hypotheses proposed are that either the bacilli were in an altered developmental non acid-fast state, or that bacilli numbers were too low to visualize (Parrish et al., 1998). In a study by Opie and Aronson in 1927, they reported that 50% of normal lung tissue studied could cause TB in guinea pigs, whereas fewer than 10% of old lesions contained live bacilli. They concluded that *M. tuberculosis* is more commonly found outside of the focal lesions and suggested that these bacilli then give rise to post-primary infection. This result is supported by the detection of IS6110 DNA in normal lung tissue from Ethiopians and Mexicans who had died from causes other than TB (Hernandez-Pando *et al.,* 2000). In this study *in situ* PCR also detected microbial DNA in cells other than macrophages, which could be revealing a strategy used by *M. tuberculosis* to evade antigen presentation. A limitation of this method of detecting mycobacteria is its inability to determine if they are viable or not.

After the introduction of chemotherapy, the surgical resection of tuberculosis lesions provided material for bacteriological studies. Studies revealed that although acid-fast bacilli could be seen in specimens, these bacilli often failed to grow in culture or cause disease in guinea pigs (Beck and Yegian, 1952). Culturing of bacilli was found to be more difficult from lesions that were "closed" (Medlar *et al.,* 1952), although improved culturing techniques were able to increase the frequency with which bacilli could be cultured from closed lesions (Hobby *et al.,* 1954). This finding revealed that bacilli could remain viable within closed lesions, and the difficulty in culturing these bacilli suggests that they may occur in a "dormant" metabolic state. Bacilli were found even in patients who had received extensive chemotherapy. Although the cultured bacilli were found to be susceptible to antibiotics, it is postulated that their suppressed metabolic state in the host may make them resistant to chemotherapy (Hobby *et al.,* 1954). The finding that prophylactic chemotherapy using isoniazid is able to reduce the risk of reactivation of latent TB however suggests that some metabolism does occur (Comstock *et al.,* 1979).

1.2.3 Modeling Persistence

In order to determine the metabolic state of persistent mycobacteria, a number of models of persistence have been developed. The simplest model of persistence is the stationary phase culture of *M. tuberculosis*, in which the number of viable bacilli remains stable. The idea that dormant bacilli in the lung are within an environment of low oxygen tension lead to the development of Wayne's model of unshaken *M. tuberculosis* cultures in 1970. The oxygen limitation in cultures of *M. tuberculosis* grown without agitation led to net growth in an arithmetic mode. This net arithmetic growth was found to reflect the continuing logarithmic replication in the upper oxygen rich layer of the culture, and the termination of replication in cells which had settled through the oxygen gradient (Wayne, 1976). *M. tuberculosis* grown without agitation was tolerant of anaerobiosis, while bacilli cultured under aerobic conditions died rapidly when placed in an anaerobic environment (Wayne and Lin, 1982). The termination of agitation of *M. tuberculosis* cultures initiated adaptation of the bacilli as they settled through the oxygen gradient. This adaptation was associated with the synthesis of URB antigen, which is found only in non-agitated cultures of *M. tuberculosis.* Isocitrate lyase and glycine dehydrogenase were upregulated in bacilli adapting to oxygen limitation (Wayne and Lin, 1982). These enzymes may be important for replenishing metabolic

intermediates under oxygen limiting conditions. The non-replicating bacilli were also resistant to rifampin and isoniazid, and susceptible to metronidazole, which has no effect on aerobic cultures of *M. tuberculosis* (Wayne and Sramek, 1994). The use of a temporal O_2 depletion gradient, generated by the slow mixing of cultures under a restricted air column, led to the identification of two stages of nonreplicating persistence (Wayne and Hayes, 1996). The first stage (NRP stage 1) was characterized by a slow increase in turbidity without a corresponding increase in colony forming units. Termination of DNA synthesis, increased glycine dehydrogenase (GDH) levels and an increase in the rate of nitrate reduction was also seen in this stage (Wayne and Hayes, 1996; Wayne and Hayes, 1998). The second anaerobic stage, NRP stage 2, showed no further increase in turbidity and a decline in GDH production (Wayne and Hayes, 1996). Bacilli from NRP stage 2 showed synchronous growth after aeration was resumed, which was not seen for bacilli in NRP stage 1. The bacilli from these two stages also showed altered sensitivity to four antibiotics. Sequencing of the genome of *M. tuberculosis* revealed two sets of genes, *narGHJI* and *narK,* which share homology with prokaryotic respiratory type nitrate reductases (Cole *et al.,* 1998). Mutant studies revealed that *narGHJI* is responsible for the nitrate reductase activity in *M. tuberculosis*, while induction of nitrate reduction by hypoxia is as a result of the induction of the nitrate transporter $narK_2$ (Sohashky and Wayne, 2003).Interestingly, the nitrate reductase does not support anaerobic growth, but appears to provide an additional energy source as *M. tuberculosis* shifts into a state of non-replicating persistence under oxygen limiting conditions. Wayne and Hayes suggest that the ability of tubercle bacilli to shift into one or both of these non-replicating states is responsible for their capacity to remain dormant in the host for extended periods and reactivate at a later stage.

The most widely used animal model of latent TB infection is the mouse model. Low-dose aerosol infection with *M. tuberculosis* results in unimpeded growth of bacilli in lungs and spleen for the first 2 to 4 weeks. The adaptive immune response of resistant mouse strains, such as C57BL/6, is then able to control the growth of organisms causing bacterial numbers to plateau. The mice show slowly progressive pathology and are capable of surviving for long periods of time. Although this persistent infection state represents an equilibrium between the host and pathogen, it does not reflect latency in humans which is characterized by low bacterial loads (reviewed in Flynn and Chan, 2001; Stewart *et al.*,2003; Gomez and

McKinney, 2004). The advantage of this model of latency is that it relies on the host immune response to control the infection.

A study investigating the fate of tubercle bacilli in the lungs and spleen of mice treated with combinations of antibiotics led to the development of the "Cornell Model" in the 1950s (Hobby *et al.,* 1954). After intravenous infection with *M. tuberculosis,* mice were treated with a combination of pyrazinamide (PZA) and isoniazid (INH) for 12 weeks. The mice appeared to be "sterilized" since bacilli could not be detected in tissue from the lungs and spleen by microscopy, culture or sub-inoculation into guinea pigs. Reactivation of the disease however occurred spontaneously in a third of the animals 90 days after the cessation of treatment and the administration of high doses of cortisone at 3 or 4 months after treatment was able to increase the percentage of reactivation to 100% (McCune *et al.,* 1966a, b). The bacilli isolated after reactivation were found to be drug susceptible. De Wit *et al.* (1995) demonstrated that although the mice appeared to be sterilized, large amounts of bacterial DNA could be detected in the organs of the mice, suggesting that the bacilli may be in a non-culturable state. No standard protocol has been developed for the Cornell Model and variations have demonstrated that the outcome of the model is highly dependent on parameters such as size of the *M. tuberculosis* inoculum, dose of antibiotics used and method of immune suppression (Scanga *et al.,* 1999). Although the model has undetectable numbers of bacilli, which is analogous to human infection, the disadvantage is the artificial induction of latency by chemotherapy. The model has demonstrated that a subpopulation of bacteria exist *in vivo* that are tolerant to the effects of antibiotics (reviewed in Gomez and McKinney, 2004).

Latency models in other animals used to study TB, including guinea pigs, rabbits and non-human primates have not been widely used. This is due to economic and logistical factors, and also since extensive research has been done on the immunology and chemotherapy of the mouse (Flynn and Chan, 2001). It is believed that by developing a therapeutic agent which targets genes or pathways involved in persistence, treatment will become more effective and regimes will be shortened. Therefore, the ability to model persistence is essential for the development of new therapeutic agents for the control of TB.

1.3. STRATEGIES FOR CONTROLLING TUBERCULOSIS

1.3.1 Vaccination

Despite the use of BCG as a vaccine against tuberculosis for more than 80 years, its efficacy in preventing pulmonary tuberculosis in adults continues to be debated. Studies have shown that BCG provides protection against tuberculosis meningitis and disseminated forms of the disease in children (Reviewed in Walker *et al.,* 2006). However, trials conducted to investigate its efficacy in adults have produced contradictory findings and show a wide range of protective efficacy against *M. tuberculosis.* There are various reasons proposed for this variability, including differences in BCG strains, doses, immunisation age, host genetic background, infecting *M. tuberculosis* strains and interference from environmental mycobacteria. In a meta-analysis of the published literature, Colditz *et al.* (1994) found that vaccination with BCG reduces the risk of tuberculosis by an average of 50%. Protection was observed for both pulmonary and extra-pulmonary tuberculosis, with higher levels of protection observed against disseminated forms of the disease. BCG efficacy was not affected by age at vaccination, while latitude and the data validity scores of the studies were shown to contribute to some of the variability observed.

As a result of the inefficiency with which BCG protects against pulmonary tuberculosis in adults, there are a number of strategies being pursued to develop a new TB vaccine. Since the majority of the world's population has been exposed to environmental mycobacteria, vaccinated with BCG or infected with TB, an ideal vaccine would induce protection in previously exposed populations as well as in individuals not previously exposed (Franco-Paredes *et al.,* 2006). The development of acquired resistance against *M. tuberculosis* is complex and involves various subsets of T-cells (Andersen, 2001). Animal models indicate that Th1-type $CD4^+$ T-cells, which produce IFN-γ, are important for protection (Franco-Paredes *et al.,* 2006). The recurrence of TB as a result of either re-infection or reactivation indicates that the immune response to *M. tuberculosis* infection is inefficient. Therefore, a new vaccine should elicit an immune response which is superior to that induced by natural infection. Currently, the best correlate of protection against *M. tuberculosis* in humans is IFN-γ, which is the major activator of macrophages and is required for the protective response against intracellular pathogens (Raja, 2004).

1.3.2 Approaches for Development of a New TB Vaccine

1.3.2.1 Subunit Vaccines

Subunit vaccines deliver mycobacterial immunogenic antigens in the form of proteins, peptides, DNA or live vectors, which induce specific subpopulations of $CD4^+$ T-cells (Franco-Paredes *et al.,* 2006). Antigens which have been investigated include those derived from the culture filtrate of *M. tuberculosis* (Orme, 2005) and proteins from the RD-1 region of *M. tuberculosis*, which is absent from BCG. More specifically, DNA vaccination involves immunization with a bacterial plasmid encoding an antigen, under the control of a suitable promoter. This results in the transfection of host cells and the endogenous production of the antigen, which generates both a humoral and cellular immune response. The advantages of DNA vaccines include stability, ease of preparation, low cost and safety in immune-compromised individuals. However, despite their ability to induce protection in mice, DNA vaccines have not performed better than BCG (Huygen, 2003).

1.3.2.2 Whole-cell Vaccines

Despite its inefficient protection, BCG has many advantages as a vaccine and therefore attempts have been made to modify it with the aim of enhancing its immunogenicity. Recombinant BCGs which have been constructed include those expressing cytokines and antigens, such as IFNγ and Ag85B (Eddine & Kaufmann, 2005). In an attempt to improve $CD8^+$ T cell stimulation by facilitating the escape of BCG from the phagolysosome, rBCG expressing listeriolysin O (LLO) from *Listeria monocytogenes* was constructed. LLO BCG recombinants showed an improved level of protection in mice relative to BCG (Grode *et al.,* 2005). The availability of the genome sequence of *M. tuberculosis* and the assignment of function to various mycobacterial genes has facilitated the production of attenuated strains of *M. tuberculosis and M. bovis* BCG. The rationale behind using these strains for vaccination is that they would cause active infection, but that the duration of infection would be limited. Auxotrophic mutants, in which an amino acid biosynthetic pathway has been disrupted, have been generated by this approach (von Reyn & Vuola, 2002). Whole-cell inactivated vaccines, such as *Mycobacterium vaccae*, have shown protection against TB in animal models (Franco-Paredes *et al.,* 2006). However in a study in KwaZulu Natal, the addition of immunotherapy with *M. vaccae* to standard chemotherapy was shown to have no benefit (Mayo & Stanford, 2000).

1.3.2.3 Prime-boost Vaccines

Prime-boost vaccines involve the successive administration of the same mycobacterial antigen. In a phase I trial, a recombinant smallpox vaccine expressing mycobacterial antigen 85A (MVA85A) was administered to BCG vaccinated and BCG-naïve individuals. Vaccination with MVA85A was found to boost pre-existing anti-mycobacterial immune responses induced either by BCG or exposure to other mycobacteria (McShane *et al.*, 2004). This approach is thought to be favourable as the protective effects of BCG might be retained.

Although the various strategies being pursued have produced promising vaccine candidates, it will be several years before a new vaccine for TB becomes available. With ongoing research in both host and pathogen biology, it is hoped that a better understanding of the disease will translate to more effective control of the epidemic through vaccine development.

1.3.3 Chemotherapy

Prior to the discovery of antibiotics, treatment for tuberculosis consisted primarily of bed rest in sanatoria and the collapsing of the affected portion of the lung by surgery or injection of air into the pleural cavity. The mortality rate of pulmonary tuberculosis was as high as 50% in this pre-antibiotic era.

The discovery of streptomycin and proof of its anti-tubercular activity in guinea pigs led to the initiation of studies on the treatment of tuberculosis by the British Medical Research Council (Reviewed in Fox *et al.*, 1999). The findings of these studies, conducted between 1946 and 1986, resulted in the development of modern chemotherapy. In 1947, a study comparing patients receiving streptomycin plus bed rest to those on bed rest alone showed the benefit of streptomycin. After 5 years however, the mortality rate was only slightly higher in the control patients since most patients developed streptomycin-resistant strains. The ability of combination therapy to reduce the development of resistance was investigated using streptomycin and p-aminosalicylic acid (PAS). Pulmonary tuberculosis patients receiving a combination of streptomycin and PAS yielded fewer positive sputums and streptomycin-resistant strains than those receiving each of the drugs individually. The introduction of isoniazid in 1952 resulted in trials using combinations of isoniazid,

streptomycin and PAS. These showed the rapid emergence of resistance when isoniazid was administered alone, but suppression of emergence of resistance when combined with streptomycin. Patients receiving isoniazid and streptomycin were found to fair slightly better than those receiving a combination of streptomycin and PAS. After screening for primary resistance in Britain revealed that resistance to two or three drugs was rare, the initial phase of treatment was increased to three drugs. This initial phase was continued for 2-3 months and followed by two drugs for a total duration of a year. Studies in India showed that chemotherapy in the sanatorium setting was no more effective than at home, and that treatment at home did not increase the risk of infection through family contact. This resulted in the move towards the domiciliary treatment of tuberculosis, making it feasible even in poor developing countries. The finding that intermittent treatment was as effective as daily therapy was also a major breakthrough in tuberculosis chemotherapy. The advantages of intermittent therapy are reduced cost, fewer adverse drug reactions and increased compliance facilitated by directly observed therapy.

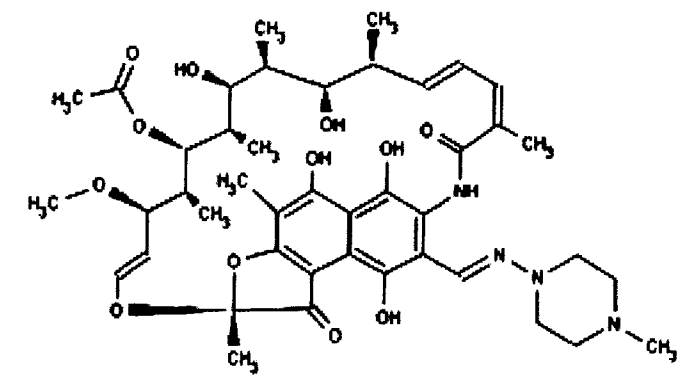

Rifampicin

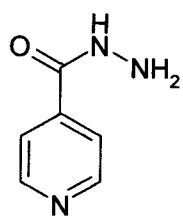

Isoniazid

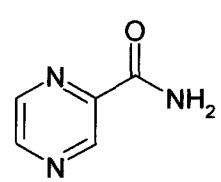

Pyrazinamide

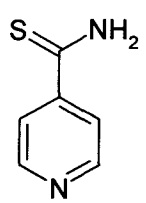

Ethionamide

Figure 1.2: Structures of some of the commonly used antitubercular drugs.

1.3.3.1 Short Course Chemotherapy

Studies in the development of the Cornell mouse model revealed interesting properties of pyrazinamide (PZA) in the murine system (McCune *et al.,* 1966a, b). Unlike isoniazid, PAS and streptomycin, which cause bacterial numbers in mice to decline and then level out, PZA has the ability to sterilize organs. This sterilizing activity was also observed for Rifampicin (RIF) in the mouse model and led to studies investigating short-course regimes including PZA and RIF to reduce relapse rates. In a study in East Africa the effect of adding RIF, PZA or thioacetazone to a 6-month daily regime of isoniazid and streptomycin was investigated (East Africa/British Research councils, 1972). All four regimes were effective; however those containing RIF and PZA had lower relapse rates after 6 months than those with thioacetazone or only two drugs. Relapse was not due to drug resistance since isolated organisms were fully sensitive. RIF and PZA regimes were also able to convert patients to culture negative faster than the other regimes. The relapse rates for a 6-month daily regime of streptomycin, isoniazid and RIF and a standard 18-month regime of streptomycin, thiocetazone and isoniazid for two months and thioacetazone and isoniazid for 16 months daily, were also found to be similar when assessed over a 5-year period (East Africa/British Medical Research Councils, 1977). Numerous other studies on short-course chemotherapy were subsequently performed in order to determine the role of each drug in the various phases of treatment, ideal dosing levels and treatment duration.

The findings of clinical trials, animal models and *in vitro* culture has led to the development of a hypothesis about the bactericidal activity of various anti-tuberculosis drugs (Mitchison, 1979). It is suggested that four bacterial populations exist within a patient with TB. The first population consists of actively growing organism, which are killed most effectively by isoniazid and to a lesser extent by streptomycin and rifampicin. The bactericidal activity of isoniazid decreases as the growth rate of organisms becomes slower. A second population of slow-growing organisms occur in an acidic environment, possibly within macrophages. These bacilli are killed primarily by PZA and to a lesser extent by RIF. Since the killing action of RIF is rapid, it is able to act against a third population of organisms which exhibit spurts of growth. These organisms are present extracellularly in solid caseous lesions. Finally, a population of dormant organisms exists against which none of the drugs has activity.

The efficacy of a treatment regime is evaluated by two criteria namely its bactericidal activity and its sterilizing activity. The measure of bactericidal activity is the proportion of patients that become sputum culture negative after two months of treatment, while the relapse rate of treatment is a reflection of the sterilizing activity of a regime (Jawahar, 2004). Current regimes use an initial intensive phase to rapidly reduce bacterial numbers and a longer continuation phase in which the killing of slower growing organisms is important. The inclusion of various drugs in these two phases is therefore dependent on their bactericidal and sterilizing activity. Generally patients receive four drugs in the initial intensive phase, and two drugs in the continuation phase of treatment. Isoniazid is given for the duration of treatment due to its high bactericidal activity, low toxicity and low cost. A commonly use regime is isoniazid, ethionamide, RIF and PZA for two months, followed by isoniazid and RIF for four months.

1.3.3.2 Multi-drug Resistant Tuberculosis (MDR TB)

Tuberculosis drug resistance can be divided into two types. Firstly primary resistance occurs in a person who has been infected with a resistant strain of *M. tuberculosis* and has not previously received treatment for TB. Secondly, acquired resistance emerges during treatment of tuberculosis and results from the inappropriate use of tuberculosis drugs (Nachega and Chaisson, 2003). MDR TB is defined as *M. tuberculosis* which is resistant to both Rifampicin and Isoniazid. The danger of MDR TB is due to its poor response to available therapeutic regimes. The risk of failure of treatment in MDR cases is 80 times higher than for drug susceptible strains in HIV negative individuals (Jawarhar, 2004). The management of MDR patients is complex as it involves determining the treatment history of the patient and the antibiotic susceptibility profile of the infecting strain. Standard drug susceptibility testing involves growing isolated strains on solid media containing critical concentrations of the drugs and results are often only available several months after patients are diagnosed. Although radiometric or fluorescence-based systems are able to reduce this period to weeks after presentation, their expense often limits application in many parts of the world (Nachega and Chaisson, 2003).

Table 1.1: Adverse Reactions associated with second line drugs used in the treatment of tuberculosis (Modified from Nachega and Chaisson 2003)

Drug	Major toxicities
Capreomycin	Auditory, vestibular and renal toxicity
Kanamycin	Auditory, vestibular(rare) and renal toxicity
Ethionamide	Gastrointestinal disturbance, hepatotoxicity, hypersensitivity
Para-aminosalicylic acid	Gastrointestinal disturbance, hepatotoxicity, hypersensitivity, sodium load
Cycloserine	Psychosis, convulsions, rash

Treatment of MDR-TB relies extensively on second line drugs (Table 1.1), which in general have poorer activity and also have more adverse reactions. Patients are treated with drugs they are known to be susceptible to or which they have not previously received. The initial phase of treatment lasts at least six months and involves the daily administration of four drugs. Three of the most active drugs are then administered for a continuation phase of 12 to 18 months. It is recommended that treatment be continued for at least 12 months after the patient's sputum cultures become negative. The treatment of MDR TB is therefore more expensive, more toxic and less successful than treatment of drug susceptible TB.

1.3.3.3 Extensively Drug-resistant Tuberculosis (XDR TB)

XDR TB is MDR TB which is resistant to three or more of the six classes of six second-line TB drugs. The first information available about the worldwide incidence of XDR TB was from a survey done by the CDC and WHO of an international network of TB laboratories (CDC, 2006). The survey found that of the 17690 TB cases between 2000 and 2004, 20% where MDR and 2% were XDR. XDR TB has been detected in all regions of the world, with the highest prevalence occurring in Asia and Eastern Europe. XDR TB is virtually untreatable and is associated with a high mortality rate. At a meeting in September 2006 between the South African Medical Research Council, WHO and the CDC, a seven-point plan to combat XDR TB was released. This included improvements in the diagnosis, containment and management of XDR TB cases, increased support for research into drugs

and diagnostic methods for XDR TB and the increased access to antiretrovirals (Lancet editorial, 2006).

1.3.3.4 New Anti-tuberculosis Drugs

Little change has occurred in current regimes in the past 30 years due to the absence of new drugs. A new drug should be highly active to facilitate shorter chemotherapy, should kill persistent bacilli to prevent relapse and should be active against MDR strains. Ideally, it should be specific for *M. tuberculosis* and compatable with existing drugs (Cole & Alzari, 2005).

The activity which fluoroquinolones possess against mycobacteria has been exploited in the treatment of patients with MDR TB. Current interest is in C-8-methoxy-fluoroquinolones, such as moxifloxacin, which are more active against *M. tuberculosis*. In a study evaluating five fluoroquinolones, moxifloxacin was the only compound which showed both bactericidal activity against slow growing organisms and sterilizing activity against persisters (Hu *et al.,* 2003). These compounds could potentially be used as first line drugs following their evaluation in clinical trials. A strategy being employed in the search for new drugs is the modification of existing antibiotics in an attempt to make them more active against *M. tuberculosis.* Rifalazil is a rifampicin derivative which has shown improved activity in the murine model when used in combination with isoniazid (Shoen *et al.,* 2000). However, its usefulness is limited by the fact that RIF-resistant strains confer resistance to all rifampicins.

PA-824 is a nitroimidazopyran which has a sub-micro molar MIC for *M. tuberculosis* and also has activity against MDR strains (Stover *et al.,* 2000). It also has activity against non-replicating microaerophilic cultures comparable to that of metronidazole. In the mouse and guinea pig model of MTB, PA-824 showed activity comparable to isoniazid at safe doses. PA-824 inhibits a step in the synthesis of cell wall mycolates, and like isoniazid is a pro-drug which requires activation. The oral activity and chemical properties which make it amenable to large-scale synthesis, makes PA-824 an attractive drug candidate. Resistance to PA-824 in *M. tuberculosis* is associated with the loss of a glucose-6-phosphate dehydrogenase (FGD1), loss of its cofactor F_{420} and mutations in hypothetical protein

Rv3547, which are all involved in the reductive activation of PA-824 (Manjunatha *et al.*, 2006).

Another promising drug candidate is a diarylquinoline R207910 (Andries *et al.*, 2005). The compound was identified through a whole-cell screening assay using *M. smegmatis* and was found to function by inhibiting ATP synthase. R207910 is highly bactericidal and was as effective against MDR strains as drug susceptible strains. In the murine model, substitution of RIF, isoniazid or PZA with R207910 resulted in increased potency of the treatment regime. The sterilizing activity of R207910 requires further investigation. Phase I human trials have shown good oral absorption, sustained plasma levels and good tolerability of R207910.

The development of MDR and more recently XDR TB has highlighted the need for the continuous development of new anti-tubercular drugs. The validation of new targets for therapeutic agents is an essential part of this process.

1.4. Low Molecular Weight Thiols

1.4.1 The Role of Thiols in Cellular Metabolism

The presence of thiols in living systems is critical for the functioning of cellular metabolism. This critical role is demonstrated by the numerous identified functions of glutathione, which the most extensively studied low molecular weight thiol.

1.4.1.1. Glutathione

Glutathione (GSH), a tripeptide (L-γ-glutamyl-L-cysteinyl-glycine), occurs in most cells in the millimolar range (Dickinson & Forman, 2002) and its functions include the detoxification of free radicals, metals and other electrophilic compounds. In order to prevent lipid peroxidation and the disruption of metabolic processes, all aerobic organisms require a mechanism to detoxify the intermediates generated during aerobic metabolism. The ability of GSH to react with carbon centered radicals is important in its role as an antioxidant (1 & 2). GSH also functions to store cysteine, since free cysteine rapidly auto-oxidises resulting in the production of oxygen radicals. Although glutathione does not react directly with hydroperoxides, it is involved in the enzymatic reduction of hydroperoxides by glutathione peroxidase (3 & 4) and the peroxiredoxin family of enzymes (5) (Dickinson & Forman, 2002).

Free radical reactions

$$R + GSH \longrightarrow RH + GS \qquad \text{.....1}$$

$$2GS \longrightarrow GSSG \qquad \text{.....2}$$

Enzymatic detoxification of H_2O_2:

$$H_2O_2 + 2GSH \xrightarrow{\text{Glutathione peroxidase}} 2H_2O + GSSG \qquad \text{.....3}$$

$$ROOH + 2GSH \xrightarrow{\text{Glutathione peroxidase}} 2ROH + GSSG \qquad \text{.....4}$$

$$H_2O_2 + 2GSH \xrightarrow{\text{Peroxiredoxins}} OH^- + GSSG + H_2O \qquad \text{.....5}$$

The reduction of GSSG by the enzyme glutathione reductase (6) is the primary mechanism for maintaining the redox state of the cell. GSSG constitutes 1% of total glutathione in cells, and only a transient increase in GSSG levels is observed during oxidative stress. Under severe oxidative stress, GSSG is transported out of cells by an ATP-dependent transport mechanism.

$$GSSG + NADPH + H^{+} \xrightarrow{\text{Glutathione reductase}} NADP^{-} + 2GSH \qquad \ldots\ldots 6$$

The reaction of glutathione with electrophilic compounds occurs either spontaneously or by the catalytic action of glutathione-S-transferase (7). The formation of the thioester bond between GSH and the electrophile usually results in a less reactive, more water soluble product (Eaton & Bammler, 1998). The conjugation of GSH to foreign chemicals, endogenous compounds and metals serves to limit their chemical reactivity and facilitate elimination from the cell (Wang and Ballatori, 1998).

$$\text{Electrophile (E)} + GSH \xrightarrow{\text{Glutathione-S-transferase}} GS\text{-}E \qquad \ldots\ldots 7$$

An aerobic environment also results in the oxidation of protein disulphides, which could alter the catalytic activity of enzymes. Reduction of these disulphides occurs by a thiol-disulphide exchange in the presence of GSH. GSSG can also exchange with protein sulphydryls to produce protein-glutathione mixed disulphides in a concentration dependant manner (Brigelius *et al.*, 1983). Thioredoxin (Trxs) and Glutaredoxins (Grxs) are enzymes which catalyse thiol-disulphide exchange reactions at the cysteines within their active site motif CXXC (Holmgren *et al.*, 2005). Unlike Trxs which are reduced by NADPH, Grxs are reduced by GSH, which allows the reactions to proceed by either a dithiol or monothiol mechanism (8-11). The latter mechanism is required for the reduction of protein-GSH mixed disulphides (R-S-SG) (Holmgren *et al.*, 2005).

Dithiol mechanism:

$$R\text{-}S_2 + Grx\text{-}(SH)_2 \longrightarrow R\text{-}(SH)_2 + Grx\text{-}S_2 \qquad \ldots\ldots 8$$

$$Grx\text{-}S_2 + 2GSH \longrightarrow Grx\text{-}(SH)_2 + GSSG \qquad \ldots\ldots 9$$

Monothiol mechanism:

$$R\text{-}S\text{-}SG + Grx\text{-}(SH)_2 \longrightarrow R\text{-}SH + Grx\text{-}S\text{-}SG \qquad \ldots\ldots 10$$

$$Grx\text{-}S\text{-}SG + GSH \longrightarrow Grx\text{-}(SH)_2 + GSSG \qquad \ldots\ldots 11$$

Since a significant number of signaling proteins have critical thiols, GSSG may act as a non-specific signaling molecule in response to a change in the redox state of the cell (Dickinson & Forman, 2002). GSH may also signal indirectly by determining the rate of H_2O_2 removal.

1.4.2 Thiol Biosynthetic Enzymes as Potential Drug Targets for TB

Mycobacterium tuberculosis synthesizes two major thiols, namely mycothiol (MSH) and ergothioneine (ESH). Since these biosynthetic pathways are not present in the human host, they are attractive targets for the development of new therapeutic agents against tuberculosis.

1.4.2.1. Mycothiol

The biosynthesis of mycothiol (MSH) which is the trivial name assigned to the compound 1-D-myo-inosityl-2-(N-acetyl-L-cysteinyl)amino-2-deoxy-α-D-glucopyranoside, appears to occur exclusively in Actinomycetales bacteria (Newton *et al.,* 1996). Mycothiol is present in high levels in mycobacteria and its synthesis is a multi-step process (Fig. 1.2). The generation of mutants of various enzymes of the biosynthetic pathway of MSH has provided insight into the role of MSH in mycobacteria. Chemical and transposon generated MshC mutants in *Mycobacterium smegmatis* (*M. smegmatis*) showed increased sensitivity to free radicals and alkylating agents and altered sensitivity to a range of antibiotics (Rawat *et al.,* 2002). In *M. tuberculosis Erdman* the MshC (Sareen *et al.,* 2003) and MshA (Buchmeier & Fahey, 2006) were found to be essential, suggesting that MSH is required for growth of this strain under laboratory conditions. The enzyme mycothiol-S-conjugate amidase has been shown to detoxify MSH conjugates of anti-mycobacterial drugs in a manner similar to GSH (Newton *et al.,* 2000b) and its inhibition may therefore increase the sensitivity of mycobacteria to established chemotherapeutic agents. The enzymatic reduction of MSSM to MSH is catalysed by mycothiol reductase, which is thought to have the same function as GSH disulphide reductase in maintaining the redox state of the cell (Patel and Blanchard, 2001). Currently, much work is being done to design and test potential inhibitors of the mycothiol biosynthetic enzymes as potential therapeutic agents.

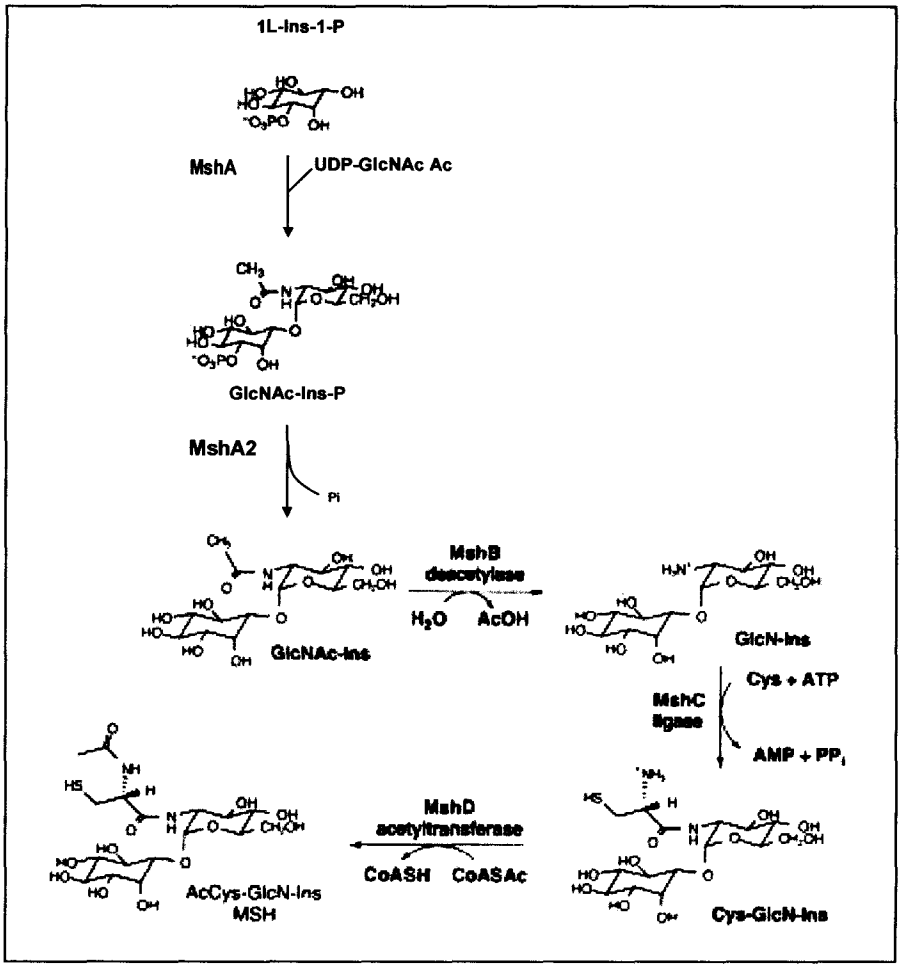

Figure 1.3: Biosynthetic pathway of MSH. The genes encoding MshA (Rv0486) (Newton *et al.*, 2003), MshB (Rv1170) (Newton *et al.*, 2000a), MshC (Rv2130c) (Sareen *et al.*, 2002) and MshD (Rv0819) (Koledin *et al.*, 2002) in *M. tuberculosis* have been identified. MshA2 is yet to be identified. (Modified from Sareen *et al.*, 2003)

1.4.2.2 Ergothioneine

Ergothioneine (ESH), the betaine of 2-thio-L-histidine, has been detected in millimolar concentrations in plants, fungi, bacteria, animals and humans. Animals obtain ESH from dietary sources, while plants are thought to obtain it from the soil (Hand and Honek, 2004). A specific transporter for ESH has been identified in humans, which suggests it has an essential

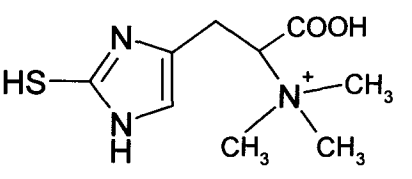

Figure 1.4: Ergothioneine (ESH)

function (Gründerman *et al.*, 2005) Certain fungi and Actinomycetales bacteria synthesize ESH (Genghof, 1970).

1.4.2.3 Biochemistry of Ergothioneine

Ergothioneine differs from GSH and MSH in that it exists as a thione under physiological conditions and consequently differs in its reactivity. Unlike other thiols, ESH exists in its reduced form in aerated aqueous solutions (Chaudiere and Ferrari-Iliou, 1999). Typical intracellular ESH concentrations are in the range 0.1-1mM, and it possesses antioxidant properties in this range. Ergothioneine reacts with the $^{\cdot}OH$ radical at a diffusion controlled rate and has the ability to chelate transition metal ions, which prevents the generation of $^{\cdot}OH$ by reaction of H_2O_2 with these ions (Akanmu *et al.*, 1991). Pulse radiolysis indicates a co-operative interaction between vitamin C and ESH. Vitamin C is an established water-soluble antioxidant and its interaction with ESH may contribute to its biological redox protection (Asmus *et al.*, 1996). The protection of α_1- antiproteinase (α_1-AP) from inactivation by HOCl showed that ESH is a good scavenger of HOCl (Akanmu *et al.*, 1991). ESH concentrations of up to 2mM were shown to slightly reduce oxidant dependent cell death, which occurs as a result of exposure to H_2O_2. This suggests that H_2O_2 scavenging may not be a major function of ESH *in vivo* (Aruoma *et al.*, 1999). ESH also possesses UV-radiation protective properties (van den Broeke, 1993), and a study on UV-irradiated human dermal fibroblast revealed this protection is partly attributable to its ability to scavenge superoxide and singlet oxygen (Obayashi *et al.*, 2005).

ESH may also combat nitrosative stress caused by molecules such as peroxynitrite ($ONOO^-$) and nitric oxide ($NO^{\cdot}$). The ability of ESH to scavenge peroxynitrite was demonstrated by its protection against the nitration of tyrosine and inactivation of α_1-AP in the presence of $ONOO^-$ (Aruoma *et al.*, 1997). Peroxynitrite-induced oxidative damage to calf thymus DNA and DNA in N-18-RE-105 cells was inhibited by ESH (Aruoma *et al.*, 1999). S-Nitrosothiols are produced through the reaction of thiols with NO^+ and $ONOO^-$. ESH was found to drive the decomposition of S-nitrosoglutathione at a rate faster than GSH, generating ammonia as the major nitrogen-containing product (Misiti *et al.*, 2001).

Although ESH was not able to inhibit lipid peroxidation stimulated by Fe^{2+} or Fe^{3+}, it does not stimulate peroxidation as some thiols do. ESH was able to inhibit peroxidation of arachidonic acid induced by H_2O_2 and hemoproteins (Akanmu *et al.*, 1991). Heavy metals

are able to auto-oxidise thiols such as GSH, to form disulphides and peroxides. This does not occur with ESH, which has the ability to chelate divalent metal ions (Hanlon, 1971). ESH was also able to inhibit certain Cu-requiring metalloenzymes (Hanlon, 1971). The ability of ESH to complex with metals may be important in the protection of oxyhemoglobin (Hb) and myoglobin (Mb) from oxidation. Pre-incubation of oxyhemoglobin with ESH prevented copper induced oxidation of hemoglobin. Addition of 1mM of ESH was also able to prevent oxidation of Mb by H_2O_2 (Akanmu *et al.*, 1991).

1.4.2.4 Bioactivity of Ergothioneine

In early work done on fungi, hercynine (an intermediate in ergothioneine biosynthesis) and ergothioneine were studied as growth regulatory substances. Hercynine was identified as a fruiting inducing substance isolated from *Agaricus bisporus* (Roure and Bouilliant, 1986), while ergothioneine accumulates in spores of *N. crassa* (Brody, 1981 in Roure and Bouilliant, 1986). Although the ergothioneine does not induce germination in *Claviceps purpurea*, its presence is able to counter the inhibition of germination by hydrogen peroxide. It is therefore thought to play a protective role against hydrogen peroxide during infection (Garay, 1956).

The Fenton reaction which involves transition metals, results in the generation of highly reactive hydroxyl radical species from hydrogen peroxide (12).

$$H_2O_2 + Fe^{2+}\ (Cu^{+}) \longrightarrow Fe^{3+}\ (Cu^{2+}) + OH^{\cdot} + OH^{-} \qquad .....12$$

Deiana *et al.* utilized a Fenton chemistry model to evaluate the antioxidant protection to the kidney afforded by dietary ESH. Oral supplementation with ESH, 7days prior to exposure to an acute dose of ferric-nitrilotriacetate, was shown to reduce oxidative damage in the liver and kidneys of rats. Supplementation protected the organs against lipid peroxidation and against the loss of endogenous antioxidants glutathione and α-tocopherol (Deiana *et al.*, 2004). In an *in vivo* rat retinal model, in which the over stimulation of *N*-methyl-D-aspartate (NMDA) subtype of glutamate receptor leads to neuronal cell death, ergothioneine was found to be neuroprotective. Since over stimulation of NMDA results in increased free radical production, the protective effect of ESH may be due to its antioxidant properties (Moncaster *et al.*, 2002). The transcription factor NFκβ is involved in the transcriptional activation of Interleukin-8, which is an inflammatory cytokine. ESH was

shown to have an anti-inflammatory effect in human alveolar epithelial cells by inhibiting the H_2O_2- and TNFα- mediated activation of NFκβ (Rahman *et al.*, 2003).

Since part of the immune response to *M. tuberculosis* infection involves the generation of reactive oxygen and nitrogen species, the production of ESH by mycobacteria may be indicative of its protective role against oxidative stress. The inhibition of ESH production may therefore be a novel drug target, by limiting the bacilli's ability to survive in this hostile environment.

1.4.2.5 Biosynthesis of Ergothioneine

The biosynthesis of ESH has been studied in *Neurospora crassa* and *Claviceps purpurea* due to the high levels present in these organisms. Initial work showed that intact histidine was incorporated into ergothioneine, while thiolhistidine does serve as a precursor for ESH (Melville *et al.*, 1957, Heath & Wildy 1957). Synthesis of ESH involves the trimethylation of histidine (Melville *et al.*, 1959) and the formation of hercynine as an intermediate (Askari and Melville, 1962). Cell-free extracts from *N. crassa* were able to catalyse the methylation of histidine, α-N-methyl-L-histidine and α-N, N-dimethyl-L-histidine to form hercynine in the presence of the methyl donor S-adenosylmethionine (Reinhold *et al.*, 1970), and Ishikawa and Melville (1970) showed that the trimethylation of histidine is catalysed by a single enzyme in *N. crassa*.

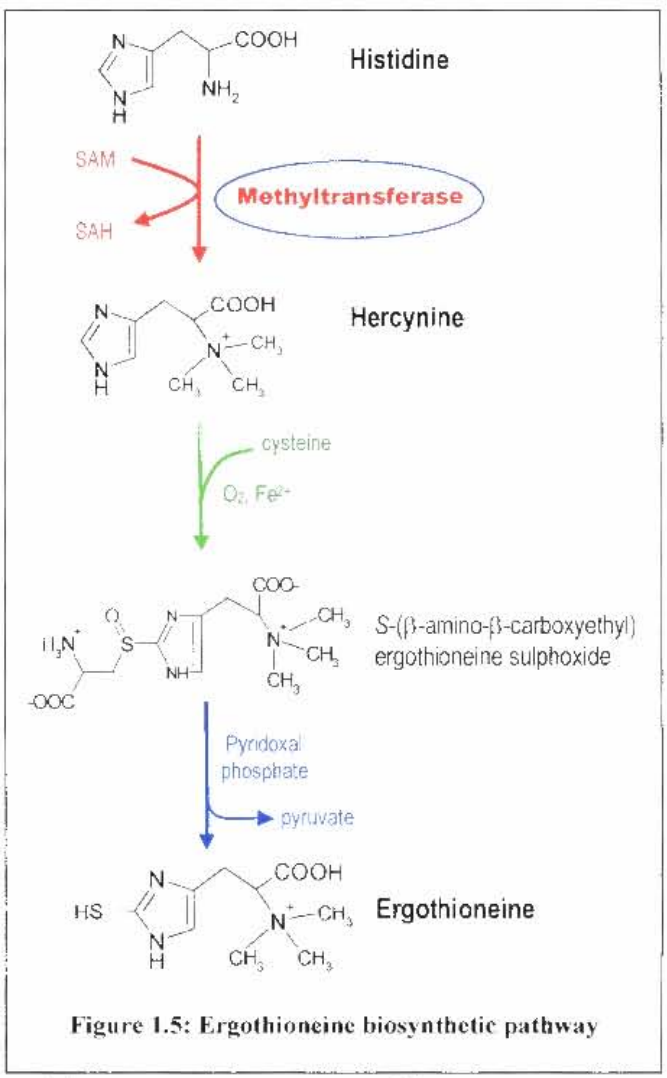

Figure 1.5: Ergothioneine biosynthetic pathway

The sulfhydryl group of ESH in *N. crassa* is provided by cysteine (Melville *et al.,* 1957) and this reaction involves the formation of an intermediate compound S-(β-amino-β-carboxyethyl) ergothioneine sulphoxide (Ishikawa *et al.,* 1974). This is distinct from the transsulfuration pathway in methionine and cysteine metabolism, which proceeds via cystathionine (Banerjee *et al.*, 2003). S-(β-amino-β-carboxyethyl) ergothioneine sulphoxide is converted to ergothioneine and pyruvate by a pyridoxal phosphate-dependant enzyme (Ishikawa *et al.,* 1974).

The use of radiolabelled precursors of ESH indicated that a similar biosynthetic pathway exists in mycobacteria (Genghof and van Damme, 1964). In actively growing cultures of *M. smegmatis,* ergothioneine synthesis was limited by the amount of sulfur present, while hercynine accumulated in sulfur-limiting cultures. Experiments using resting *M. smegmatis* cell cultures showed that cysteine is a good sulfur donor in ergothioneine synthesis, and that other compounds which could easily be converted into cysteine could also be utilized (Genghof and van Damme, 1968). The addition of L-histidine to the media was found to increase hercynine synthesis. Ergothioneine and Hercynine were both detected in the buffer fluid in which resting preparations of *M. smegmatis* were incubated, which may indicate that these compounds are being exported from the cells (Genghof and van Damme, 1968).

Despite the fact that the biosynthetic pathway of ergothioneine was elucidated in mycobacteria in the 1960s (Figure 1.3) and that the complete genome of *M. tuberculosis* $H_{37}Rv$ was sequenced in 1998 (Cole *et al.,* 1998), the genes involved have never been identified. The bottleneck in validating ergothioneine biosynthetic enzymes as potential drug targets is therefore in the identification of the genes. Performing an annotation keyword search of the *M. tuberculosis* $H_{37}Rv$ genome using the TIGR database (http://cmr.tigr.org/) reveals no matches to the terms "sulphoxide", "sulphoxide synthase" or "sulphoxide lyase". A search for the terms "methyltransferase" and "methylase" provides a total of 70 matches, 8 of which are putative or probable. The available annotations for the *M. tuberculosis* $H_{37}Rv$ genome therefore provides no indication of the genes involved in ergothioneine biosynthesis.

In the case of mycothiol, the first biosynthetic enzyme was identified by the generation of chemical mutants, which were screened for reduced mycothiol production using immunoblotting (Newton *et al.,* 1999). The resultant Isoniazid-resistant phenotype of mycothiol-deficient mutants subsequently facilitated the screening for other mutants. Given that no simple technique exists for the detection of ergothioneine-deficient mutants, this is not a feasible approach. The identification of these genes therefore requires the purification of their respective enzymes. The approach taken by this study was to purify the first enzyme in the biosynthesis of ergothioneine, which is an S-adenosyl-L-methionine dependent methyltransferase.

PART A:

The Attempted Isolation of α-*N*,*N*,*N*-Histidine Methyltransferase, the First Enzyme in Ergothioneine Biosynthesis.

CHAPTER 2: INTRODUCTION

The identification of the gene of a therapeutically important enzyme facilitates the investigation of its expression and regulation, kinetic properties and cellular function. Sequence information may provide structural information about the protein, which in turn would facilitate the synthesis of inhibitors. The identification of the genes of the ergothioneine biosynthetic enzymes is therefore a critical step in validating them as a potential drug targets. The approach of this study was to purify the α-*N,N,N*-histidine methyltransferase, which is the first enzyme in ergothioneine biosynthesis. Since the methylation reaction catalyzed by this enzyme utilizes S-adenosyl-L-methionine as the methyl donor, it is classified as an S-adenosyl-L-methionine dependant methyltransferase.

2.1. S-Adenosyl-L-methionine Dependent Methyltranferases

Methyltransferases (MTases) are enzymes which catalyze the transfer of a methyl group from a cofactor to the nitrogen, oxygen, sulfur or carbon atom of a substrate molecule. S-adenosyl-L-methionine (SAM) is the most commonly used methyl donor utilized by MTases. These SAM-dependent methyltransferases (MTases) can be divided into four major substrate classes, namely DNA, RNA, proteins and small molecules. Three structurally defined classes of SAM-dependent MTases have been identified.

2.1.1. Class I

Class I MTases, which is the major class, share a common core structure referred to as an "SAM-dependent MTase fold". This core structure contains a mixed seven-stranded β-sheet, in which strand seven is anti-parallel to the other six strands. In most cases, strand 7 is inserted into the sheet between strands 5 and 6 (6↓ 7↑ 5↓ 4↓ 1↓ 2↓ 3↓), which may have functional significance. Generally, strands 1-3 interact with SAM, while strands 4-7 bind the substrates methylated by these enzymes (Cheng & Roberts 2001).

The highly conserved structure of Class I MTases is not reflective of a high degree of sequence similarity among the structurally characterized enzymes. Sequence similarities between methyltransferases were first identified in enzymes which modify DNA (Posfai *et al.* 1989). Analysis of cytosine-specific DNA methyltransferases from 11 prokaryotes and one eukaryote revealed highly conserved "core" sequences and "variable" regions (Lauster *et al.* 1989).

A

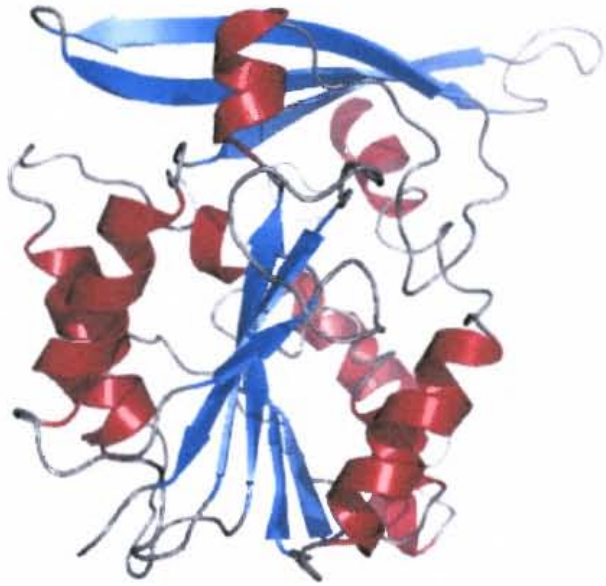

B

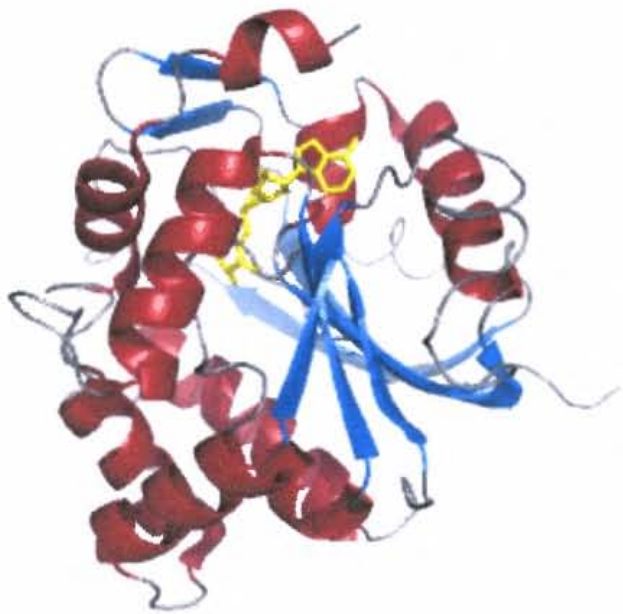

Figure 2.1: Examples of small molecule Class 1 MTases showing the SAM-dependent MTase fold. **A:** Glycine N-methyltransferase. **B:** Phenylethanolamine N-methyltransferase complexed with S-adenosylhomocysteine.

Subsequent sequence comparison of DNA, RNA, protein and small molecule methyltransferases revealed sequence similarities in three short sequences, designated regions I, II and III (Ingrosso *et al.* 1989, Wu *et al.* 1992). Regions II and III are present in most non-DNA MTases (Kagan & Clarke 1994). The similar position of these sequences in a diverse group of MTases, along with their presence in other enzymes which bind SAM or S-adenosylhomocysteine, suggested a role in SAM binding (Ingrosso *et al.* 1989). Structurally guided sequence alignments revealed that motifs I and II are involved in cofactor binding, while motif III plays a structural role. The analysis also revealed that the residues that interact with the cofactor are located in four motifs, I-IV (Velkov & Lawen 2003).

Motif I is characterized by a glycine rich stretch with the consensus sequence of GXGXG in non-nucleic acid MTases (Kagan & Clarke 1994). The conserved glycine residues in this region form hydrogen bonds with the carboxyl and amino groups of SAM. A high degree of heterogeneity exists in Motif II, which is characterized by an acidic residue followed by a hydrophobic or aliphatic residue. The conserved acidic residue forms hydrogen bonds with the hydroxyls of the adenine ribose in most structurally characterized SAM-dependent MTases, while the hydrophobic residue stabilizes the adenine ring by van der Waals packing (Velkov & Lawen 2003). In Motif III the central glycine residues are highly conserved (Kagan & Clarke 1994) and are involved in hydrogen bonding with the adenine ring of SAM. The consensus sequences have been expanded with time through manual inspection of known MTases, and designated Motif I, Post I, Motif II and Motif III (Katz *et. al.* 2003).

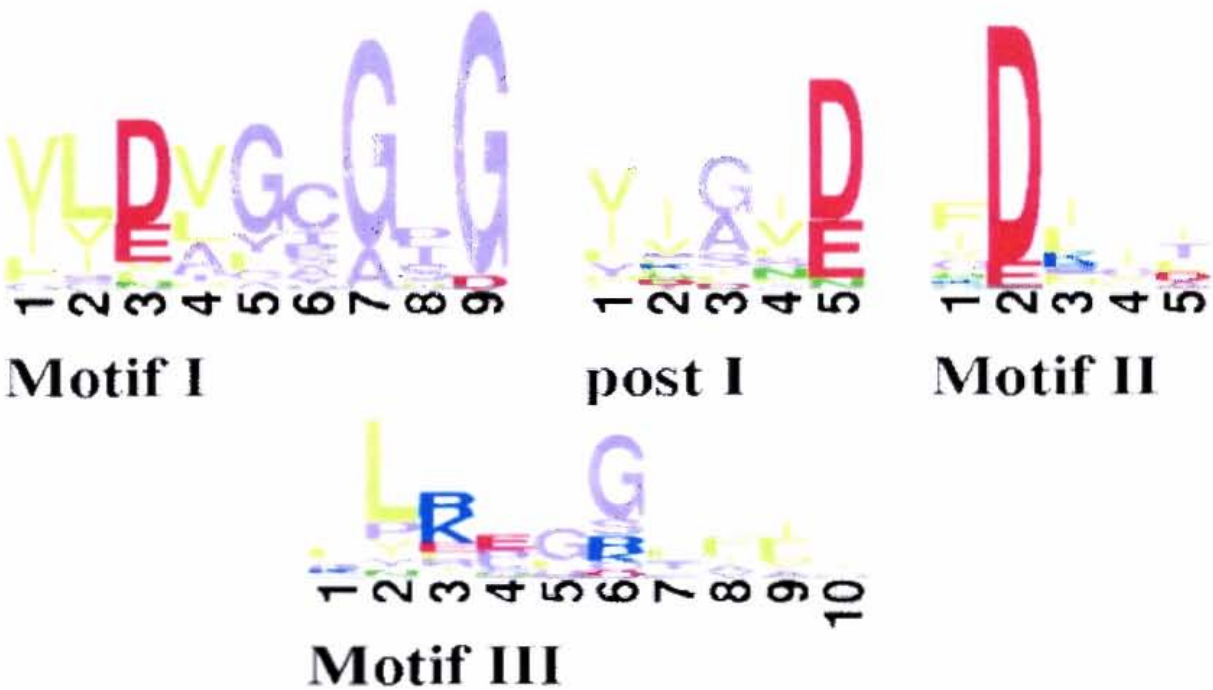

Figure 2.2: Graphical representation of the consensus sequence for each motif determined from 18 experimentally characterized yeast methyltransferases. The size of the letter is relative to the frequency at which it occurred at a particular position. (From Katz *et al.* 2003)

2.1.2. Class II

Class II SAM-dependent MTases are characterized by the SET (Su (var). Enhancer of zeste, Trithorax) domain proteins. The SET domain is rich in β-conformation consisting of several small sheets, which contain a few short strands. The structurally conserved core of the SET domain is made up of two discontinuous parts of the primary sequence, which are separated by a highly variable region. In the three structurally characterized SET domain proteins, the C-terminal region of the SET domain passed under a loop formed by the preceding sequence (Figure 2.3). These two regions have the most highly conserved sequence motifs in the SET domain protein family, and site directed mutagenesis revealed their importance in binding and catalysis (Yeates 2002)

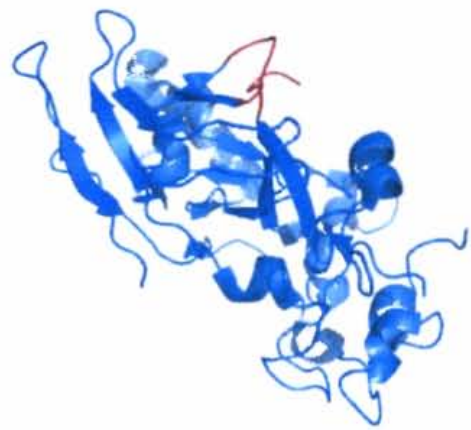

Figure 2.3: The SET domain protein DIM-5 from *Neurospora*.
The most highly conserved region is indicated in red.

2.1.3. Class III

Ste14p from *Saccharomyces cerevisiae* was the first member identified in the isoprenylcysteine carboxyl methyltransferase (ICTM) family, which characterizes the Class III MTases. Topological analysis revealed that Ste14p contains six membrane spans. Mutation studies of Ste14p identified six amino acid residues important for activity, five of which are conserved in other ICMT homologues. Sequence alignments and database searches revealed homology between members of the ICMT family in the C-terminal region. A consensus sequence (RHPxY-hyd-EE), which consists of two regions of homology flanking a hydrophobic stretch (hyd) of amino acids, was identified in this region. This sequence was also identified in two yeast phospholipid methyltransferases, ergosterol biosynthesis enzymes and a series of bacterial open reading frames of unknown function (Romano & Michaelis 2001).

2.2. The Challenge of the "Post-genomic" Era

The generation complete genome sequences for numerous organisms has forever changed the face of the biological sciences. The challenge now facing scientists in the "post-genomic" era is the analysis of genome-data to assign functions to genes and proteins and ultimately to understand the organism as a whole. Although the available genomic data has not facilitated the identification of the ergothioneine biosynthetic enzymes, the best approach to identify these enzymes would be one which incorporates sequence, structural and experimental data. In order to correctly interpret genomic data, an understanding of how it was generated and the errors associated with it is required.

2.2.1. Genome Annotation

Genome annotation has become an automated process which consists of a number of steps. The first step involves the prediction of proteins or functional RNA products from the genome sequence. This process is considerably more complicated for eukaryotic organisms due to the low coding density and the presence of introns (Bork *et. al.*, 1998).

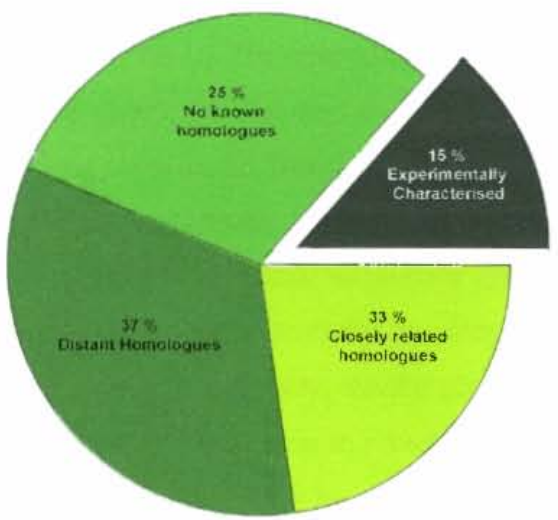

Figure 2.4: Distribution of known sequences. Only 15% of known sequences have been characterized experimentally. Of the remaining sequences, approximately 25 % have no known homologues in this group (Modified from Ofran *et. al.* 2005).

The identified genes are then compared to existing annotated databases to identify similar sequences. If similar sequences are found, their annotation is transferred to the new sequence. This process is called homology-based transfer, and although it is a powerful method it has limitations. Of the known protein sequences, only 15 % have annotations which have been functionally characterized experimentally (Ofran *et. al.*, 2005). Of the remaining 85 % of proteins, 33 % have close homologues in the annotated group, while 37 % have only distant homologues. The remaining ~25 % of proteins have no known homologues, and therefore annotation has to be done by other methods (Figure 2.4). When proteins do not share overall sequence homology, the presence of functionally significant residues can be used in predicting function. Several databases exist to detect such motifs or patterns, including PROSITE and PFAM. The PROSITE database

contains manually selected motifs which have been generated from multiple sequence alignments of homologous proteins (Sigrist *et. al.*, 2002). These motifs are described as either patterns or profiles and can be used to identify domains and new members of a protein family. PFAM is a manually curated database which contains protein families which were generated by multiple sequence alignments and translated into hidden Markov models (Bateman *et. al.*, 2002). Although PFAM is not as well annotated as PROSITE, each entry is linked to other databases and literature resources. The annotation process can also add information such as chemical and structural properties, which are determined directly from the predicted gene or derived from similarity searches with other genes (Stothard & Wishart, 2006).

The final step of the annotation process is to organize the information in a meaningful and accessible way. The degree to which genome annotation is automated varies between systems (Stothard & Wishart, 2006). In some cases the process is completely automated (BASys: http://wishart.biology.ualberta.ca/basys/), while in other systems human curators deal with problematic cases (HAMAP: http://ca.expasy.org/sprot/hamap/) or do manual revisions to the automatic annotations (PUMA2: http://compbio.mcs.anl.gov/puma2/).

Although widely used, annotation of genes by homology-based transfer can be problematic for two reasons. (i) The annotation in the database may be incomplete or incorrect. Devos & Valencia (2001) predict that as many as one third of specific annotations, such as those predicting enzymatic function, could be wrong. These errors are then perpetuated in subsequent annotations. (ii) The relationship between sequence and function is not always clear-cut. Although similar sequences generally produce similar structures (Clothia & Lesk, 1986), this does not necessarily translate to function (Reviewed in Ponting, 2001; Whisstock & Lesk, 2003). Conversely, similar structures can be generated from sequences which have no similarity, as is the case in proteins which form TIM barrels (Nagano *et. al.*, 2002). It has also been found that many biochemical reactions can be catalysed by enzymes which have no sequence and/or structural similarities (Galperin *et. al.*, 1998).

When homology-based transfer is not possible due to the absence of an experimentally annotated homologue, *de novo* prediction of functional features is required. This includes the prediction of sub-cellular localisation, post-translational modifications, protein-protein interactions and the identification of possible ligand binding sites or functional residues (Reviewed in Ofran *et. al.*, 2005). Although these methods are associated with a high degree of error, they are sufficiently accurate to guide future experimental work. The availability of several complete genome sequences can provide additional information for elucidating

protein function (Reviewed in Bork *et. al.,* 1998). For example the local context of a gene may indicate its connection to a specific pathway, as is often the case with genes in a bacterial operon.

The challenge of correctly annotating the numerous genome sequences available and continuously being generated remains a daunting task. However, improvements to annotation methods, the availability of more complete databases and increasing experimental knowledge will lead to better annotations as time progresses.

2.2.2. Identification of Putative MTases using Sequence and Structural Information

Although methyltransferases share very low overall sequence homology, the conserved motifs present in the Class I MTases have been used to identify putative MTases. These motifs were first used to scan an entire genome for putative MTases in the organism *S. cerevisiae* in 1999. This resulted in the identification of 33 candidate genes, seven of which were known methyltransferases. Four of the identified genes were previously characterized to not be associated with methylation and constitute false positives. Mutant studies on one of the identified genes revealed that it catalyzes the methylation of arginine (Niewmierzycha & Clarke 1999).

Katz *et al.* developed a semi-automated method for identifying putative methyltransferases and ranking them according to the likelihood of this assignment being correct. This involved the use of a training set of known MTases to generate log-odds matrices of amino acids and their positions in the consensus motifs. The log-odds matrices are used to estimate the rate at which each residue can change to each possible residue over time. This allows each residue in the consensus motifs to be scored and different proteins to be ranked according to their overall score. The matrices were then used to scan the genome of *S. cerevisiae* and the candidates were then evaluated as either being a known MTase, a putative MTase or a false positive. Candidate MTases were identified in yeast and other organisms and results suggested that this methodology was an improvement on those previously used.

The high degree of structural conservation in the MTase fold in Class I MTases has also been used in the identification MTases. The identification of a MTase fold in the crystal structure of the fibrillarin homologue in *Micricoccus jannaschii* revealed its function in rRNA methylation (Wang *et. al.* 2000). The MTase fold has also been identified in other structurally characterized proteins (Cheng & Roberts 2001). Although sequence and structural homology provide clues about the function of unidentified genes, the risk of incorrect assignment still exists. Furthermore, the determination of the methyl accepting substrates and the elucidation

of their role in metabolism require biochemical studies. Hence the identification and characterization of methyltransferases requires a multidisciplinary approach.

2.3. Aims:

The fungi, *Neurospora crassa* (*N. crassa*), was selected as a source for the α-N, N, N-histidine methyltransferase enzyme for two reasons. Firstly, Ishikawa & Melville (1970) had reported a purification strategy for the purification of α-N, N, N-histidine methyltransferase from *N. crassa*. Secondly, preliminary work revealed that the activity of the enzyme was much lower in crude extracts from *M. smegmatis* than the fungi *N. crassa*. The aim was therefore to purify and identify the enzyme in *N. crassa*, which would facilitate the identification of the equivalent enzyme in mycobacteria.

CHAPTER 3: MATERIALS & METHODS

3.1. Materials

Chemical/Reagent:	**Supplier:** (see Appendix C for details)
NH_4Cl	Merck
NH_4OH	Riedel-de Haën
NH_4HCO_3	Saarchem
NH_4NO_3	Riedel-de Haën
NH_4 tartrate	Sigma
H_3BO_3	Merck
$CaCl_2$	BDH
$CoSO_4$	BDH
$FeCl_3$	BDH
$NiSO_4$	Sigma
NaCl	Fluka
NaH_2PO4	BDH
Na_2HPO_4	BDH
CH_3COONa	Merck
$NaHCO_3$	BDH
$Na_2S_2O_3$	Fluka
NaOH	Fluka
KH_2PO4	Merck
K_2HPO_4	Fluka
$MnCl_2.4H_2O$	BDH
$MgSO_4.7H_2O$	Merck
$Na_2MoO_4.2H_2O$	BDH
$AgNO_3$	Merck
$ZnSO_4$	BDH
2-mercaptoethanol	Merck
Acetic acid	Merck
Acrylamide	Sigma
s-adenosylmethioneine	Fluka
s-adenosylhomocysteine	Fluka
Ammonium persulphate	Merk
Ammonium sulphate	Riedel-de Haën
Bacto Agar	Oxoid
Bis-acrylamide	Fluka
Protein assay reagent	BioRAD
Biotin	Sigma
Bovine serum abumin	Roche
Casein hydrolysed	Merck
CHAPS	Sigma
Coomasie Briliant Blue R250	Merck
Dimethylhistidine	Pharmatech International
DTT	Fermentas
1-ethyl-3-(3-dimethylaminopropyl)-carbodiamide	Fluka
Ethanolamine	BDH

Formaldehyde	BDH
Formic acid	Riedel-de Haën
Glycerol	Sigma
glycine	BDH
HCl	BDH
HEPES	Fluka
Imidazole	Fluka
Insulin	Sigma
Iodoacetamide	Sigma
Malt extract	Merck
MES	Research Organics Inc.
N-hydroxysuccinimide	Fluka
PMSF	Boeringer Ingelheim
Proteomics grade trypsin	Sigma
Ready Flow III Scintillation fluid	Beckman Coulter
Sucrose	Fluka
SDS	BDH
TEMED	BDH
Tris	Merck
TPCK	Sigma
TLCK	Sigma
Urea	BDH
Yeast extract	Fluka
Dialysis tubing	Sigma
Glass beads (0.4-0.6mm)	Biospec

Solvents:

Acetone	KIMIX
Ethanol	Sigma
Methanol	Fluka
Acetonitrile (HPLC grade)	Sigma
TFA (HPLC grade)	Sigma

Chromatography Resins:

ω-aminopentyl agarose	Sigma
activated CH-sepharose 4B	Sigma
CM-Sephadex	Whatman
DEAE Cellulose DE-52	Whatman
Dye ligand Kit	Sigma
Hydroxyappatite	BioRAD
Iminodiacetic acid agarose	Sigma
Strata Screen-C Cartridge	Phenomenex
Strata scx Cartridge	Phenomenex
Oasis mcx Cartridge	Waters

HPLC columns:

Luna 5μ C_{18} (200 x 4.6 mm)	Phenomenex
PolyHYDROXYETHYL aspartamide (200 x 4.6 mm, 5μm)	The Nest Group
Vydac 301VHP575	Vydac

Radio-chemicals:

S-[methyl-^{3}H]-Adenosyl-L-methionine,	Perkin Elmer

3.2. Methods

3.2.1. Enzyme Assay with S-[methyl-^{3}H]-Adenosyl-L-methionine

The assays were performed as previously described (Reinhold *et al.*, 1970, Ishikawa and Melville, 1970), with modifications. The enzyme assay was modified by replacing histidine with dimethylhistidine, and utilising S-[methyl-^{3}H]-adenosyl-L-methionine to monitor the reaction. The reaction mixtures contained 5 nmoles of dimethylhistidine, 12 nmoles of S-adenosylmethionine, 0.08μCi of S-[methyl-^{3}H]-adenosyl-L-methionine, 50μl of enzyme solution, 50μmoles of NH_4Cl buffer, pH8.5 and water made up to a final volume of 100μl. The assay was initiated by the addition of the enzyme solution and incubated at 25^{0}C for 30 or 60min. For control reactions, dimethylhistidine was omitted. Enzyme assays were stopped by adding 10μl of 1M HCl and stored at 4^{0}C prior to analysis either by HPLC or mini-columns.

3.2.2. HPLC Analysis

Three volumes of acetonitrile were added to the acidified assay mixtures and the precipitated protein removed by centrifugation at 16 100g for 1min. The components of the enzyme assays were separated using a Polyhydroxyethyl Aspartamide column (200x4.6mm, 5μm, 100A) under HILIC conditions. After injection of 100μl of the sample, the initial conditions of 60% (CH_3CN), 40% B (5mM ammonium formate, pH 3.0) were maintained for 5 min. The column was then eluted with a linear gradient to 60%B over 25min, maintained at 60%B for 5 min and then returned to initial conditions in 5 min. The flow-rate was 1ml.min^{-1} and the radioactivity was detected using a β-ram flow-thru scintillation counter (Insus Systems Inc.) with the counting window set between 0 and 18.6 keV. A standard curve was constructed which related the radioactivity peak area to the total product present (Appendix A).

3.2.3. Mini-column Analysis

Oasis MCX cartridges were conditioned with 2ml of Methanol and equilibrated with 2ml of 0.1M HCl. The acidified assay mixtures were centrifuged at 16 100g for 1min to remove precipitated protein. Thirty microlitres of the sample was applied to the

equilibrated column and washed with 3ml of 0.1M HCl. The product was eluted with 5ml of 20mM imidazole-acetate buffer (pH 6.05) and 1ml fractions were collected. Three millilitres of scintillation fluid to each fraction and was counted using a liquid scintillation counter (Packard) with the counting window set between 0 and 18.6 keV. The column was then washed with 3ml of 10% NH_4OH in Methanol to remove the SAM. A standard curve was constructed which related the cpm of the fractions to the total product present (Appendix A).

3.2.4. Growth of *Neurospora crassa*

N. crassa was maintained as spore suspensions in 20% sterile glycerol stored at -80°C. The spore suspensions were used to inoculate complete medium agar plates which were incubated at 28°C in the dark. After three days, the plates were flooded with sterile growth medium and the spores scraped to form a spore suspension. One millilitre of the spore suspension was used to inoculate 200ml of Fries liquid medium (Appendix A), which was incubated at 28°C with shaking (150rpm) for 48hrs. Mycelial pellets were harvested by filtration, washed with cold water and stored at -80°C.

3.2.5. Preparation of Ammonium Sulphate Fraction from *N. crassa*

The required amount of frozen mycelia was ground in a blender and divided into 80g portions. Each portion was placed in a bead-beater (Biospec products, Inc.) chamber half-filled with cold glass beads (0.5mm). The chamber was then filled with approximately 200ml of 50mM Tris-Cl buffer (pH 8.5) containing 35µM of TPCK and TLCK, 0.5mM PMSF and 1mM DTT and placed in the ice-bath jacket. The mycelia were disrupted for three one minute intervals, separated by a minute to allow cooling of the chamber. The disruption of 20g or less of mycelium was done manually using a pestle and mortar in the presence of glass beads and a minimum volume of buffer. The resulting enzyme extracts were clarified at 60 000g for 30min. The clarified supernatant was adjusted to 60% saturation with solid ammonium sulphate and kept at 4°C for 30min. The extract was centrifuged at 27 216g for 10min and the precipitate re-suspended and dialysed against the appropriate buffer to remove residual ammonium sulphate. All dialysis and subsequent purification steps were performed at 4°C unless otherwise stated.

3.2.6. Small-scale Purification of Histidine Methyltransferase using Ion Exchange Chromatography

An ammonium sulphate fraction was prepared as previously described from approximately 100g of mycelium, and dialysed against 0.1M NH_4Cl buffer, pH8.5, 1mM DTT overnight. After dialysis the extract was loaded onto a DEAE cellulose DE52 ion exchange column, which had been equilibrated with 0.1M NH_4Cl buffer,

pH8.5, 1mM DTT. Unbound protein was removed by washing and the enzyme was eluted with a linear NaCl gradient from 0 to 0.25M in a volume of 400ml. The fractions were assayed as previously described and those containing activity were pooled and precipitated by addition of ammonium sulphate to a saturation of 80%. The precipitated protein was re-suspended in 2ml of 0.1M NH_4Cl buffer, pH8.5, 1mM DTT and dialysed overnight against the same buffer. After dialysis, 100µl of the extract was loaded onto a Vydac 301VHP575 column which had been equilibrated with 0.1M NH_4Cl buffer, pH8.5. The enzyme was eluted with a linear gradient of 0-0.25M NaCl over 30min, at a flow rate of $1ml.min^{-1}$. One millilitre fractions were collected, and DTT and glycerol were added to a final concentration of 1mM and 10% respectively. HPLC was performed at room temperature and fractions were placed on ice after collection. Fractions were assayed for enzyme activity as previously described.

3.2.7. Size Exclusion Chromatography

The size exclusion resins Sephacryl S200, S300 and S400 were investigated for their ability to separate the standards Blue Dextran (2 000 000 Da) and Acyl CoA dehydrogenase (172 000 Da). Column lengths of between 25 cm and 50 cm were investigated and the standards were applied in less than 3% of the column volume. The standards were detected in the eluting fractions by determining their absorbance spectra using an Ocean Optics diode array spectrophotometer.

3.2.8. Cation Exchange Chromatography

Approximately 80g of mycelium was used to prepare an ammonium sulphate fraction as previously described. The fraction was dialysed overnight against 5mM sodium phosphate buffer, 1mM DTT, pH 6.4 and loaded onto a CM-Sephadex column (21cm, 1.5cm) equilibrated with the same buffer. The column was washed with 80ml of 10mM Tris-Cl pH7.5 and then eluted with a linear gradient from 5 to 50mM sodium phosphate in a volume of 200ml. Fractions containing protein as determined by their absorbance at 280nm were assayed for activity.

3.2.9. pH Precipitation

An ammonium sulphate fraction containing approximately 100mg of protein was dialysed overnight against 100mM NH_4Cl, 1mM DTT, pH8.5. The pH of the extract was reduced to 6.0 with acetic acid and then incubated at 4°C while stirring for 30min. Insoluble material was removed by centrifugation at 30 000g for 10min. The pH of the extract was then raised to 8.5 using NH_4OH, and the change in protein concentration and enzyme activity determined.

3.2.10. Hydroxyapatite

The supernatant from the pH precipitation was dialysed overnight against 25mM HEPES, 1mM DTT, pH8.0 and applied to a hydroxyapatite column (14cm, 2.2cm) which had been equilibrated with the same buffer. The column was washed with approximately 200ml of 25mM HEPES, 1mM DTT, pH8.0. A linear gradient from 25mM HEPES pH 8.0 to 300mM potassium phosphate in 100mM HEPES pH7.0 over 400ml was used to elute the column.

3.2.11. Immobilised Metal Ion Affinity Chromatography (IMAC)

Iminodiacetic acid (IDA) agarose was prepared and loaded with either nickel, zinc or cobalt ions. Excess ions were removed by washing the resin with water and equilibrating with 5 volumes of 25mM HEPES pH 8.0, 0.5M NaCl. An ammonium sulphate fraction which had been dialysed against 25mM HEPES pH 8.0, 0.5M NaCl overnight was loaded onto the columns and unbound material eluted. Bound proteins were then eluted with a linear gradient of 0-20mM Imidazole in 25mM HEPES pH 8.0, 0.5M NaCl in a volume of 200ml. Eluted fractions were assayed for methyltransferase activity.

3.2.12. Small-scale Purification of Histidine Methyltransferase using Ion Exchange Chromatography and IMAC

An ammonium sulphate fraction from 90g of mycelium was prepared as previously described and loaded onto a DE52 ion exchange column (17.5cm, 2.5cm), which had been equilibrated with 0.1M NH_4Cl buffer, pH8.5, 1mM DTT. The column was washed with approximately 300ml of 0.1M NH_4Cl buffer, pH8.5, 1mM DTT to remove unbound proteins. The enzyme was eluted with a linear gradient of 0 to 0.25M NaCl in a volume of 400ml at a flow rate of $1ml.min^{-1}$. The fractions were assayed as previously described and those containing activity were pooled and concentrated by ultrafiltration. The concentrated sample was dialysed overnight against Buffer B (50mM HEPES, 0.5M NaCl, 1mM imidazole, pH 8.0). The dialysed extract was applied to an IDA-agarose column (9.5cm, 1.5cm) loaded with zinc ions and equilibrated with buffer B. The column was washed with approximately 120ml of buffer B and then eluted with a linear gradient of 0-20mM imidazole in buffer B in a volume of 200ml at a flow-rate of $0.5ml.min^{-1}$. Fractions containing methyltransferase activity were pooled and precipitated with 80% ammonium sulphate. Precipitated protein was re-suspended in 1ml of 0.1M NH_4Cl buffer, pH8.5 and dialysed overnight against the same buffer. After dialysis, the extract was loaded onto a Vydac 301VHP575 column which had been equilibrated with 0.1M NH_4Cl buffer (pH8.5), 10% glycerol. The enzyme was eluted with a linear gradient of 0-0.25M NaCl over 30min, at a flow rate of $1ml.min^{-1}$. One millilitre fractions were collected, and DTT was added to a final concentration of 1mM.

Fractions were assayed for enzyme activity as previously described. Trichloroacetic acid precipitation (see appendix) was used to concentrate 600 µl of the samples for SDS-PAGE analysis.

3.2.13. Chromatofocusing

The active fractions from a zinc IMAC column were concentrated by ultrafiltration using a PM10 membrane and dialysed overnight against 25mM MOPS, pH 7.0. The dialysed extract was applied to a Polyexchanger 94 column (23.5cm, 1cm), which had been equilibrated with 25mM MOPS pH 7.0. The column was eluted with Polybuffer 74 which had been diluted 1 in 9 and adjusted to pH 4. The fractions eluting from the column were adjusted to a pH between 8 and 9 with NH_4OH and DTT was added to a final concentration of 1mM.

3.2.14. Dimethylhistidine Affinity Chromatography

Dimethylhistidine (DMH) was coupled to ω-aminopentyl agarose in the presence of 1-ethyl-3-(3-dimethylaminopropyl)-carbodiamide (EDC) and *N*-Hydroxysuccinimide (NHS) (Sehgal & Vijay 1994). Approximately 5ml of ω-aminopentyl agarose was washed with water and 25mM MES pH6.55. A six-fold excess of DMH was dissolved in the MES buffer containing 1mole EDC and 15moles NHS and mixed with the resin in a final volume of 10ml. The mixture was incubated at room temperature for 16hrs with gentle agitation. Uncoupled DMH was removed by washing the resin with three cycles of 0.1M sodium acetate, 0.5M NaCl pH4 and 0.1M Tris-Cl, 0.5M NaCl, pH 8.0. Samples of the reaction were taken at the start and end of the incubation to determine the efficiency of coupling.

Analysis of coupling efficiency was performed by HPLC using a polyHYDROXYETHYL Aspartimide column (200x4.6mm, 5µm, 100A). An aliquot of the coupling reaction was centrifuged and 50µl of the supernatant was injected. The initial conditions of 60% A (CH_3CN) 40% B (5mM ammonium formate pH 3.6) were maintained for 10min. The column was then eluted with a linear gradient to 40% A over 20min, maintained at 40% for 5min and then returned to 60% A in 5min. DMH was monitored at 220nm and the change in the peak area was used to determine the coupling efficiency

An ammonium sulphate fraction containing 9.5mg of protein was prepared as previously described and dialysed against 50mM NH_4Cl, 1mM DTT, pH 8.5 (buffer A) overnight. The prepared resin was re-suspended, packed and equilibrated with 50mM NH_4Cl, 1mM DTT, pH 8.5. and the extract applied. The column was washed with buffer A to remove unbound material and eluted stepwise with 100mM, 500mM NaCl and 50mM histidine, 500mM NaCl in buffer A.

3.2.15. S-Adenosylhomocysteine Affinity Chromatography

3.2.15.1. Coupling at α-amino

S-Adenosylhomocysteine was coupled to activated CH-Sepharose 4B according to the manufacture's instructions. Approximately 1ml of resin was re-suspended and washed with 100ml of 1mM HCl on a sintered glass filter. The resin was then washed with water and re-suspended in 0.1M $NaHCO_3$ pH 9.0. A five-fold excess of ligand was dissolved in 200 µl of 1mM HCl and then mixed with the resin in a final volume of 2ml. The reaction was allowed to proceed at room temperature overnight with gentle agitation. Samples of the supernatant of the coupling reaction were taken at the start and end of the reaction to determine the coupling efficiency. Excess ligand was removed by washing with 5 volumes of coupling buffer. The resin was incubated with 1M ethanolamine pH8.0 for 1hr to block any unreacted groups. The coupled resin was washed with three cycles of 0.1M sodium acetate, 0.5M NaCl pH4 and 0.1M Tris-Cl, 0.5M NaCl, pH 8.0.

Analysis of coupling efficiency was performed by HPLC using a Luna 5µ C_{18} column (250x4.6mm). The coupling reaction samples were diluted 10 fold and ten microlitres injected. The initial conditions of 95% A (CH_3CN) 5% B (0.1% TFA) were maintained for 5min. The column was then eluted with a linear gradient to 10% A over 30min, maintained at 10%A for 5min and then returned to 95% A in 5min. S-Adenosylhomocysteine was monitored at 260nm and the change in the peak area was used to determine the coupling efficiency.

An ammonium sulphate fraction was prepared as previously described and dialysed against 100mM phosphate buffer pH 8.0 (buffer C) overnight. The prepared resin was equilibrated with buffer C and approximately 12mg of protein loaded. The column was washed with buffer C to remove unbound material and eluted stepwise with 100mM, 500mM NaCl in buffer C.

3.2.15.2. Coupling at N_6 position

The coupling of S-adenosylhomocysteine to activated CH-Sepharose 4B was modified by using 50mM sodium phosphate buffer pH 6.0 as the coupling buffer. Analysis of coupling efficiency was performed as described above. An ammonium sulphate fraction containing approximately 10mg of protein was prepared as previously described and dialysed against 50mM NH_4Cl, 1mM DTT, pH 8.5 (buffer A) overnight. The prepared resin was equilibrated with 50mM NH_4Cl, 1mM DTT, pH 8.5 and the extract applied. The column was washed with buffer A to remove unbound material and eluted stepwise with 100mM, 500mM NaCl in buffer A containing 10% glycerol.

3.2.16. Dye-ligand Chromatography

The following pre-packed 3ml dye-ligand columns (Sigma) were investigated: Yellow 3, Blue 4, Green 19, Red 120, Blue 72, Brown 10, Cibacron blue, Green 5, Yellow 86. The columns were washed with half a column volume of 6M urea in 0.5M NaOH, followed by several column volumes of 10mM NaCl to remove any leaked dye. Columns were then equilibrated with 10mM Tris-Cl pH7.5. An ammonium sulphate fraction from 80g of mycelium was prepared as previously described and dialysed against 10mM Tris-Cl pH7.5 overnight. The dialysed extract was diluted to a total volume of 20ml, of which 2ml was applied to each column. Unbound protein was removed by washing with 10mM Tris-Cl pH7.5, and the columns were then eluted step-wise with 10mM Tris-Cl, 0.5M NaCl pH8.5 and 10mM Tris-Cl, 1.0M NaCl pH8.5. Eluted fractions with the highest absorbance at 280nm were assayed for activity.

3.2.17. Large-scale Purification of Histidine Methyltransferase

The *N. crassa* mycelium used for the large-scale purification was purchased from the BioTechnology Institute at the University of Minnesota. Three hundred grams of frozen mycelia was broken into pieces and ground in a blender. Eighty grams of ground mycelia and approximately 200ml of 50mM Tris-Cl buffer (pH 8.5) containing 35μM of TPCK and TLCK, 0.5mM PMSF, 1mM DTT and 1mM EDTA, were placed in a bead-beater chamber and disrupted as previously described. The resulting enzyme extract was clarified at 30 000g for 20min. Streptomycin sulphate to a final concentration of 0.5% w/v was added to the enzyme extract over a period of 30min. The precipitate was removed by centrifugation at 27 216g for 10min. The clarified supernatant was then adjusted to 60% saturation with solid Ammonium sulphate and kept at 4^0C for 30min. The extract was centrifuged at 27 216g for 10min and the precipitate re-suspended in a minimum volume of 0.1M NH_4Cl buffer, pH 8.5, 1mM DTT.

3.2.17.1. DEAE Cellulose Chromatography

The extract was desalted by applying fifty millilitres at a time to a Sephadex G25 column (45cm, 2.2cm), which was eluted with 0.1M NH_4Cl buffer, pH 8.5, 1mM DTT. The active fractions from successive Sephadex columns were pooled and applied to a DEAE cellulose column (15.5cm, 4.4cm) which had been equilibrated with 0.1M NH_4Cl buffer, pH 8.5, 1mM DTT. The column was eluted stepwise with 50, 150 and 500mM NaCl in 0.1M NH_4Cl buffer, pH 8.5 containing 1mM DTT. Protein from the 150mM elution step was precipitated by adding solid ammonium sulphate to a saturation of 80%. The proteins were pelleted by centrifugation at 27 216g for 10min and stored at 4 °C.

3.2.17.2. Zinc IMAC

The pellets from three successive DEAE columns were pooled, resuspended and divided into four aliquots. Each aliquot was dialysed overnight against 50mM HEPES pH8.0, 0.5M NaCl, 1mM imidazole (Buffer B). The dialysed aliquot was clarified at 12 000g for 10min and then applied to an IDA-sepharose column (14.3cm, 2cm) loaded with Zn^{2+} and equilibrated with Buffer B. The unbound protein was removed by washing with Buffer B and the enzyme was then eluted with 20mM imidazole in buffer B. The fractions eluted with 20mM imidazole from the four successive IDA-sepharose columns were pooled. The protein was precipitated by adding solid ammonium sulphate to a saturation of 80%. The precipitated protein was divided in half and pelleted by centrifugation and stored at 4 °C.

3.2.17.3. Chromatofocusing

Half of the precipitated protein from the IDA-sepharose columns was resuspended in 25mM MOPS, pH 7.0 and dialysed overnight against the same buffer. The dialysed extract was applied to a Polyexchanger 94 column (24cm, 1cm), which had been equilibrated with 25mM MOPS pH 7.0. The column was eluted with Polybuffer 74 which had been diluted 1 in 9 and adjusted to pH 4. The fractions eluting from the column were adjusted to a pH between 8 and 9 with NH_4OH and DTT was added to a final concentration of 1mM. The second half of the precipitated protein was processed in the same way.

3.2.17.4. HPLC Ion Exchange Chromatography

The active fractions from the Chromatofocusing column were pooled and concentrated by ultrafiltration through a PM10 membrane, to a volume below 10ml. The concentrated sample was then dialysed against 10mM Tris-Cl pH 8.5 overnight. Six millilitres of the dialysed sample was injected onto a Vydac 301VHP575 column which had been equilibrated with 10mM Tris-Cl, pH 8.5. Unbound protein was removed by washing with 10mM Tris-Cl, pH 8.5 at a flow-rate of 0.5ml.min^{-1}. The column was eluted with a linear gradient of 0-0.25M NaCl in 30min.

3.3. General Methods:

3.3.1. SDS-Polyacrylamide Gel Electrophoresis of Proteins

SDS-polyacrylamide gel electrophoresis was performed on vertical slab gels (Laemmli, 1970). The resolving gel (approximately 11.5cm x 14cm x 0.016cm) consisted of 0.4M Tris-Cl pH 8.8, SDS 0.1% (w/v), acrylamide 12% (w/v), bis-acrylamide 0.33% (w/v), ammonium persulphate 0.03% (w/v) and TEMED 0.002% (v/v). This was overlaid with a stacking gel consisting of 0.12M Tris-Cl pH 6.8, SDS 0.1% (w/v), acrylamide 4.36% (w/v), bis-acrylamide 0.12% (w/v), ammonium persulphate 0.03% (w/v) and TEMED 0.002% (v/v). Protein samples were mixed with $1/10^{th}$ the volume of Sample Treatment Buffer (0.125M Tris-Cl pH 6.8, 4.1% (w/v) SDS, 0.2% (v/v) glycerol, 0.1% (v/v) 2-mercaptoethanol) and heated at 80°C for 5min before loading. A tank buffer consisting of 25mM Tris-Cl, 0.1% SDS, 0.19M glycine was used and gels were electrophoresed at 30mA. The electrophoresis Calibration Kit from Pharmacia and the Fermentas protein Molecular Weight Marker (Appendix B) were used to estimate protein size.

3.3.2. Native Polyacrylamide Gel Electrophoresis

Native PAGE was performed on vertical slab gels in the absence of SDS. The resolving gel (approximately 11.5cm x 14cm x 0.016cm) consisted of 0.4M Tris-Cl pH 8.8, acrylamide 6% (w/v), bis-acrylamide 0.33% (w/v) and riboflavin. This was overlaid with a stacking gel consisting of 0.12M Tris-Cl pH 6.8, SDS 0.1% (w/v), acrylamide 4.36% (w/v), bis-acrylamide 0.12% (w/v) and riboflavin. Protein samples were mixed with $1/10^{th}$ the volume of Sample Treatment Buffer (0.125M Tris-Cl pH 6.8, 0.2% (v/v) glycerol, 0.1% (v/v) 2-mercaptoethanol) and heated at 80°C for 5min before loading. A tank buffer consisting of 25mM Tris-Cl, 0.19M glycine was used and gels were electrophoresed at 30mA. Gels were stained as described above.

3.3.3. Visualisation of Proteins Separated by PAGE

Gels were stained overnight in a solution of 0.45% methanol and 0.18% glacial acetic acid, containing 0.25% Coomasie Brilliant Blue R250. Destaining was performed in a solution containing 20% ethanol and 10% acetic acid. In cases where coomasie staining was not sufficiently sensitive, silver staining was performed on the destained gel.

Table 3.1: Silver Staining Protocol

Solution:	Composition:	Incubation time*:
Fixer soln.	50% methanol, 5% acetic acid	20min
Washing soln.	50% methanol	10min
Water		2hrs/overnight
Sensitizing soln.	1mM $Na_2S_2O_3$	1min
Water		2x1min
Silver solution	0.1% $AgNO_3$	20min @ 4°C
Water		2x1min
Developing soln.	2% Na_2CO_3, 0.04% formalin	5-10min
Stop solution	5% acetic acid	3x1min

*All steps were performed on a shaker

3.3.4. In-gel Tryptic Digest for LC-MSMS

The protocol used was written by David Miyamoto and is based on the method from Shevchenko *et al.*, (1996). Bands were excized from coomasie or silver stained gels, cut into pieces and placed in Eppendorf tubes. Heavily stained bands were destained by vortexing the gel pieces three times (10min each) in 500µl of 6 mM potassium ferricyanide. The gel pieces were then vortexed with 500µl of 100mM NH_4HCO_3 for 10min, to remove residual potassium ferricyanide. After the removal of the NH_4HCO_3, the gel pieces were covered with acetonitrile and allowed to dehydrate at room temperature for 10min. Excess acetonitrile was removed and the gel pieces were dried using a Speed-vac for 10min. Gel pieces were rehydrated with 100mM NH_4HCO_3 containing 10mM DTT and incubated for 1hr at 56°C. After allowing the tubes to cool, the NH_4HCO_3 containing DTT was replaced with an equal volume of 100mM NH_4HCO_3 containing 55mM iodoacetamide. The tubes were incubated in the dark at room temperature for 45min, with occasional vortexing. The iodoacetamide solution was removed, replaced with an equal volume of 100mM NH_4HCO_3 and incubated at room temperature for 20min. Gel pieces were dehydrated by replacing the NH_4HCO_3 solution with acetonitrile and incubating at room temperature for 10min. The NH_4HCO_3 wash and dehydration steps were repeated and the gel pieces then dried in a Speed-vac for 10min.

A solution of proteomics grade trypsin (Sigma) was prepared according to the manufacturer's instructions and diluted with 50mM NH_4HCO_3 to give a final concentration of 10ng.ul^{-1}. The gel pieces were allowed to rehydrate in 100 µl of the

digestion solution for 45min on ice. Excess digestion solution was removed and 100 µl of 50mM NH_4HCO_3 buffer added to each tubes. The digestion mixture was incubated at 37°C overnight and then centrifuged at 16 100g for 1min. The digestion supernatant was removed and place in a PCR tube. One hundred microlitres of extraction solution containing 5% Formic acid and 50% acetonitrile was added to the remaining gel pieces, and incubated at room temperature for 20min. Gel pieces were centrifuged for 1min at 16 100g and the extraction supernatant removed and added to the digestion supernatant. The extraction step was repeated three times and the pooled supernatants were evaporated to dryness using a Speed-vac.

3.4. Bioinformatics Tools:

DNA alignments were performed using the multiple sequence alignment function in DNAMAN v. 4.0 (Lynnon BioSoft). Cartoon structures were generated using PyMOL (DeLano Scientific LCC) from PDB files obtained from www.rcsb.org/**pdb**/ .

3.4.1. MASCOT MS/MS Ion Search

The ion spectra files obtained for various samples were used to perform a MASCOT MS/MS Ion Search (www.matrixscience.com). The search was performed on the NCBIr database, with the taxonomy limited to fungi. The peptide tolerance and the MS/MS tolerance were set to ± 0.5 Da and ± 0.6 Da respectively. One missed cleavage was allowed and a peptide charge of 2^+ and 3^+ were selected.

3.4.2. PEAKS *de novo* and Database Search

PEAKS online was accessed at www.bioinformaticssolutions.com and used to perform a *de novo* and database search. The search parameters were set the same as for the MASCOT search.

4.1. Development of Methylation Assay

The development of a reliable and specific enzyme assay is essential for enzyme purification. The assay developed for the α-N-methylation of histidine, is based on previous work done by Reinhold *et al.*, (1970) and Ishikawa and Melville (1970). In the study by Reinhold *et al.*, (1970), histidine, mono-, di and trimethylhistidine were separated by chromatography on Whatman paper, while Ishikawa and Melville (1970) used Amberlite IRA-410 ion exchange resin to separate hercynine from histidine, mono- and dimethylhistidine. In the present study, the assay volume was reduced from 1ml to 100 µl and HPLC was used to separate S-adenosylmethionine and hercynine. A Polyhydroxyethyl Aspartamide column was investigated for its ability to separate the assay product from S-adenosylmethionine under HILIC conditions (Figure 4.1). Hydrophilic interaction chromatography (HILIC) involves passing a mainly organic, hydrophobic phase over a hydrophilic stationary phase. Solutes elute in increasing order of hydrophilicity as the organic percentage of the mobile phase is reduced. At a low pH the stationary phase has a slight positive charge, which facilitates separation on the basis of both hydrophobicity and charge.

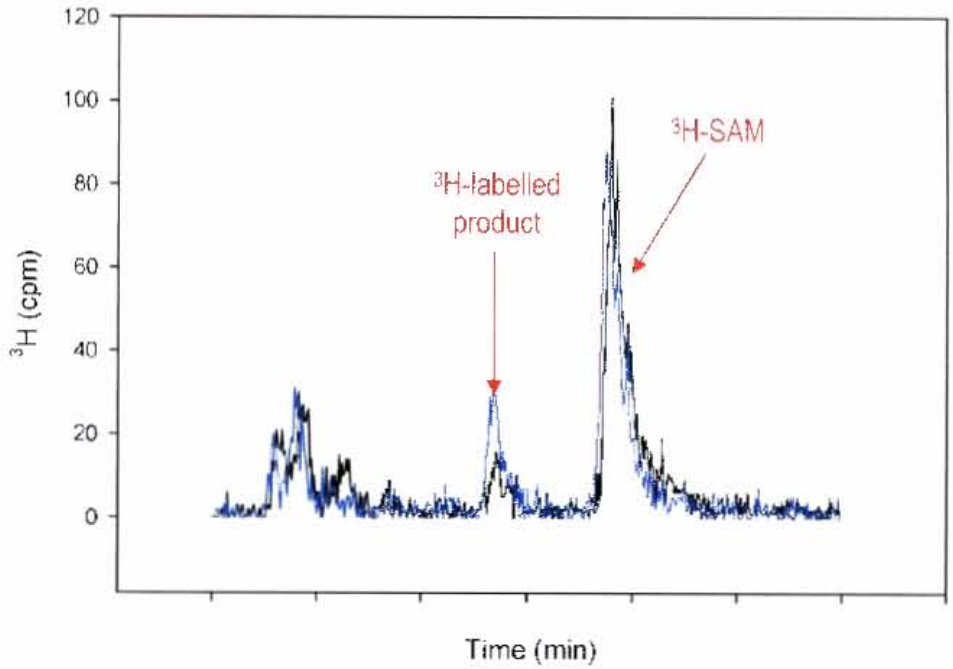

Figure 4.1: Separation of ^{3}H labelled assay components on Polyhydroxyethyl Aspartimide column under HILIC conditions. Black trace shows the utilisation of histidine as a substrate, while blue trace shows utilisation of dimethylhistidine. Radioactivity was detected by means of a β-ram flow-thru counter (Insus Systems Inc.)

Under these conditions the [^{3}H]-labelled methyl donor, S-adenosylmethionine elutes at 19 min, while the radiolabelled products elute at 14min. The product elutes in the same position as the dimethylhistidine and hercynine standards, which co-elute under these conditions. After 30min of incubation, the rate at which hercynine formed from dimethylhistidine (blue) was shown to be faster than the product formation from histidine (black). This is consistent with the findings of Ishikawa and Melville (1970). All subsequent assays were performed utilising dimethylhistidine as a substrate.

While different separation methods for the purification of the methyltransferase were being investigated, the HPLC assay described above was used. During the subsequent large-scale purification, a simpler and less time-consuming assay was required. This led to the development of a mini-column assay which involved the use of pre-packed cartridges.

4.2. Mini-column Assays

Two cation exchange cartridges, namely Strata-scx and Strata-Screen-c and one mixed mode cation/reverse phase exchanger namely the Oasis-mcx cartridge, were evaluated for their ability to separate [^{3}H] S-adenosylmethionine and [^{14}C] Histidine. The columns were conditioned according to the manufacturer's instructions and equilibrated with 0.1M HCl. After applying the radiolabelled standards the columns were washed with 0.1M HCl until the radioactivity returned to background levels. Under these conditions, both SAM and hercynine are positively charged (see Figure 3.1) and bind the cartridges. The columns were then eluted stepwise with 20mM Histidine (acetic acid) pH 6.1, which causes the hercynine to loose its charge and elute from the column. The imidazole in the buffer also competes with the hercynine for binding to the cartridges. Finally, the pH is raised further to elute the SAM from the cartridge using 10% NH4 in Methanol. The ability of the three columns to separate SAM and histidine

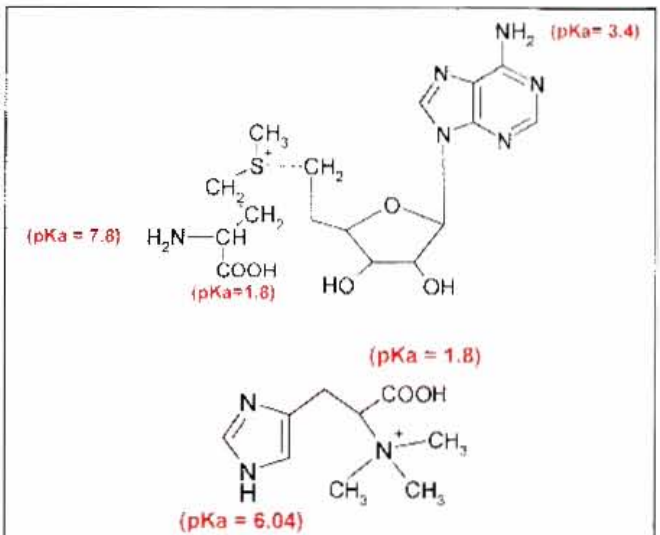

Figure 4.2: pKa values for ionisable groups of S-adenosylmethionine and hercynine

is shown in Figure 4.3. The values were corrected for spill-over from ^{14}C into the ^{3}H window. The Oasis column was found to be most effective, although a small percentage of SAM eluted with the histidine. The reverse phase properties of this cartridge could explain the improved retention of SAM compared to the cation exchangers.

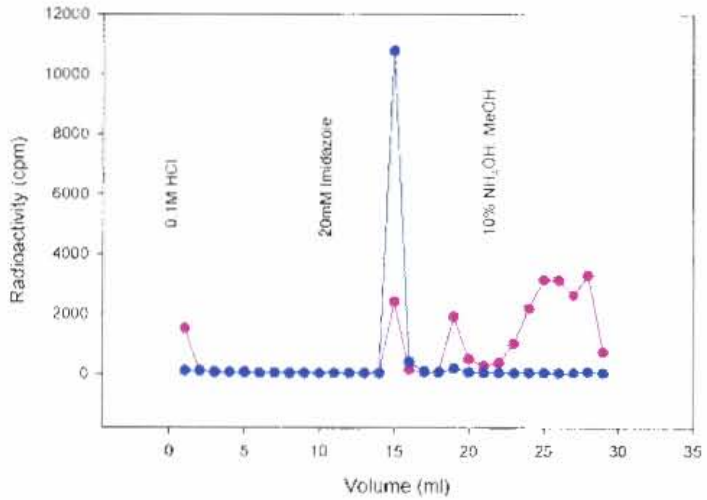

Figure 4.3A: Separation of [^{3}H] S-adenosylmethionine (pink) and [^{14}C] Histidine (blue) on a strata-scx™ column.

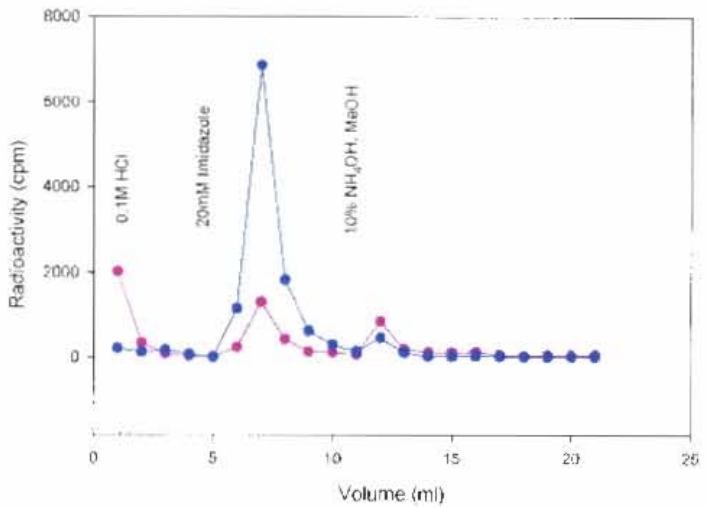

Figure 4.3B: Separation of [^{3}H] S-adenosylmethionine (pink) and [^{14}C] Histidine (blue) on a strata-Screen-c™ column.

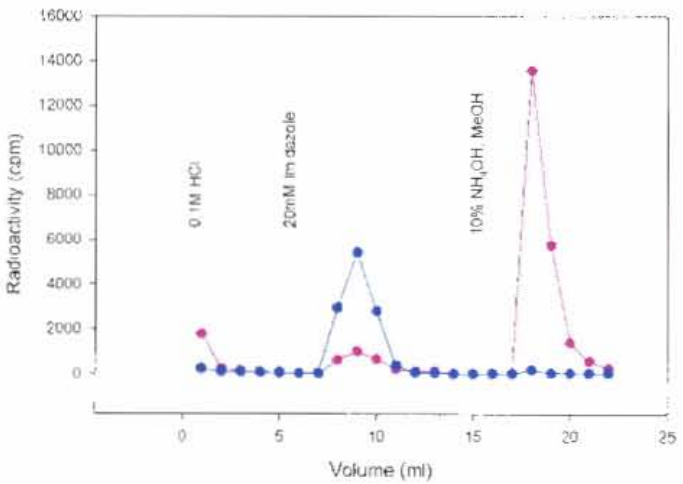

Figure 4.3C: Separation of [^{3}H] S-adenosylmethionine (pink) and ^{14}C Histidine (blue) on an Oasis-mcx™ column.

4.2.1. Evaluation of Oasis Mini-column Assay

In order to validate the oasis mini-column assay, the same reaction mixture was separated using both HPLC and the mini-columns. A control reaction excluding the substrate was also evaluated. The results are shown below.

Assay:	**Total Activity**
HPLC	0.19 nmoles.min^{-1}
Oasis	0.18 nmoles.min^{-1}
Oasis control	0.12 nmoles.min^{-1}

Although the total activity determined using the HPLC and oasis assays were similar, a high background was observed for the oasis control. When the control assay was separated by HPLC, there was no radioactivity observed where the product was expected. It is possible that SAM either degrades spontaneously or is modified by one of the enzymes in the extract, resulting in a product which co-elutes with hercynine from the oasis cartridge. If this breakdown or modification occurs when DMH is present, one would expect the total activity in the assay to be higher. However, it cannot be ruled out that the total activity observed in the oasis assay is due both to hercynine and another product. Therefore, these assays were only employed as a screen for activity and not a quantitative measure. Control assays were included for each sample and subtracted from the assay to determine if activity was present.

4.3. Small-scale Purification of Histidine Methyltransferase using Ion Exchange Chromatography

The purification of α-N,N,N-methyltransferase from *N. crassa* by Ishikawa and Melville (1970) utilized ammonium sulphate fractionation, molecular exclusion chromatography on Bio-Gel A-0.5m and ion exchange chromatography on DEAE cellulose and DEAE sephadex. Similar methods were therefore investigated.

A dialysed ammonium sulphate fraction (0-60%) was loaded onto a DEAE cellulose column. Since the enzyme could not be eluted from DEAE cellulose with 0.2 M NH_4Cl as previously reported, the method was modified to elute the enzyme with a NaCl gradient. The gradient fractions are shown in Figure 4.4, which revealed a broad band of activity spread over the gradient. Since no elution profiles were shown by Ishikawa and Melville (1970), it is not clear if they encountered a similar phenomenon. They did however indicate that when the DEAE cellulose column was eluted with a 1 000 ml gradient, the highest methyltransferase activity eluted between 730 and 900ml. This volume suggests that spreading of the activity may have been observed.

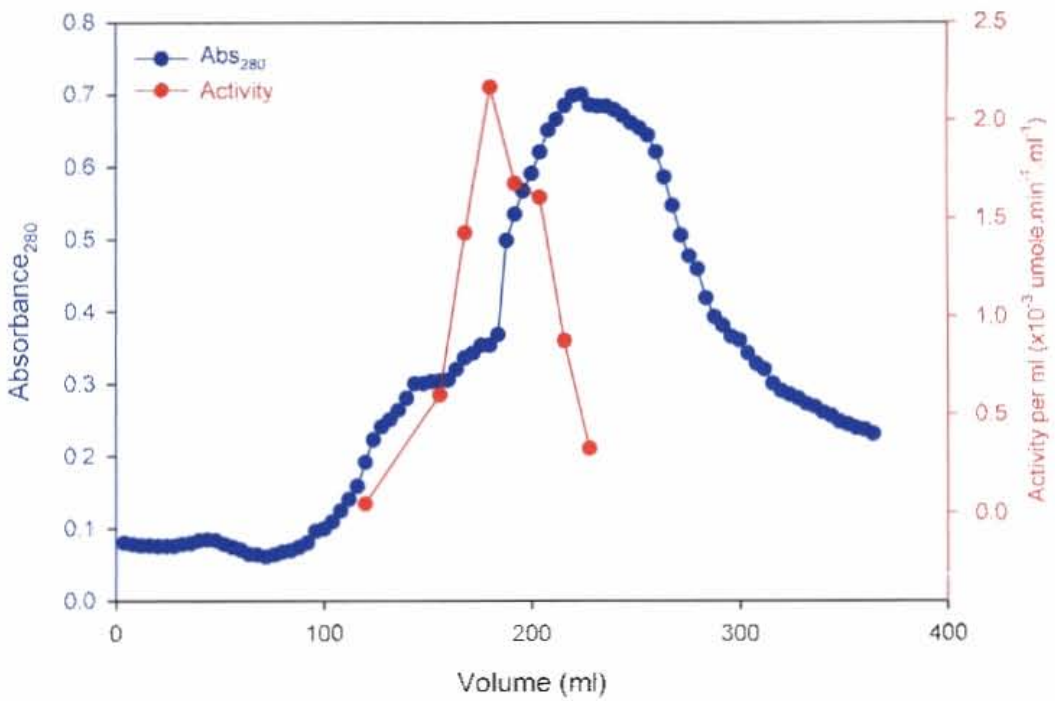

Figure 4.4: Elution profile of 0-0.25M NaCl gradient from DEAE-cellulose column. Absorbance at 280nm shown in blue, activity shown in red.

The spreading of activity may be due to the degradation of the enzyme by endogenous proteases, since it has been reported that the ε-N-l-lysine methyltransferase from *N. crassa* is highly susceptible to degradation (Borum and Broquist, 1977). However, PMSF, TPCK and TLCK were included in the lysis buffer to prevent proteolysis. It is also possible that more than one isozyme of the enzyme occurs, or that more than one enzyme is responsible for the methylation of histidine. Ishikawa and Melville (1970) have shown that the relative substrate activities remain constant throughout the purification, suggesting a single enzyme.

The second ion exchange column investigated was a Vydac 301VHP575 HPLC column. This column was chosen since it offers superior resolution of components compared with the low pressure chromatography. The active fractions were pooled, concentrated by ammonium sulphate precipitation and dialysed overnight. One-twentieth of the dialysed extract from the above DEAE column was loaded onto a Vydac 301VHP575 ion exchange column. The enzyme was eluted with a salt gradient from 0 to 0.25M NaCl and the activity of the gradient fractions are shown in Figure 4.5.

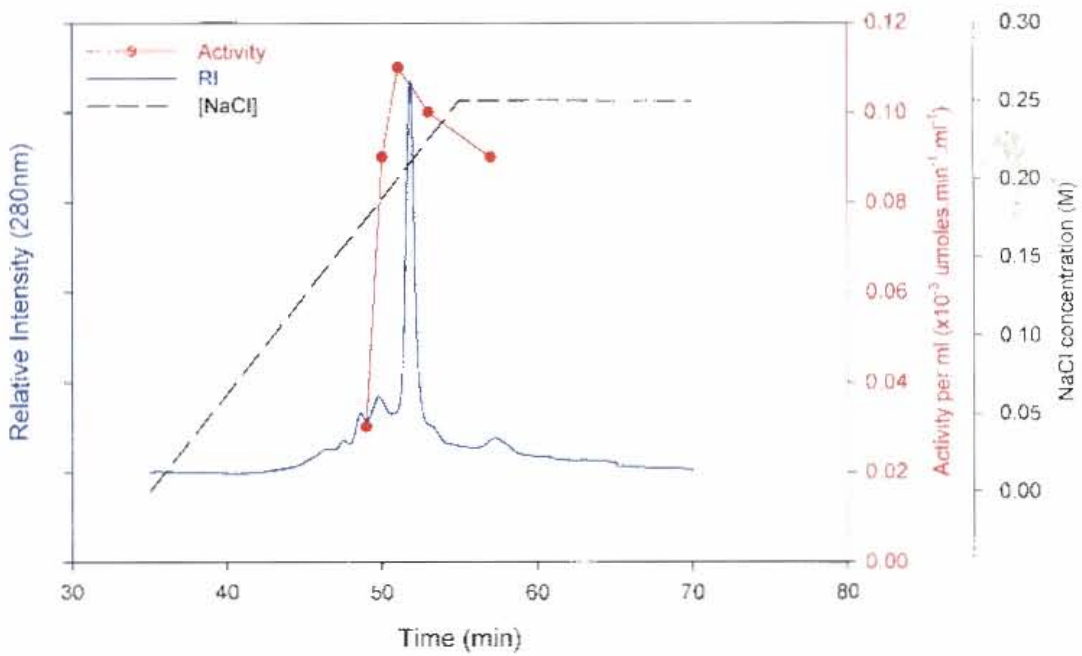

Figure 4.5: Elution profile of 0-0.25M NaCl gradient from Vydac HPLC column. Relative Intensity at 280nm shown in blue and activity shown in red.

Since Ishikawa & Melville (1970) used native PAGE as the criterion of purity, this method was compared to SDS PAGE for the purification performed. Gradient fractions eluted from the HLPC ion exchange column showing maximal activity were electrophoresed on both native and SDS PAGE gels (Figure 4.6).

The native PAGE gel after these three steps revealed a single band corresponding to the fractions with the highest activity. This is similar to the result obtained by the authors. However, when the same fractions were separated by SDS PAGE, several protein bands were visible. This suggests that the criterion of purity used by Ishikawa & Melville (1970) was inadequate, and that the methods used were insufficient to purify the α-N, N, N-histidine methyltransferase.

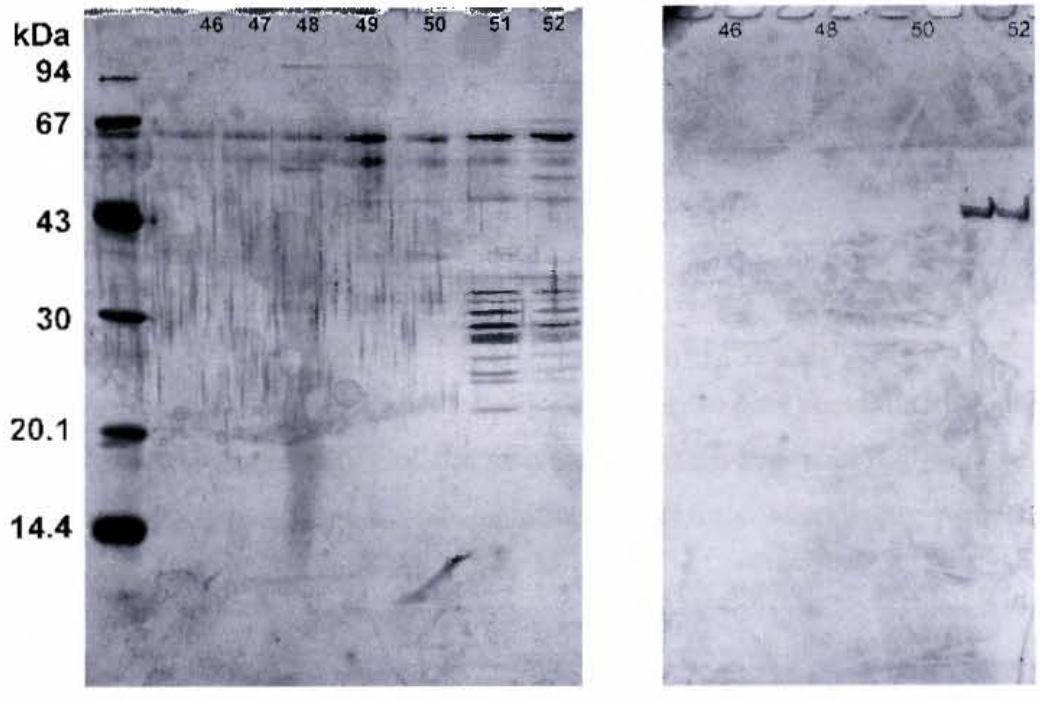

Figure 4.6: SDS PAGE (left) and Native PAGE (right) electrophoresis of fractions from Vydac ion exchange column.

4.4. Investigation of Alternative Purification Methods

Since the purification methods previously reported failed to yield a pure enzyme, a number of other methods were investigated.

4.4.1. Size Exclusion Chromatography

Ishikawa and Melville (1970) utilized Bio-Gel A-0.5m, which has an exclusion limit of 500 000, for size exclusion chromatography. However, since this resin is no longer available, resins with similar fractionation ranges were investigated. Sephacryl S200, S300 and S400, which have fractionation ranges of $5x10^3 - 2.5x10^5$, $1x10^4 - 1.5x10^6$ and $2x10^4 - 8x10^6$ respectively, were evaluated on their ability to separate Blue Dextran (2 000 000 Da) and acyl CoA dehydrogenase (172 000 Da). None of these resins were able to separate these two standards. They were therefore not considered useful for the purification of the methyltransferase, which has an apparent molecular weight of between 270 000 and 300 000 Da (Ishikawa & Melville, 1970).

4.4.2. Cation Exchange Chromatography

Given that the enzyme binds to anion exchange resins, it was predicted that it would not bind tightly to cation exchange resins such as CM-Sephadex. Cation exchange chromatography was however investigated for its ability to bind contaminating proteins, and thereby improve the purity of the enzyme. Although the resin did not retain the enzyme as expected, it also did not significantly retain contaminating proteins and therefore was not useful (data not shown).

4.4.3. pH Precipitation and Hydroxyapatite Chromatography

Ishikawa and Melville (1970) reported that the enzyme has a pI of between 4.9 and 5.0, as determined by isoelectric focussing. This property was utilized by performing a pH precipitation at pH 6.0 on an ammonium sulphate fraction. Although this method was able to increase the specific activity from 1.22 to 1.93 x 10^{-3} $\mu moles.min^{-1}.mg^{-1}$, it was not significant enough to be useful. This result did demonstrate that the methyltransferase was stable at low pH. The resulting fraction was then used to investigate hydroxyapatite chromatography.

After dialysis against HEPES buffer, the resulting preparation was applied to a hydroxyapatite column. Unbound protein was removed by washing with 200ml of HEPES buffer. A gradient to 300mM potassium phosphate was then applied resulting in most of the protein eluting in a single peak, which corresponded to the enzyme activity (Figure 4.7). Again, this method did not prove useful as it was unable to separate the enzyme activity from contaminating proteins.

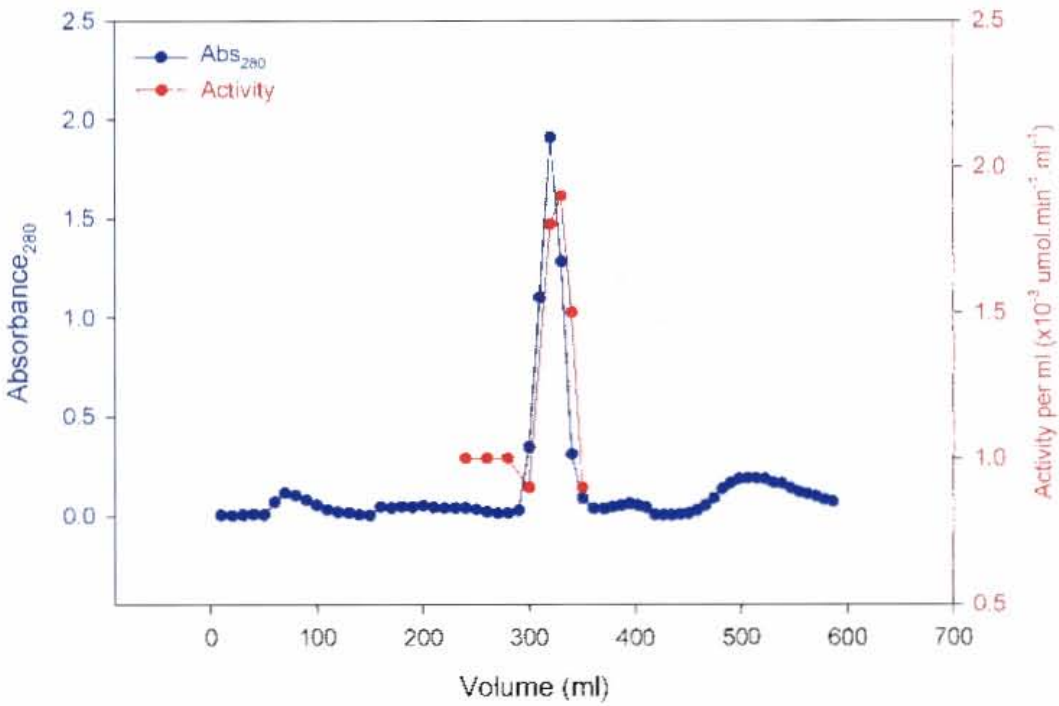

Figure 4.7: Elution profile from hydroxyapatite column. Column was washed with approximately 200ml of 25mM HEPES buffer, 1mM DTT, pH 8.0 and then eluted with a linear gradient to 300mM KPi in 400ml. Absorbance is shown in blue and activity in red.

4.4.4. Metal Ion Affinity Chromatography:

Three immobilized metals ions, nickel, zinc and cobalt, were investigated for their ability to bind the enzyme and remove contaminating proteins. Ammonium sulphate fractions were dialysed against 25mM HEPES pH 8.0, 0.5M NaCl and applied to IDA resin loaded with one of the three metals. Enzyme assays of the flow-through revealed that cobalt was unable to bind the enzyme, while nickel and zinc retained it. The nickel and zinc columns were eluted with a linear gradient of 0-25mM imidazole in 200 ml, which caused the bound protein to elute as a single peak.

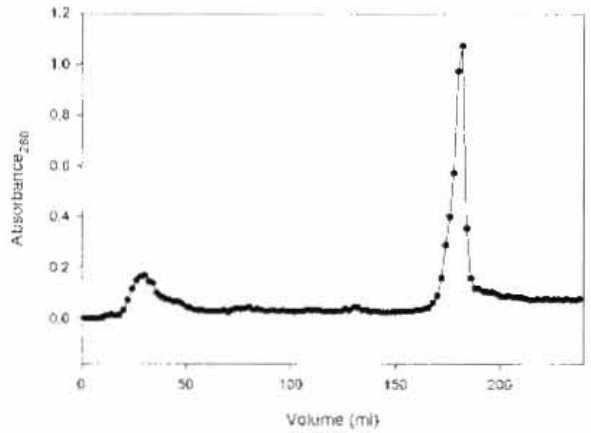

Figure 4.8A: Elution profile of IMAC loaded with nickel. Activity present in peak eluting between 150 and 200ml (Total protein loaded ~ 20mg)

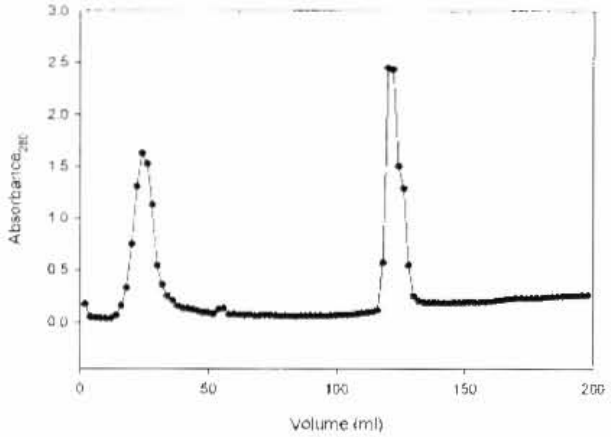

Figure 4.8B: Elution profile of IMAC loaded with zinc. Activity present in peak eluting between 100 and 130ml (Total protein loaded ~ 50mg)

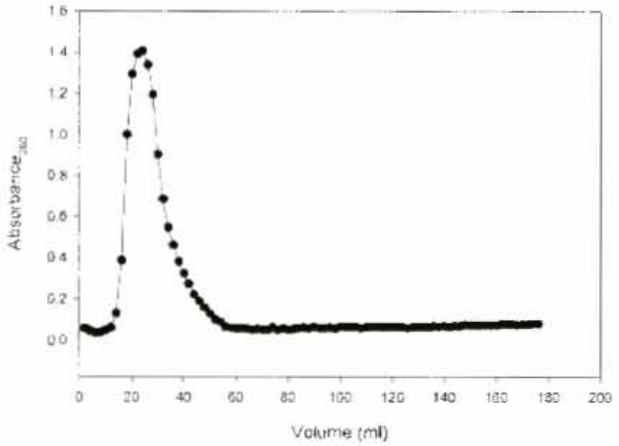

Figure 4.8C: Elution profile of IMAC loaded with cobalt. Activity present in flow-through.
(Total protein loaded ~ 10mg)

The affinity of these ions for proteins decreases as follows: $Ni^{2+} > Zn^{2+} > Co^{2+}$. This trend could clearly be seen, and zinc was selected for future purification as it was able to effect a better separation of the enzyme from contaminants than nickel. It has previously been shown that nickel, cobalt and zinc are able to inhibit the α-N, N, N-histidine methyltransferase, with zinc causing a decrease in activity by 74 % (Ishikawa & Melville, 1970). These authors suggest that zinc interacts with the active site of this enzyme. However, the results for IMAC with zinc do not show significantly tighter binding of this enzyme when compared with other retained proteins, as they elute in a single peak.

4.5. Small-scale Purification of α-N, N, N-Histidine Methyltransferase

Approximately 90g of frozen mycelium was used to prepare an ammonium sulphate fraction and ion exchange chromatography on DEAE cellulose was performed as previously described. The activity of the gradient fractions is shown in Figure 4.9.

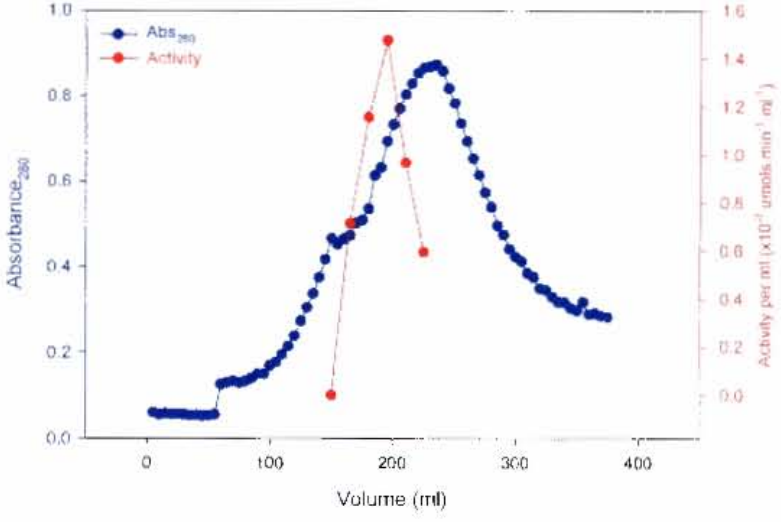

Figure 4.9: Elution profile of 0-0.25M NaCl gradient from DEAE-cellulose column. Absorbance at 280nm shown in blue, activity shown in red.

The active fractions were pooled, concentrated by ultrafiltration and dialysed overnight against Buffer B (50mM HEPES pH 8.0, 0.5M NaCl, 1mM imidazole). The extract was applied to an IDA agarose column loaded with zinc. A linear gradient of 1-20mM imidazole in buffer B was used to elute the enzyme (Figure 4.10). Table 4.1 indicates the purification obtained with these steps.

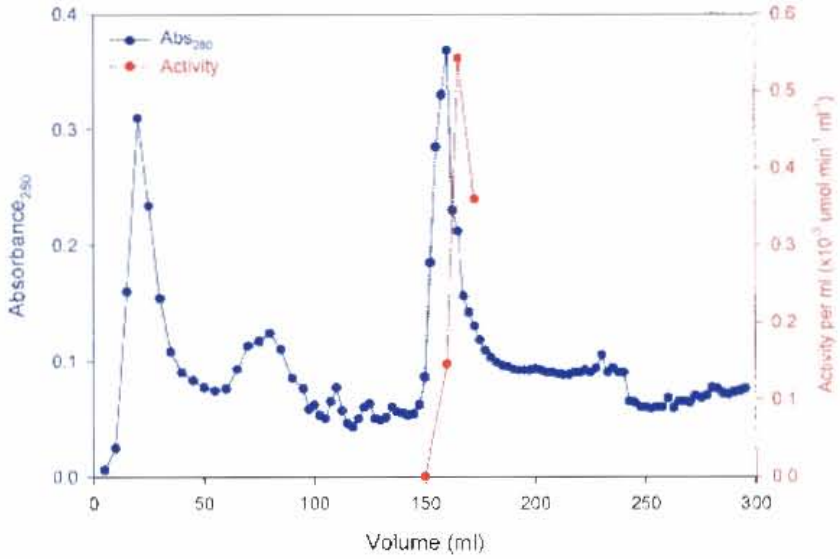

Figure 4.10: Elution profile Zn^{2+} IMAC of DEAE cellulose fraction. Absorbance shown in blue and activity in red.

Table 4.1: Purification Table for Histidine Methyltransferase from *N. crassa*

Purification Step	Total Protein (mg)	Volume (ml)	Total Activity (nmole.min^{-1})	Specific Activity (nmole.min^{-1}.mg^{-1})
0-60% $AmSO_4$	206	24	0.050	0.248X10^{-3}
DEAE cellulose Ultra-filtration (UM2)	18.8	4.18	0.012	0.648X10^{-3}
Zn^{2+} IMAC	0.139	1.0	0.004	28.78X10^{-3}

The combination of DEAE cellulose and Zinc IMAC chromatography resulted in almost a 100-fold increase in specific activity after ammonium sulphate fractionation. The fractions from the zinc IMAC column with the highest activity were pooled, concentrated and dialysed overnight against 0.1M NH_4Cl pH 8.5, 1mM DTT. Ion exchange chromatography was performed using a Vydac 301VHP575 column on this fraction. The elution profile of the NaCl gradient is shown in Figure 4.11, with the activity indicated in red.

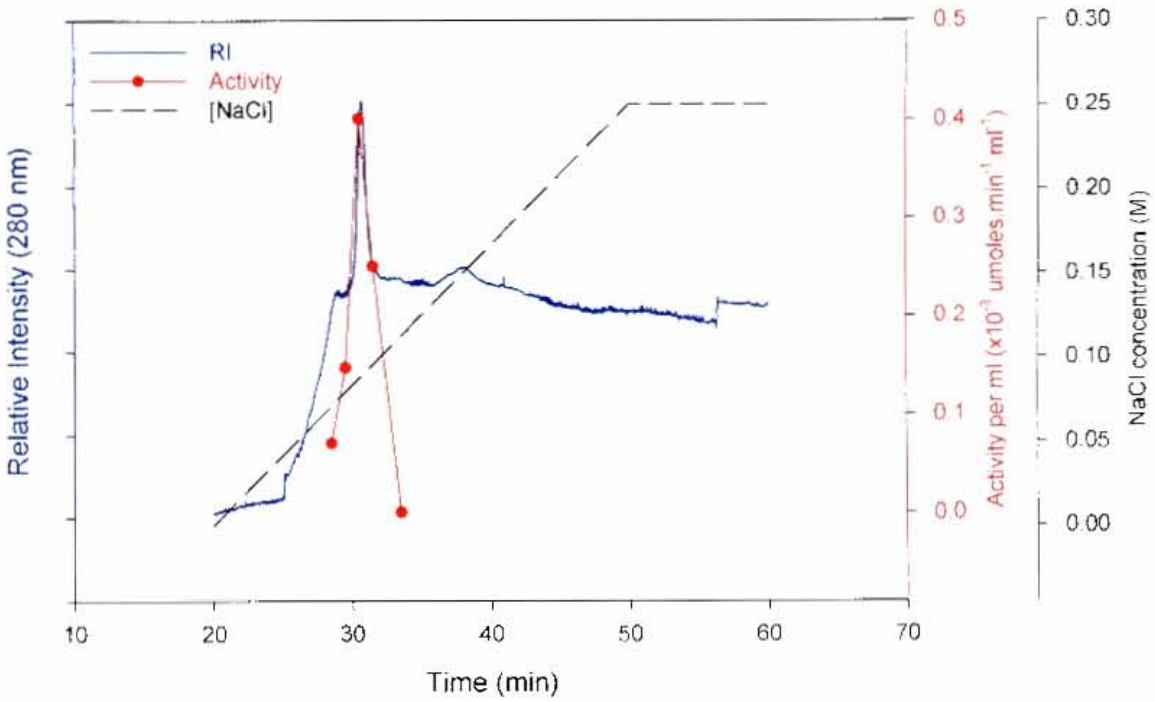

Figure 4.11: Elution profile of NaCl gradient from Vydac 301VHP575 column. Relative Intensity at 280nm is shown in blue and activity in red

The fractions exhibiting the highest activity were separated by SDS PAGE and visualized by silver staining (Figure 4.12).

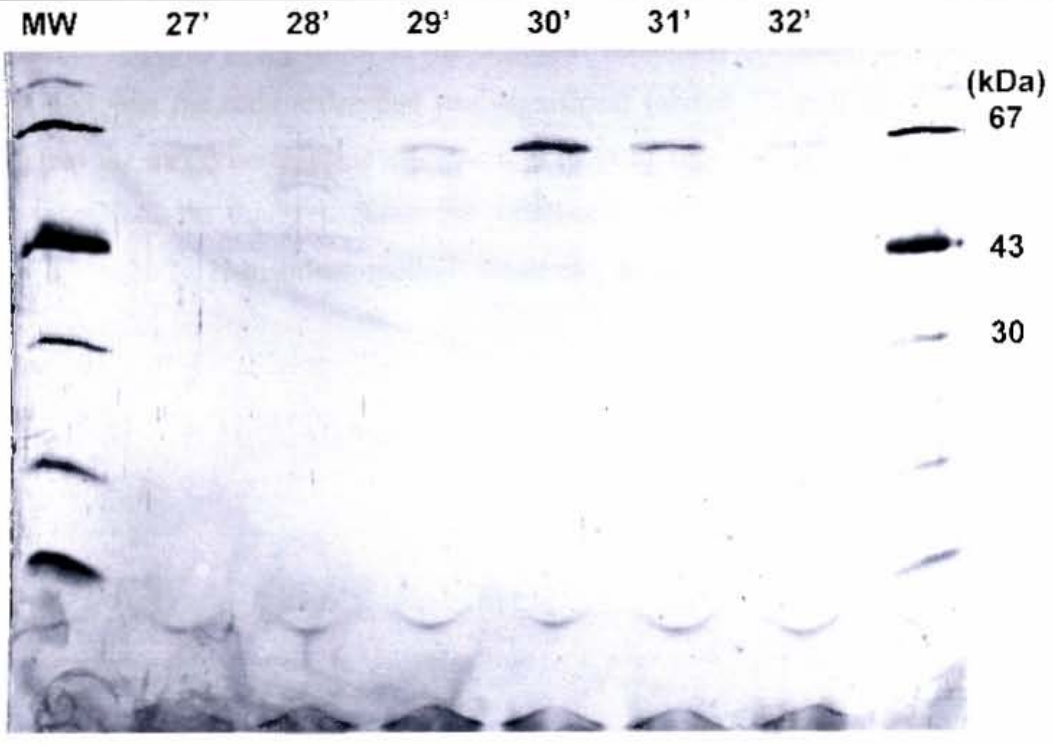

Figure 4.12: SDS PAGE electrophoresis of most active fractions from Vydac ion exchange chromatography.

Since the prominent band at 66 kDa appeared to correspond to the activity it was excized, digested with trypsin and submitted for LC-MSMS analysis. The fragment ion spectra obtained were analysed using MASCOT (www.matrixscience.com) MS/MS Ion Search program (Matrix Science, London). The protein was identified to be a probable sulphate adenyltransferase from *N. crassa* (Figure 4.13), which has a predicted mass of 64 421 Da.

1	MSNPPHGGVL	KDLIARDLPR	HAELEAEAET	LPALLLSERQ	LCDLELILNG
51	GFSPLEGFMN	QEDYNDVVKE	NRLASGLLFS	MPITLDVSEE	TISELGLKAG
101	ARITLRDFRD	DRNLAILTVD	DVYKPDKALE	AKEVFGGDEE	HPAVKFLYET
151	AKFYYVGGKL	EAVNKLQHYD	FVDLRYSPAE	IRTHFDKLGW	SRVVAFQTRN
201	PMHRAHRELT	VRAARSHHAN	VLIHPVVGLT	KPGDIDHFTR	VRVYKALLPR
251	YPNGMAVLGL	LPLAMRMGGP	REAIWHAIIR	KNHGATHFIV	GRDHAGPGKN
301	SKGVDFYGPY	DAQYAVEKYR	DELGIEVVPF	QMMTYLPDSD	EYAPVDQIPK
351	GVPTLNISGT	ELRAPLRSGR	EIPEWFSYPE	VVKVLRESHP	PRSQQGFTVI
401	FTGYPNSGKD	QIAMALQVTL	NQQGGRSVSL	FLGENIRHEL	SSELGYNRED
451	RDKNIARIAF	VASELTRSGA	AVIAAPIAPF	EKARQNAREL	VEKYGDFYLV
501	HVATPLEYCE	KTDKRGIYAK	ARAGEIENFT	GVNDPYETPA	KPDLVVDCEK
551	QSVRSIVHQI	ILLLESQGLL	DRF		

Figure 4.13 Probable sulphate adenyltransferase from *N. crassa* identified by MASCOT MS/MS Ion search. Identified peptide fragments indicated in red.

The probability of this being an incorrect match is low, firstly since MASCOT matched 7 peptides as opposed to 1 peptide in the next best candidate. Secondly, the probability score of 153 was the only score that was significant (above 32, $p<0.05$). It therefore appears that the methyltransferase enzyme is present in very low abundance and could not be visualized on this gel. Since the small-scale purification performed did not identify the α-N, N, N-histidine methyltransferase, additional purification steps were investigated.

4.6. Chromatofocusing

Ishikawa and Melville (1970) determined by isoelectric focussing that the pI of the α-N, N, N-histidine methyltransferase was between 4.9 and 5.0. The investigation of precipitation by lowering pH as a purification method revealed that the enzyme was stable at low pH. Chromatofocusing was therefore investigated for its purification potential. The active fractions from a Zinc IMAC column were pooled and applied to PE94 resin which had been equilibrated at pH7. The column was eluted by washing with diluted Polybuffer 74, pH 4. The elution profile is shown below, with the pH of the fractions indicated in black. The activity was detected over a broad pH range between 200 and 300ml (indicated by red arrow). Since this method was able to remove a large amount of proteins which were not retained by the column, it was included in the subsequent large-scale purification.

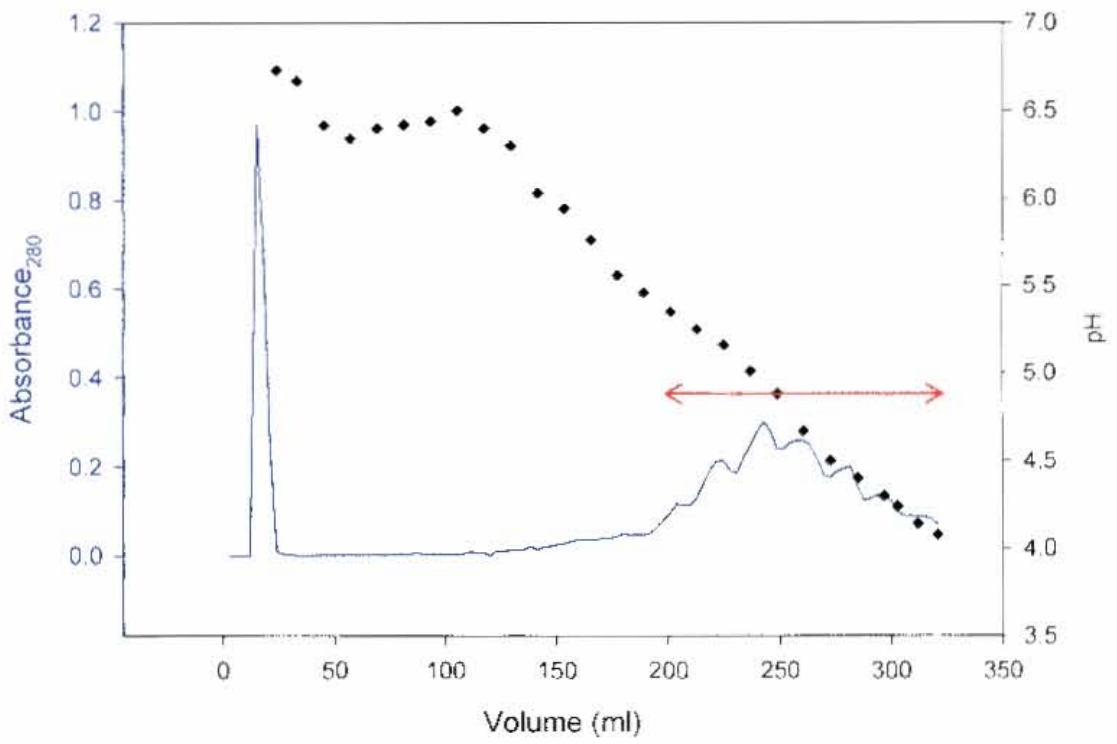

Figure 4.14 Elution profile of chromatofocusing column. Absorbance shown in blue, pH in black and the region in which activity was present is indicated by red arrow

4.7. Affinity Chromatography:

Affinity Chromatography was investigated using both the substrate dimethylhistidine and the product S-adenosylhomocysteine of the methylation reaction.

4.7.1. Dimethylhistidine Affinity Chromatography

Immobilised histidine has been tested as an affinity ligand for a number of proteins (Kanoun *et al.,* 1986). Since the histidine methyltransferase was shown to methylate dimethylhistidine (DMH) faster than histidine, DMH was chosen as an affinity ligand. Dimethylhisitidine (DMH) was coupled to ω-aminopentyl agarose and the coupling efficiency was monitored by HPLC. The area of the DMH peak decreased from 91 588 536 to 81 313 584, which indicates that 11% of the DMH was coupled. Given that a total of 300 μmoles of DMH was present, in the reaction this is equivalent to 33 μmoles of DMH. The resin was estimated to have a total of 50 μmoles of aminopentyl coupling groups, and therefore the coupling efficiency was 66%.

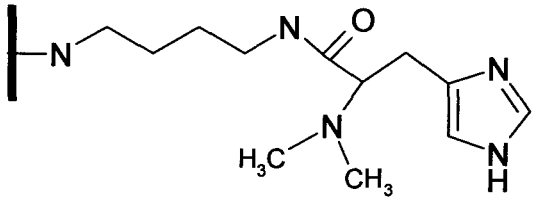

Figure 4.15: Schematic of the DMH-agarose resin which was synthesized

The binding conditions selected for affinity chromatography were similar in salt and pH to those used in the assay.An ammonium sulphate fraction was dialysed against Buffer A (50mM NH_4Cl, 1mM DTT, pH8.5) and then applied to the DMH-agarose resin. The protein was eluted stepwise with Buffer A containing 100mM, 500mM NaCl and 50mM histidine + 500mM NaCl. The protein for each step was pooled and assayed for activity. Under these conditions the histidine methyltransferase bound to the DMH-agarose, and was eluted with 100mM NaCl along with a number of contaminating proteins. Ninety-three percent of the activity was recovered after this chromatography step and the Specific Activity increased approximately 10-fold from 0.097×10^{-3} to 1.037×10^{-3} $\mu moles.min^{-1}.mg^{-1}$.

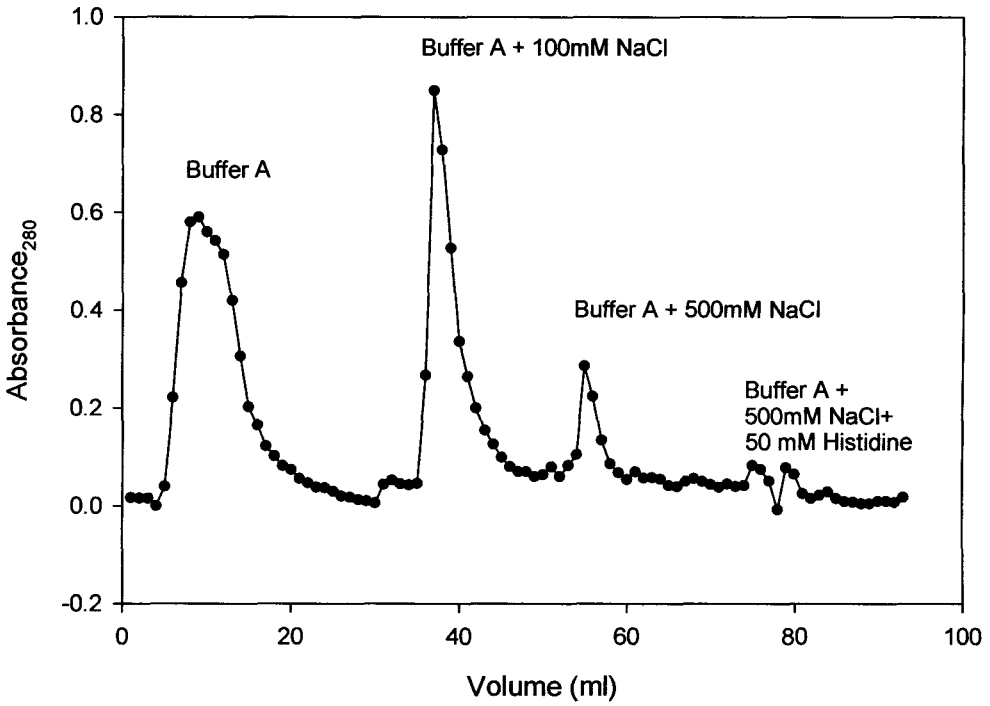

Figure 4.16: DMH Affinity Chromatography of ammonium sulphate fraction. Activity was detected in peak eluted with Buffer A containing 100mM NaCl

Elution of the enzyme by salt rather than its substrate suggests that it is not binding to DMH-agarose by biospecific interactions, but by more general interactions. Kanoun *et al.* (1986) suggest that histidine binds proteins by hydrophobic interactions with the imidazole ring and ionic interactions with the carboxyl group. They also suggest that the zwitterionic nature of histidine may result in dipole-induced interactions with proteins. It is possible that the coupling of DMH via its carboxyl group removes an important ionic interaction with the enzyme. This is supported by the fact that the enzyme is not inhibited by imidazole, histamine, histidine methyl ester and dimethylhistidine methyl ester (Ishikawa & Melville, 1970), in which the carboxyl is either missing or masked. The weakening of this interaction between the enzyme and its substrate may explain the premature elution of the enzyme by salt rather than its substrate. Affinity chromatography is a powerful method, which can achieve a high degree of purification in a single step. An example of this is the 296-fold purification achieved using adenosine-agarose in the purification of narigenin 7-O-methyltransferase (Rakwal *et al.*, 2000). Since a similar purification factor could not be achieved here, the method was excluded in favour of chromatography steps utilising resins which were cheaper and readily available. This was a consideration because of the large scale-up which was required for this enzyme.

4.7.2. S-Adenosylhomocysteine (SAH) Affinity Chromatography

S-adenosylhomocysteine (SAH) is a known inhibitor of methyltransferase enzymes, and more specifically has been shown to inhibit this enzyme (Ishikawa & Melville, 1970). SAH was therefore investigated as an affinity ligand.Activated CH-Sepharose 4B was used to couple S-adenosylhomocysteine (SAH) via its amino groups. The pre-activation of CH-Sepharose 4B is achieved by the esterification of its carboxyl group with N-hydroxysuccinimide (NHS), which facilitates the spontaneous coupling of ligands containing amino groups. This is important since addition of NHS to the coupling buffer would result in the amino and carboxyl groups of SAH coupling to each other. The wide pH range at which coupling to activated CH-Sepharose 4B occurs (5-10) allows the coupling of SAH to be directed to either of its amino groups by choosing an appropriate pH. At pH 9.0, coupling occurs preferentially at the α-amino group since it is more reactive. Lowering the pH of the coupling reaction facilitates coupling at the N_6 position.

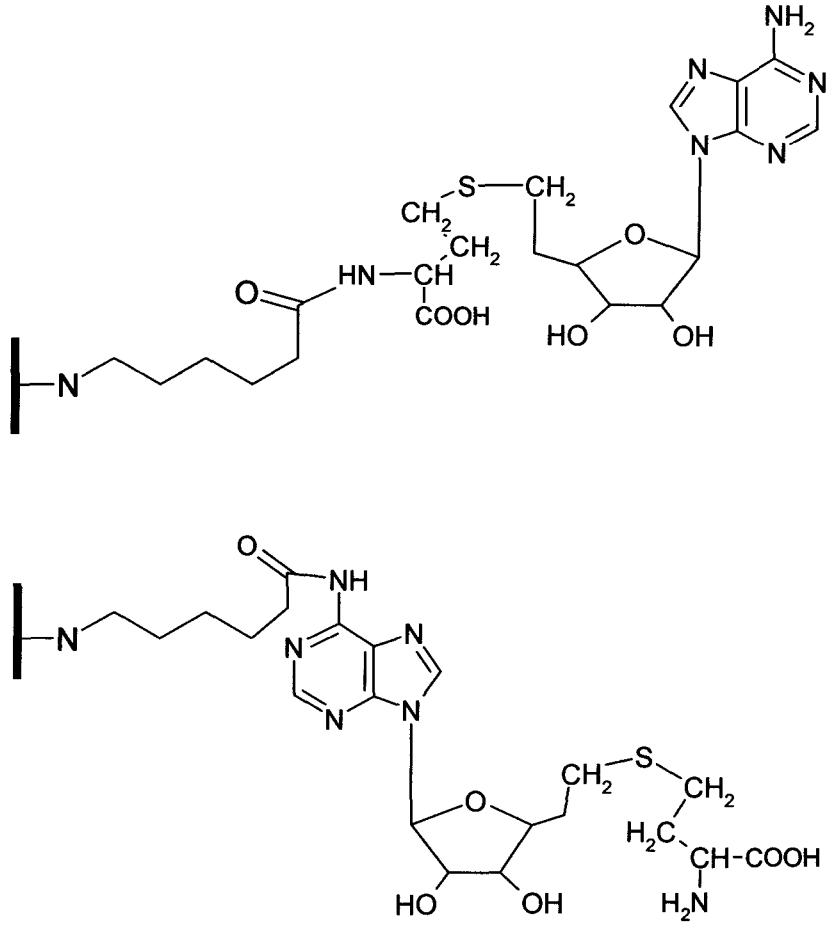

Figure 4.17: Schematic of the SAH-agarose resins which were synthesized. In the top figure SAH is coupled via the α-amino group and in the bottom figure it is linked via the N_6 position

4.7.2.1. Coupling via α-amino Group

The coupling efficiency was determined by HPLC using a C_{18} column and detecting the reaction components at 260nm. The area of the SAH peak decreased from 10 625 177 to 6 985 481, which indicated that approximately 7.7 μmoles of SAH had been coupled. The resin is estimated to contain between 10 and 14 μmoles of coupling groups, and therefore the coupling efficiency was between 55 and 77 %.

An ammonium sulphate fraction was dialysed against 100mM phosphate buffer and then applied to the SAH (α)-agarose resin. The protein was eluted stepwise with phosphate buffer containing 100mM and 500mM NaCl. The enzyme did not bind to the resin and the total activity recovered was 130%, suggesting that an inhibitor of the activity had been removed. Since the resin was unable to bind the enzyme or a significant percentage of the contaminating proteins, it was not utilized further.

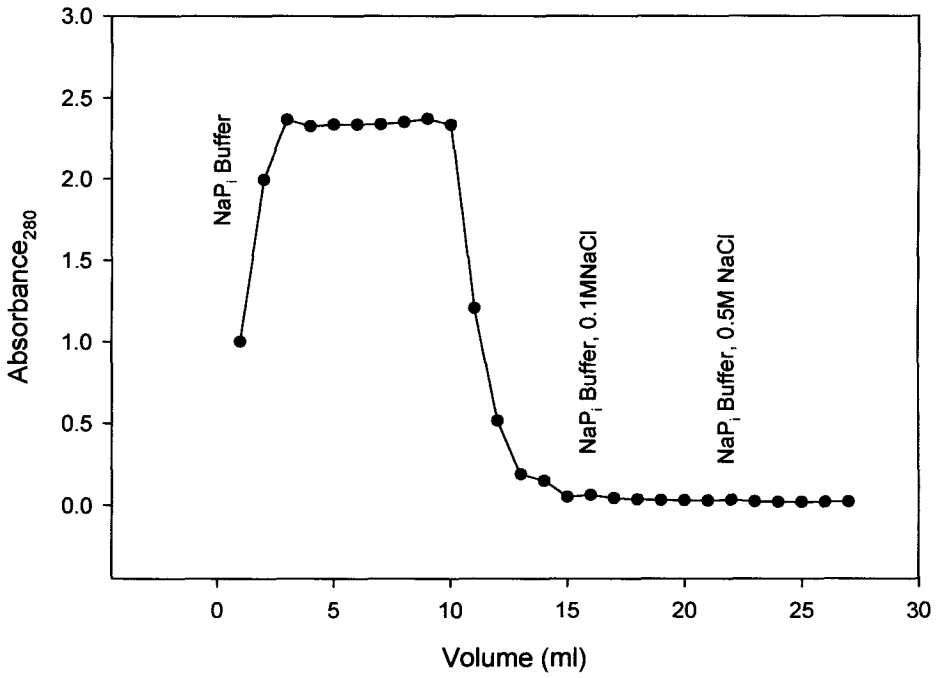

Figure 4.18: SAH (α-amino) Affinity Chromatography of ammonium sulphate fraction. Activity was detected in flow-through

4.7.2.2. Coupling via the N_6 amino Group

The efficiency of coupling was determined by HPLC as previously described. A reduction from 201 949 888 to 158 052 192 in the area of the SAH peak indicated that approximately 8.1 μmoles of SAH had been coupled. The resin is estimated to contain between 10 and 14 μmoles of coupling groups, and therefore the coupling efficiency is between 58 and 81 %.

An ammonium sulphate fraction was dialysed against Buffer A (50mM NH_4Cl, 1mM DTT, pH8.5, 10% glycerol) and then applied to the SAH-agarose resin. The protein was eluted stepwise with Buffer A containing 100mM, 500mM NaCl and 5mM SAM + 500mM NaCl. The enzyme activity was detected in the flow-through, however only 72 % of the enzyme activity could be recovered. No activity was detected in any of the subsequent fractions, suggesting that a portion of the enzyme was either irreversibly bound or was inactivated during the chromatography.

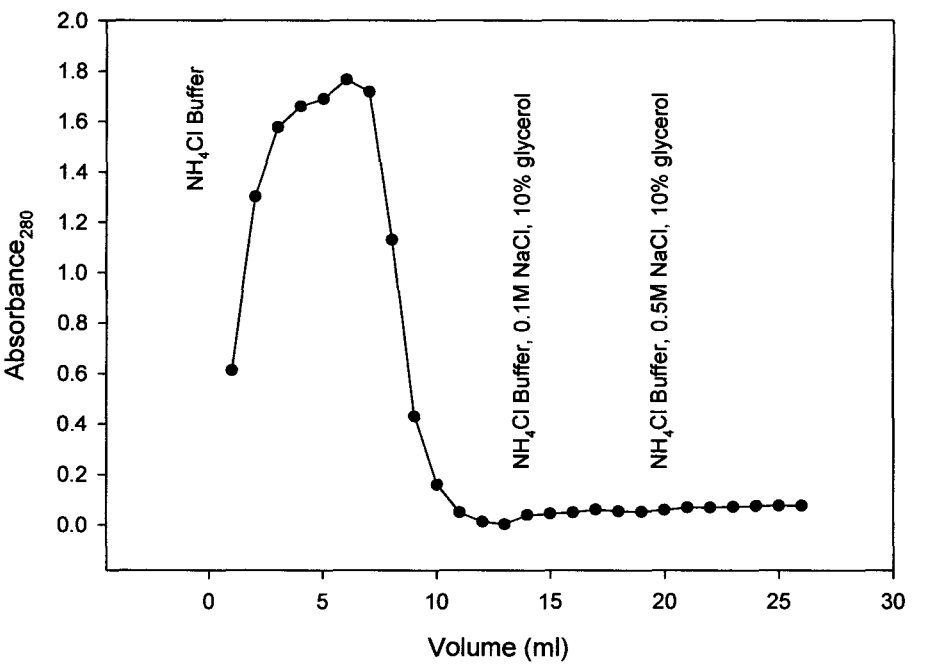

Figure 4.19: SAH (N_6) Affinity Chromatography of ammonium sulphate fraction. Activity was detected in flow-through

Mack & Slaytor (1978) indicate that the requirement for the two amino groups of SAH for binding to SAM-dependent enzymes is variable. They suggest that the preferred linking position is the carboxyl group. The inhibition data obtained by Ishikawa and Melville (1970) for the methylation of hercynine implies that dimethylhistidine is the first substrate to bind and hercynine is the last product to leave. It is therefore possible that the binding of dimethylhistidine is required for the binding of S-adenosylmethionine and the formation of S-adenosylhomocysteine. This could explain the inability of the free enzyme to bind the SAH affinity resin. S-adenosylmethionine was not investigated as a ligand due to its chemical and enzymatic instability.

4.7.3. Dye-ligand Chromatography

One of the first dyes used in dye-ligand chromatography, Cibacron Blue, has been shown to act as an analogue for ADP-ribose and has the ability to bind enzymes with AMP, IMP, ATP, NAD, NADP and CTP binding sites (Scopes, 1994). Since S-adenosylmethionine contains adenosine, it is conceivable that the histidine methyltransferase may bind Cibacron Blue or a related dye. A screening kit containing 9 different dyes was therefore investigated for its ability to bind the enzyme. Chromatography was performed using an ammonium sulphate fraction and the results are shown in Figure 4.20. The fractions with the highest absorbance for each elution step were assayed for activity. The dyes were able to bind certain proteins, which were eluted by increasing the NaCl concentration to 0.5 M. However none of the dyes were able to bind the histidine methyltransferase. The inability of the dyes to bind the enzyme may be due to the absence of important interactions with the amino, carboxyl and sulphur groups on the methionine. In structurally defined methyltransferases, the conserved glycine residues in Motif 1 have been found to hydrogen bond with the amino and carboxyl groups of SAM and SAH (Kagan & Clarke, 1994). The need for the protein to first bind its substrate may also play a role. Given that the proportion of protein that did bind the column was small and did not improve the purity significantly, these columns were not utilized further.

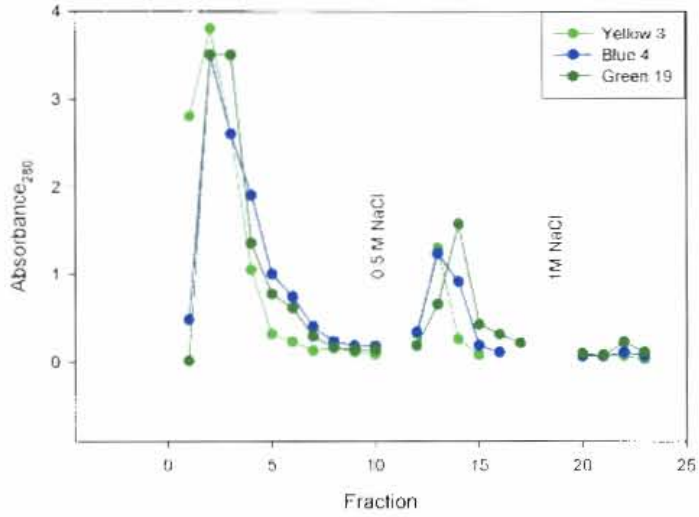

Figure 4.20A: Dye-ligand Chromatography of ammonium sulphate fraction using Yellow 3, Blue 4 and Green 19

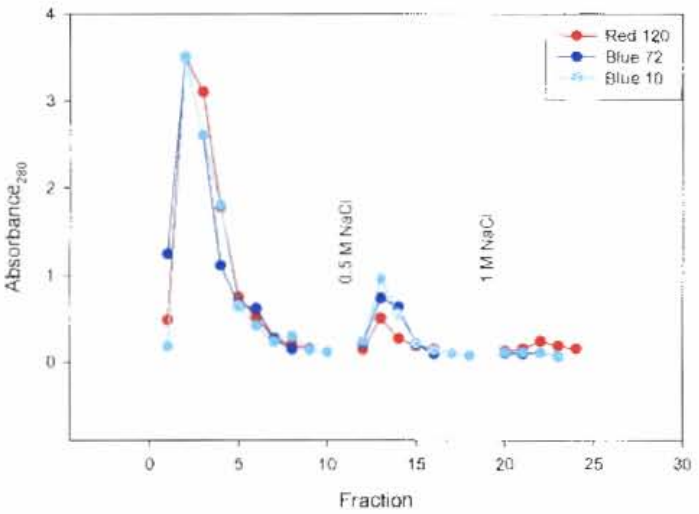

Figure 4.20B: Dye-ligand Chromatography of ammonium sulphate fraction using Red 120, Blue 72 and Blue 10

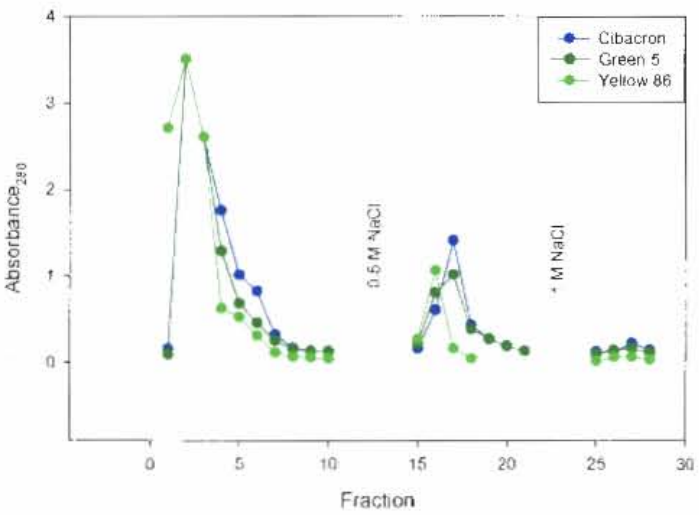

Figure 4.20C: Dye-ligand Chromatography of ammonium sulphate fraction using Cibacron, Green 5 and Yellow 86

4.8. Large Scale Purification of α-N, N, N-Histidine Methyltransferase

Since the histidine methyltransferase was not visible on SDS PAGE after the small scale purification performed, a 10-fold scale-up was performed. In order for a large-scale purification to be performed, the purification methods developed had to be modified to handle the increased volumes within a reasonable timeframe. For this reason, a streptomycin sulphate precipitation was included to allow clarification of the extract at a lower speed by centrifugation. Effectively, this allowed the clarification of 1.5 l of extract, by centrifuging at 14 000 rpm in a JA14 rotor for 10 min, as opposed to 320 ml by centrifuging at 22 000 rpm using a JA 30.50 Ti rotor. After ammonium sulphate fractionation, desalting was performed using Sephadex G25 rather than dialysis. Ion exchange chromatography and Zinc IMAC chromatography were both modified from gradient elution to step-wise elution. Since the enzyme activity was spread over a large volume of the gradient for both these methods, the use of step-wise elution did not drastically reduce the purification obtained. The storage of the protein as an ammonium sulphate pellet was found to be most effective in retaining the activity and was therefore used between purification steps.

The Purification Table for three successive DEAE columns is shown below. The enzyme activity eluted in the 150mM NaCl step.

Table 4.2 Purification Table for three DEAE cellulose columns

Purification Step	Total Protein (g)	Volume (ml)	Total Activity ($nmol.min^{-1}$)	Specific Activity ($\mu mole.min^{-1}.mg^{-1}$)
$AmSO_4$/G-25	2.0	260	0.150	0.070×10^{-3}
DEAE	0.598	580	0.298	0.498×10^{-3}
$AmSO_4$/G-25	1.3	230	0.214	0.165×10^{-3}
DEAE	0.236	310	0.272	1.153×10^{-3}
$AmSO_4$/G-25	1.89	200	0.123	0.065×10^{-3}
DEAE	0.358	291	0.171	0.479×10^{-3}

The protein from three successive DEAE columns was pooled, precipitated and divided into four aliquots. Zinc IMAC Chromatography was performed on each aliquot and the results are shown below.

Table 4.3 Purification Table for four Zinc IMAC columns

Purification Step	Total Protein (mg)	Volume (ml)	Total Activity ($\mu mol.min^{-1}$)	Specific Activity ($\mu mole.min^{-1}.mg^{-1}$)
Zn IMAC 1	69.5	102	0.171	2.46×10^{-3}
Zn IMAC 2	109	72	0.285	2.62×10^{-3}
Zn IMAC 3	103	70	0.222	2.16×10^{-3}
Zn IMAC 4	70.6	74	0.208	2.94×10^{-3}

The results from successive DEAE and zinc IMAC columns showed that the purification using these methods was consistent and the yield of activity was excellent.

4.8.1. Chromatofocusing 1

The active fractions from four zinc IMAC columns were pooled and concentrated by ammonium sulphate precipitation (0-80%). The protein was divided in half and used to run two chromatofocusing columns. In the first chromatofocusing column, a large percentage of the protein eluted in the flow through, while the enzyme activity eluted in a very broad peak between pH 5 and pH 4. SDS PAGE was performed on the active fractions from the first chromatofocusing column (Figure 4.21). Since a single band corresponding to the activity could not be identified, all the active fractions were pooled and concentrated by ultrafiltration.

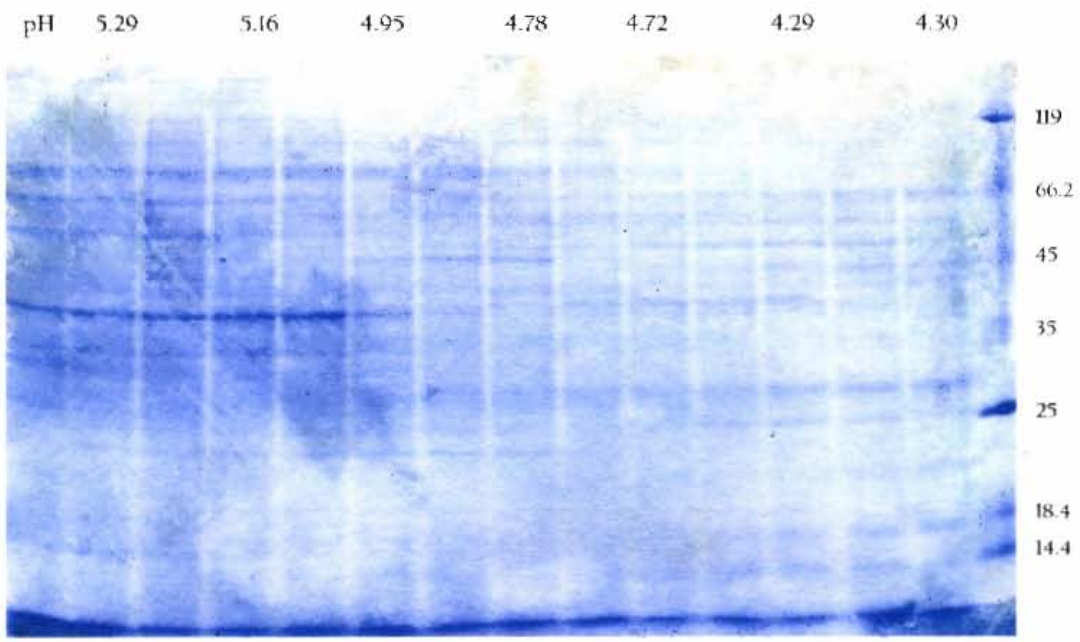

Figure 4.21: SDS PAGE of every third fraction in the region of activity from Chromatofocusing column. The pH of fractions is shown above and MW is indicated in kDa.

The fraction had a total activity of 0.072 μmoles.min^{-1} and given that the total activity loaded on the chromatofocusing column was approximately 0.4 μmoles.min^{-1}, only 18% of the activity was recovered. Due to this massive loss of activity, the Specific Activity only increased slightly to 4.0 x 10^{-3} μmoles.min^{-1}.mg^{-1}. Ishikawa and Melville (1970) reported that "some precipitation of the activity" had occurred during isoelectric focussing. It is therefore possible that a percentage of the enzyme is denatured during the chromatofocusing step and may remain bound to the column or elute as inactive enzyme. In hindsight it may have been more useful to use the DMH-agarose step rather than chromatofocusing, since the recovery of the enzyme is much better. However, the DMH-agarose step was only investigated using an ammonium sulphate fraction and therefore its effectiveness at a later stage in the purification would have to be determined.

4.8.2. DEAE Vydac Ion Exchange 1

The pooled fraction from Chromatofocusing 1 was dialysed against 10 mM Tris-Cl pH 8.5 and one-fifth was applied to a Vydac HPLC Ion Exchange column. Unbound protein was removed by washing the column with 10mM Tris buffer and this fraction was found to contain a small amount of activity. The column was then eluted with a linear gradient of 0-0.25M NaCl over 30min. The elution profile and the activity of fractions 45min to 63min are shown in Figure 4.22.

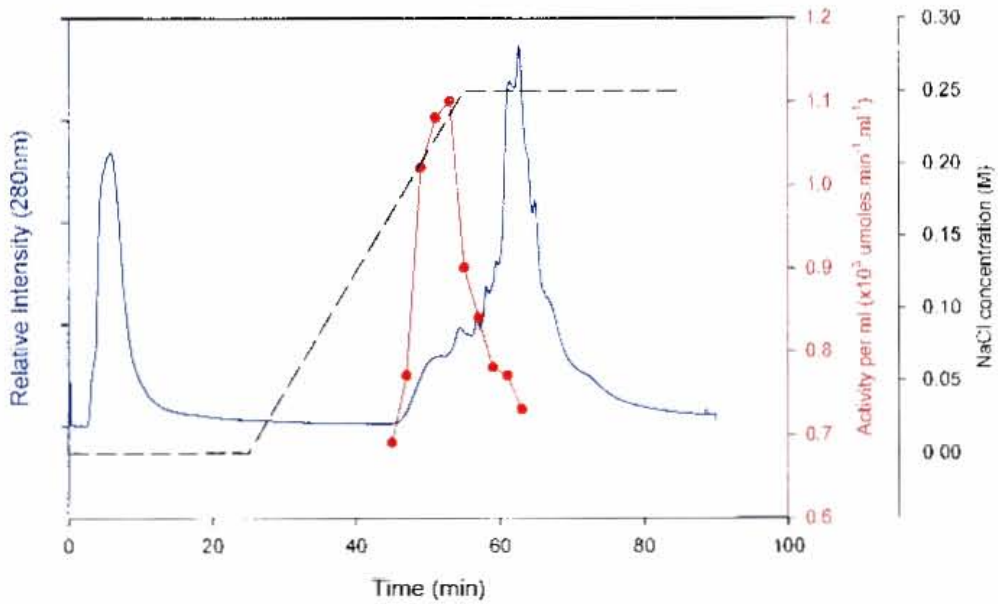

Figure 4.22: Elution profile of Vydac HPLC ion exchange column. Relative Intensity at 280nm shown in blue, NaCl concentration in black and Activity in red.

The assayed fractions had a combined activity of approximately 0.007 μmoles.min^{-1}. Since the total activity loaded on the chromatofocusing column was 0.014 μmoles.min^{-1} (1/5th of 0.072), approximately 50% of the activity was recovered. In order to obtain sufficient protein for LC-MSMS, 600ul of fractions 47 and 79 were separated and visualized by SDS PAGE (Figure 4.23). The proteins that were most intense in the most active fraction were selected and designated samples A-E. These bands were excised, processed and submitted for LC-MSMS.

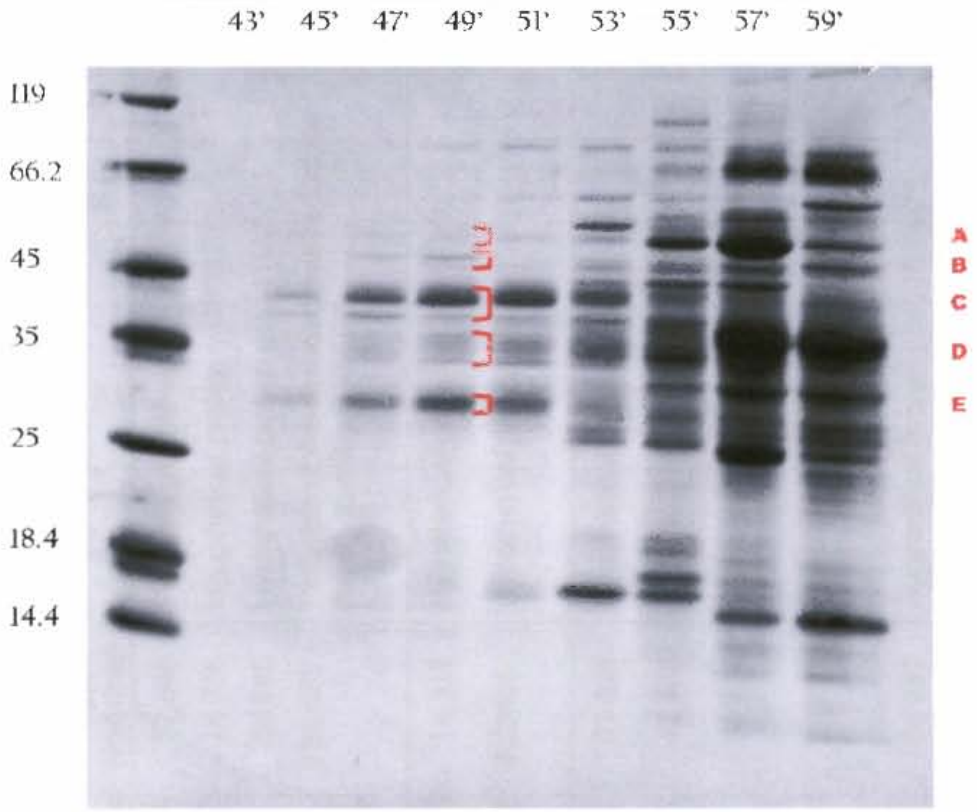

Figure 4.23: SDS PAGE of Vydac ion exchange column fractions surrounding highest activity. The bands designated A-E in red were submitted for LC-MSMS

The fragment ion spectra obtained for samples A-E were analysed using MASCOT MS/MS Ion Search program (Matrix Science, London). The proteins identified as being significant matches for each sample are indicated in Table 4.4.

Table 4.4: *Neurospora crassa* protein candidates obtained for samples A-E using MASCOT MS/MS Ion Search

Sample	MASCOT score	Matched peptides	Molecular weight Observed	Molecular weight Nominal	Annotation & Accession no.	Conserved Domains
A	201	3	49 700	57 843	Probable glucokinase gi|38567331	Hexokinase, Nag C
	110	1		74 326	Hypothetical protein gi|85080705	WD 40 domain/repeats
	79	1		56 985	Hypothetical protein gi|85118357	Proteosome subunit
	49	1		130 623	Probable alpha-aminoadipate reductase large subunit gi|9367276	AMP-binding. CaiC, Ent E, EntF, Acs,FAA1,COG3320, WcaG, 3Beta_HSD, RfbD, Epimerase, COG1086
B	404	22	46 000	74 326	Hypothetical protein gi|32403350	WD40 domain
	169	3		232 155	Hypothetical protein gi|32405530	Eukaryotic SMC protein, Cromasome segregating ATPase, HOOK protein
C	73	7	40 000	61 024	Hypothetical protein gi|85113050	Glucose-1-phosphate uridylyltransferase
	42	1		42 485	Hypothetical protein gi|85111594	Nucleotide hydrolase
D	146	2	35 000	38 174	Thiamine biosynthesis protein NMT 1 gi|15822513	ABC transporter
	58	1		39 033	Hypothetical protein gi|85076244	Aldo/keto reductase family/ Predicted oxidoreductase
	38	1		98 267	Hypothetical protein gi|85079300	Domain of unknown function Uncharacterised conserved protein
E	166	3	30 000	26 981	Probable 20s proteasome subunit Y7 gi|18376026	alpha-proteosome subunit
	96	3		61 024	Hypothetical protein gi|85113050	Glucose-1-phosphate uridylyltransferase

4.8.3 LC-MSMS Analysis and Identification of Candidate Proteins from DEAE Vydac 1

A MASCOT MS/MS Ion search performed on samples A-E from the first Vydac column revealed 12 candidate proteins from *N. crassa* that were significant (score > 37, $p < 0.05$). Of these proteins, 1 had a definitive annotation, 3 contained the word "probable" in their annotation and the remaining 8 were annotated as "hypothetical proteins". None of the candidate proteins were annotated as methyltransferases. A BLASTp search revealed conserved domains for all 12 proteins, but again no similarity with methyltransferases were observed. One of the hypothetical proteins, which has a glucose-1-phosphate uridylyltransferase conserved domain, was matched to the protein bands observed at 40 000 Da and 30 000 Da. A similar discrepancy in observed and predicted mass was observed for most of the candidate proteins. Taken with the fact that the protein has a predicted mass of 61 024 Da, this could indicate that proteolysis had occurred.

4.8.4. Chromatofocusing 2

The second half of the Zinc IMAC fraction was used to run a second chromatofocusing column. The second chromatofocusing column yielded better resolution and the activity appeared to be in two distinct peaks (Figure 4.24). This could indicate the presence of more than one enzyme or multiple isoforms of the same enzyme. Since the first peak corresponded to the pI previously reported by Ishikawa and Melville (1970), these fractions were pooled and taken to the next step of purification. These pooled fractions had a combined activity of approximately 0.013 μmole.min^{-1}, which is a recovery of only 3 % of the activity loaded.

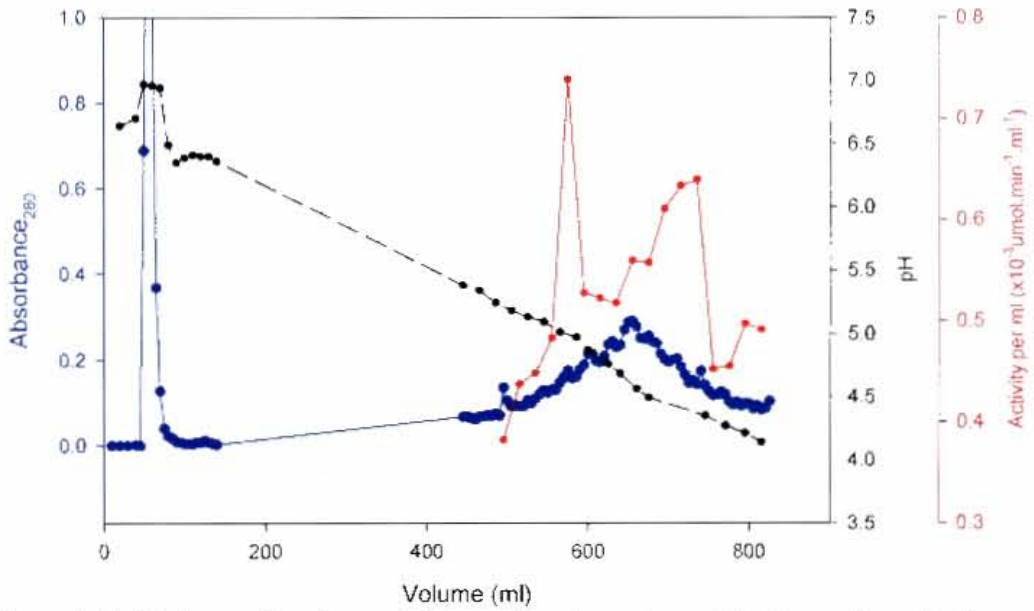

Figure 4.24: Elution profile of second chromatofocusing column. Absorbance shown in blue, pH in black and Total Activity in red.

4.8.5. DEAE Vydac Ion Exchange 2

The DEAE Vydac method was modified by the addition of 1 mM CHAPS to all the buffers. The position at which enzyme activity eluted from the Vydac 301VHP575 column was similar for the protein from chromatofocusing columns 1 and 2. The addition of 1mM CHAPS to the buffers used for the second Vydac 301VHP575 column did not significantly reduce the spreading of the enzyme activity, but it did result in the appearance of a minor peak of activity which eluted later. The inclusion of only the first peak of activity in the chromatofocusing column 2 resulted in less protein eluting with the activity, and this could clearly be seen when the active fractions were visualized on SDS PAGE (Figure 4.26).

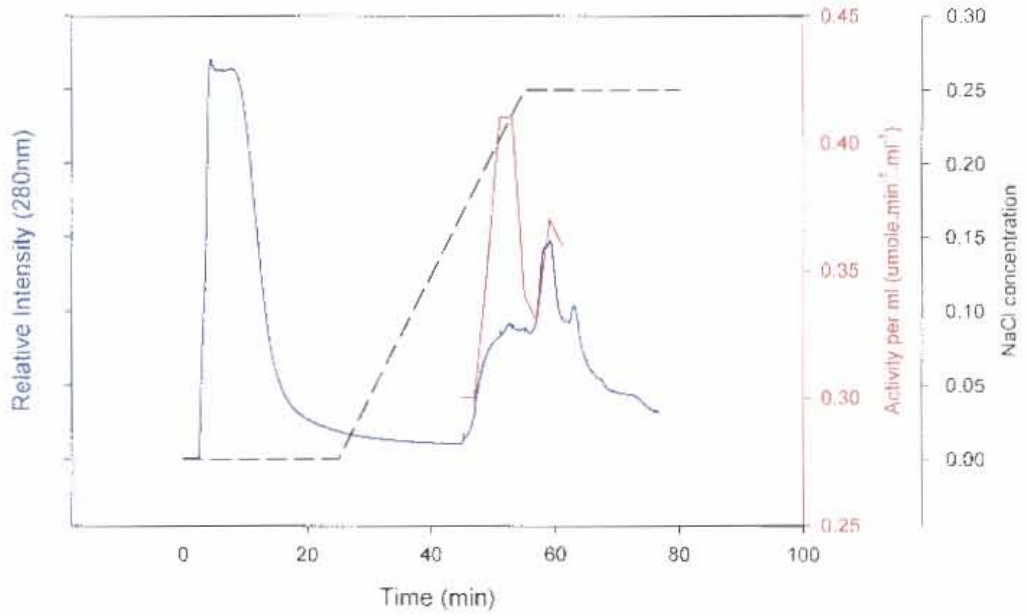

Figure 4.25: Elution profile of second Vydac ion exchange column. Relative Intensity at 280nm is shown in blue, NaCl concentration in black and activity in red.

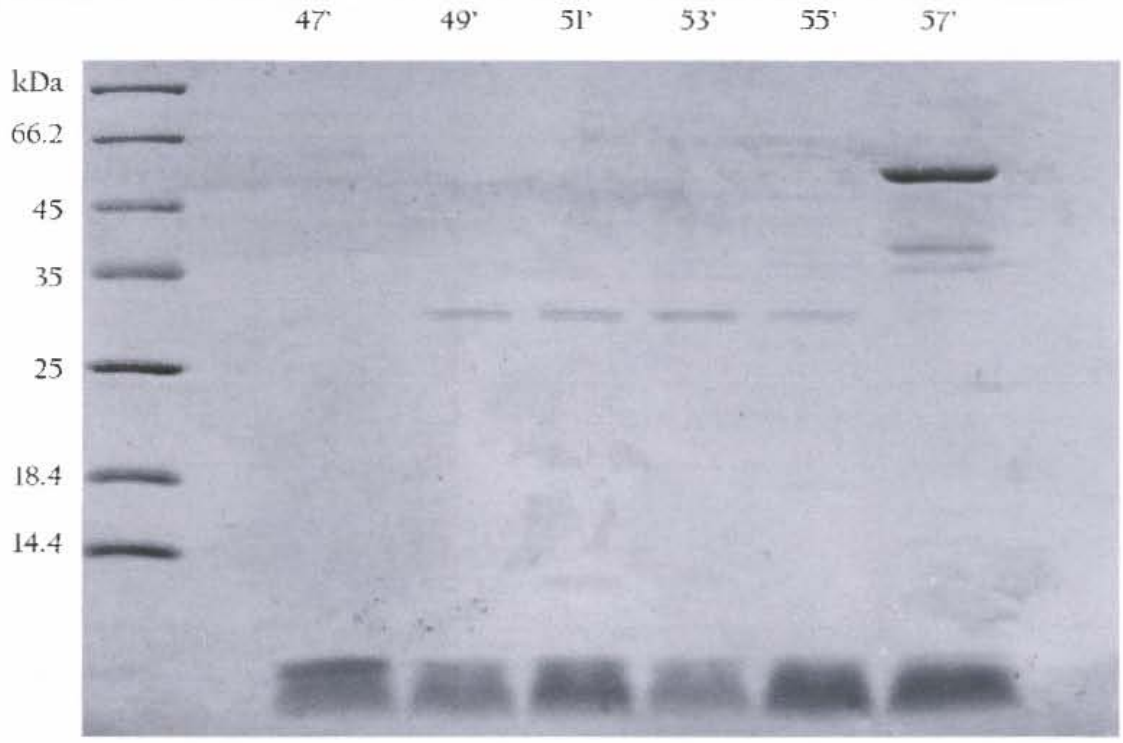

Figure 4.26: SDS PAGE of Vydac ion exchange column fractions containing highest activity. A TCA precipitation was performed to concentrate 600 ul of each fraction between 47 and 57 min.

The activity during the purification of the second half of the zinc IMAC fraction was significantly lower and this was due to storage of the protein for 6 weeks before the last two steps were performed. Although storage of the protein as an ammonium sulphate pellet at 4 °C was found to be the best method, it was not able to prevent a decrease in activity. Time constraints are therefore a limiting factor when considering the feasibility of the scale-up required to obtain sufficient material for identification of the enzyme.

The two protein bands (~ 30 000 Da) from lane 49 (Figure 4.26) were excised, processed and submitted for LC-MSMS. The upper band was designated A, and the lower band B. The fragment ion spectra obtained were analysed using MASCOT MS/MS Ion Search program (Matrix Science, London). The proteins identified as being significant matches for each band are indicated in Table 4.5.

Table 4.5: *Neurospora crassa* protein candidates obtained for samples A and B using MASCOT MS/MS Ion Search

Sample	MASCOT score	Matched peptides	Molecular weight Observed	Molecular weight Nominal	Annotation	Conserved Domains
A	141	6	30 000	61 024	Hypothetical protein gi|85113050	Glucose-1-phosphate uridylyltransferase
B	240	3	30 000	25 732	Vacular ATP synthase subunit E gi|85114075	ATP synthase subunit
	118	6		61 024	Hypothetical protein gi|85113050	Glucose-1-phosphate uridylyltransferase
	47	1		29 940	Hypothetical protein gi|85089532	Proteosome_beta Ntn_hydrolase

4.8.6. LC-MSMS Analysis and Identification of Candidate Proteins from DEAE Vydac 2

The most active fractions for the second Vydac column revealed only two bands, designated A and B. Sample A revealed only one significant match when a MASCOT MS/MS Ion search was performed, namely the hypothetical protein containing the glucose-1-phosphate uridylyltransferase conserved domain. This hypothetical protein was also a significant match for Sample B. Since bands A and B were very close together, this could be due to inaccurate separation of the bands during excision. MASCOT analysis of Sample B also revealed two candidate proteins, which were not seen previously in samples A-E. This may indicate the need for the removal of more abundant proteins by purification before those which occur in very low abundance can be detected. The importance of fractionation of complex protein samples was demonstrated in a study involving the detection of human growth hormone (hGH) in plasma (Wu *et al.,* 2002). Pre-fractionation by reverse-phase HPLC or separation of complex mixtures by 1D and 2D gel electrophoresis was shown to increase the sequence coverage and detection of hGH by LC-MS/MS. McCormack *et al.* (1997) were able to demonstrate using simple mixtures of proteins that proteins within a 30-fold difference in molar quantities could be reproducibly detected in the femtomole range. This detection however is dependent on the complexity of the protein sample being analysed and the resolving power of the HPLC step prior to mass spectrometry. Therefore, purification steps which reduce the complexity of protein mixtures prior to LC-MS/MS facilitate the detection of proteins of low abundance.

One of the requirements for identification of candidate proteins by MASCOT is that the gene of interest has been correctly predicted. Since errors are prevalent, especially in eukaryotes, a *de novo* peptide identification method was employed for Samples A and B to evaluate the MASCOT results. The programme used was an online version of PEAKS (available at www.bioinformaticsolutions.com) and the *N. crassa* proteins which were identified are listed in Table 4.6. While MASCOT searches databases with un-interpreted MS/MS data, PEAKS uses a computational algorithm to determine all possible sequences for the peptides, scores the peptides to determine the best sequence and then uses these peptides to search the selected database (Ma *et al.,* 2003). The analysis of Samples A and B by PEAKS *de novo* and database method selected the same five candidate proteins as MASCOT.

Table 4.6: *Neurospora crassa* protein candidates obtained using the PEAKS *de novo* and database method for samples A and B

Sample	PEAKS score	Matched peptides	Annotation	Conserved Domains
A	79.3 %	6	Hypothetical protein gi|32419014	Glucose-1-phosphate uridylyltransferase
	2.44 %	2	probable isoamyl alcohol oxidase gi|21622328	FAD binding domain FAD/FMN-containing dehydrogenase
	2.3%	2	Hypothetical protein gi|32417282	Serine/Threonine protein kinases, catalytic domain
B	97.64 %	3	Vacuolar ATP synthase subunit E gi|2493134	ATP synthase subunit
	93.31 %	6	Hypothetical protein gi|32419014	Glucose-1-phosphate uridylyltransferase
	76.21 %	1	Hypothetical protein gi|32414343	Proteosome_beta Ntn_hydrolase
	7.06 %	1	Hypothetical protein gi|32417214	REC signal receiver domain Response regulator containing CheY-like receiver domain
	3.88 %	1	Hypothetical protein gi|32407695	Glycosyl hydrolase family 10 Fungal-type cellulose-binding domain

In addition, the PEAKS analysis also identified four new protein candidates. The PEAKS score of these candidates were all below 10 and therefore could be chance events. One of the weaknesses of this identification method is that no significance cut-off is indicated, as is the case with MASCOT.

For both the MASCOT and PEAKS searches, the hypothetical protein with a uridylyltransferase conserved domain was the only candidate protein for band A. The predicted mass of this protein however is 61 024 Da, while it appears at approximately 30 000 Da on the SDS PAGE gel. To explore this discrepancy, the matched peptides for the MASCOT and PEAKS were examined. Interestingly, the peptides matched in the hypothetical protein containing a glucose-1-phosphate uridylyltransferase conserved domain by the MASCOT and PEAKS methods were identical (Figure 4.27). This indicates the power of the MASCOT search, despite the fact that it relies on un-interpreted LC-MS/MS spectra.

```
1   MAQAIRSALP DRLMPSNGDE EFAKRHHGKT RSHMVSTILS LCHHPSNKMT
51  VQEELTHRQA FENTSTSIAA AQMRNALTKL AETVKDPDQK KLFETEMDNF
101 FSLFRRYLND KAKGNEVNWD KIAPPAPHQI VDYESLANNN SVDFLNKLAV
151 LKLNGGLGTS MGCVGPKSVI EVRDGMSFLD MSVRQVEHLN RTYGSNVPIL
201 LMNSFNTDDD TAAIIKKYEG HNVDILTFNQ SRYPRIYKDS LLPVPKSFDS
251 PLHDWYPPGH GDVFESLYNS GILDKLIERG IEIIFLSNAD NLGAVVDLRI
301 LQHMVETDAE YIMELTNKTK ADVKGGTIID YEGSVRLLEI AQVPKEHVNE
351 FKSIKKFKYF NTNNIWMNVQ AVKRVVENNE LELEIIPNEK TIPGDKKGES
401 DISIVQLETA VGAAIKHFKG AHGVNVPRRR FLPVKTCSDL MLVKSDLYTV
451 KHGQLQMSSA RFGDAPLIKL GNDFKKVSDF QKRIPSIPKI IELDHLTITG
501 AVNLGRGVTL KGTVIIVATE GQTIDIPPGS ILENVVVQGS LRLLFH
```

Figure 4.27: Protein sequence of Hypothetical protein gi|85113050 The peptide fragments matched by the MASCOT MS/MS Ion search and PEAKS *de novo* and database methods are indicated in red.

The peptides matched all occurred between residues 185 and 390 and the estimated molecular weight of this region is approximately 24 000 Da. It is therefore possible that the ends of the protein have been removed by proteolytic degradation, resulting in a discrepancy between the observed and expected masses. In the reported purification of the Glucose-1-phosphate uridylyltransferase from *N. crassa* by Tovar & Ruiz-Herrera (1986), the activity was found to correspond to a single protein band after non-denaturing disc electrophoresis. When this band was excised and subjected to denaturing PAGE, four bands of molecular masses 63 000, 61 000, 57 000 and

55 000 Da were visible on the gel. The authors concluded these were four polypeptides which combined in different ratios to give an enzyme with a molecular mass of 580 000 Da. A search for all the genes in the *Neurospora crassa* database (www.broad.mit.edu/annotation/genome/neurospora/Home.html) containing the "glucose-1-phosphate uridylyltransferase conserved domain" yielded two hypothetical proteins, one annotated as a glucose-1-phosphate uridylyltransferase (NCU02797.3) and the second annotated as a UDP-*N*-acetylglucosamine pyrophosphorylase (NCU02109.3). The first gene corresponds to the hypothetical protein gi|85113050, which was consistently identified as a protein candidate by the MASCOT and PEAKS programmes for sample A (Vydac 2). It is possible that the band observed by Tovar J & Ruiz-Herrera J at 61 000 Da corresponds to this hypothetical protein and that the other bands are proteolytic fragments or contaminating proteins.

LC-MS/MS analysis and subsequent database searching failed to identify a protein candidate containing "methyltransferase" in its annotation. This is despite the removal of a large number of contaminating proteins and visualisation of two protein bands which appeared to correspond to the methyltransferase activity. There are two possible explanations for this discrepancy. Firstly, the histidine methyltransferase may occur at such low levels that it could not be visualized after SDS PAGE. In a purification of a similar enzyme, namely the S-adenosylmethionine:ε-N-l-Lysine Methyltransferase from *N. crassa*, the purified protein only constituted 0.00001% of the initial protein (Borum & Broquist, 1977). This purification utilized several kilograms of fungal mat to produce 122 g of protein in the crude extract. It is therefore conceivable that the scale on which the purification was attempted was too small to obtained sufficient protein for LC-MSMS analysis. A technique which could be used to confirm the presence of the enzyme at levels below the sensitivity of silver staining is photoaffinity labelling with [methyl-^{3}H] SAM. The method was used by Mosli Waldhauser *et al.* (1997) to detect low levels of *N*-7 methyltransferase from protein extracts of *Coffea Arabica L.* Although this method would indicate the position SAM-binding proteins after SDS PAGE, it would not necessarily allow the identification of the protein by LC-MSMS because of the low protein concentration. Another concern regarding the applicability of this method is the order of substrate binding to the histidine methyltransferase. The kinetic data reported previously and the difficulties experienced in this work with SAH affinity chromatography suggest the need for dimethylhistidine to bind to the enzyme before SAM. If this is the case, SAM photoaffinity labelling may not be possible.

Interestingly, despite the fact that a successful purification has been published for the S-adenosylmethionine:ε-N-l-Lysine Methyltransferase from *N. crassa*, the gene has as yet not been identified.

The second possible explanation for none of the candidate proteins being annotated as methyltransferase is that their annotations are incorrect. A case in point is the annotation of CbiT and all its homologues in sequence databases as "precorrin 8w-decarboxylases", as a result of sequence-based reasoning. The subsequent resolution of the crystal structure of CbiT revealed an SAM-dependent MTase-fold and an SAM binding pocket, which suggests that it functions as a methyltransferase. The protein has no structural similarity to proteins with decarboxylase activity and it is no longer clear if it is a decarboxylase (Keller *et al.*, 2002).

The hypothetical protein which contained a glucose-1-phosphate uridylyltransferase conserved domain was consistently identified in MASCOT searches. Since it belonged to the enzyme family of transferases, it was selected for further analysis to confirm its annotation.

4.9. Sequence Analysis of Hypothetical Protein Containing Glucose-1-phosphate Uridylyltransferase Conserved Domain from *N. crassa* (HP-GlcPU)

The first analysis tool used was BLAST (Altschul *et al.*, 1997), which aligns nucleotide or protein sequences with sequences in a database and calculates the statistical significance of the alignment. The analysis of HP-GlcPU showed a high degree of sequence conservation of the glucose-1-phosphate uridylyltransferase conserved domain (pfam01704.12) across species. The three best alignments where with hypothetical proteins and showed an overall sequence identity of 85.65% (Figure 4.28).

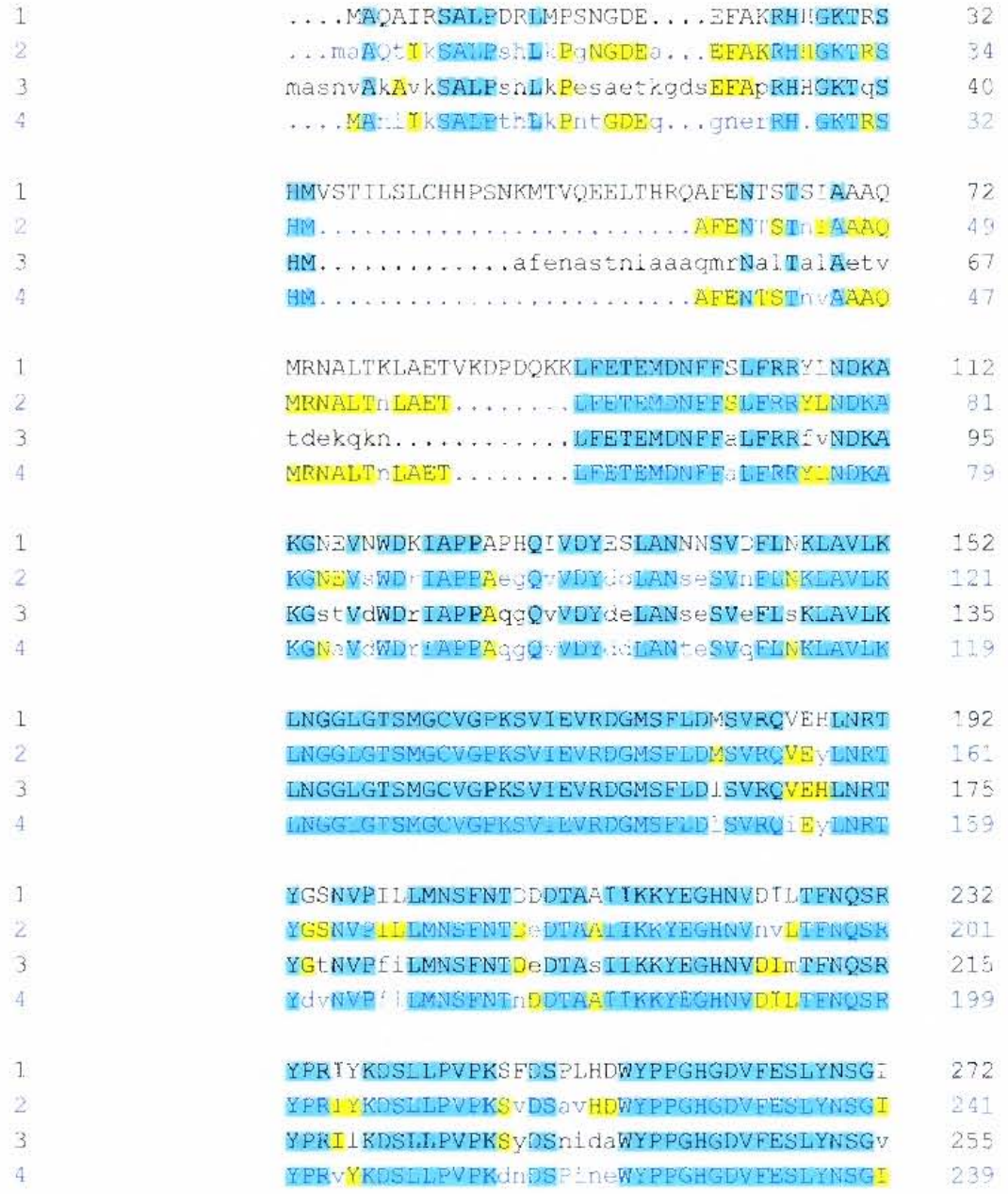

Figure 4.28: Alignment of three best BLAST hits for gi|85113050| (conserved hypothetical protein [Neurospora *crassa* OR74A]). Blue shaded region indicates sequence identity shared between all four sequences while the yellow shaded region shows sequence identity with gi|85113050|. The sequences share an overall identity of 85.65%.

1: gi|85113050| conserved hypothetical protein [Neurospora crassa OR74A]

2: gi|116181760| conserved hypothetical protein [Chaetomium globosum CBS 148.51]

3: gi|39951977| hypothetical protein MG01631.4 [Magnaporthe grisea 70-15]

4:gi|46107282| conserved hypothetical protein [Gibberella zeae PH-1]

The best scoring hit, of which the function had been confirmed by enzymatic studies, was the UDP-glucose pyrophosphorylase from *Cricetulus griseus* (gb|AAC53343.1|). HP-GlcPU had a 55% identity with this protein. The high degree of sequence conservation observed between proteins containing the pfam01704.12 domain suggests a common function, since sequence homology generally translates into structural homology (Clothia & Lesk, 1986). The opposite however is not necessarily true, since a lack of sequence homology between proteins does not rule out functional similarities. This is clearly illustrated by the family of Class 1 SAM-dependent methyltransferases. Proteins in this class contain four conserved motifs, but have a very low overall sequence homology. Despite their low sequence conservation, Class 1 MTases possess a highly conserved core structure known as the SAM-dependent MTase-fold. It is therefore not sufficient to rely solely on sequence information when investigating function, but also to utilize structural information.

4.10. Structural Analysis of Hypothetical Protein Containing the Glucose-1-phosphate Uridylyltransferase Conserved Domain (HP-GlcPU)

The second analysis tool used to confirm the annotation of the hypothetical protein was GenTHREADER (Jones 1999), which uses a combination of sequence and structural properties to predict protein structure. GenTHREADER analysis includes three steps. Firstly, a sequence alignment profile is generated using PSI-BLAST. This profile is then used to make alignments with each member of the fold library to generate scores according to their structural (e.g. solvation energy sum) and sequence (e.g. sequence length) properties. Finally, these scores are fed into a trained feed-forward neural network which generates an output between 0 and 1 for each alignment (McGuffin & Jones, 2003).

The structures with the three highest scores are shown in Table 2.7. and they were the N-acetylglucosamine 1-phosphate uridyltransferase (GlmU) from *E.coli,* the human UDP-*N*-acetylglucosamine pyrophosphorylase (ADPGlcNAc PPase) and the potatoe tuber ADP-glucose pyrophosphorylase (ADP-Glc PPase). Despite the fact that these proteins had very low sequence identity with HP-GlcPU, (12,6 % 14,5 % and 9.1 % respectively) the GenTHREADER scores were all above 0.9 (out of 1), indicating the importance of structural parameters in the calculation of the overall GenTHREADER scores.

Table 4.7: Three highest scoring structures for the GenTHREADER search of HP-GlcPU

GenTHREADER score: 0.933

Description:
Crystal Structure of N-acetylglucosamine 1-phosphate uridyltransferase from *E coli* bound to *N*-acetyl-*D*-glucosamine. Chain: a Fragment: truncated form after r331.

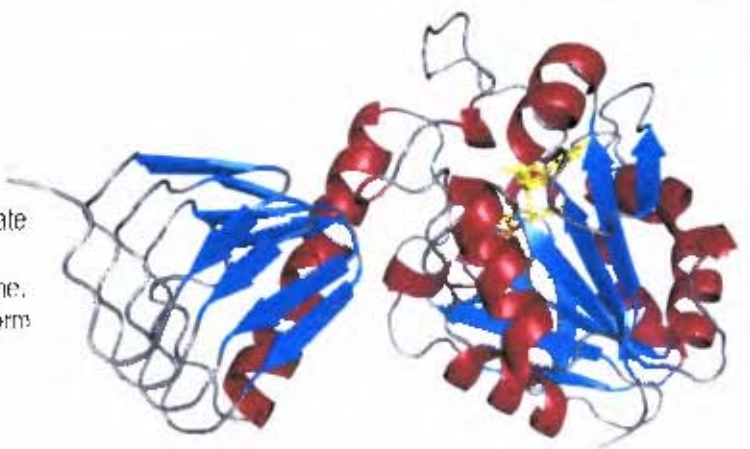

GenTHREADER score: 0.922

Description:
UDP-*N*-acetylglucosamine pyrophosphorylase (**Human AGX1**) bound to *N*-acetyl-*D*-glucosamine (Chain: a)

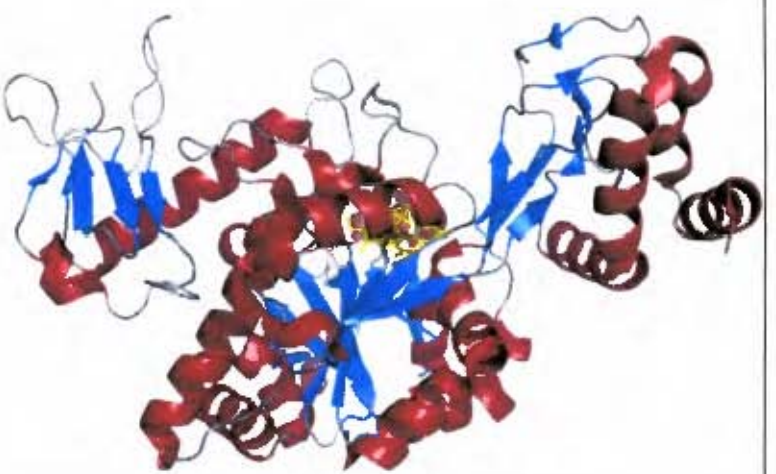

GenTHREADER score: 0.910

Description:
Crystal structure of potato tuber adp-glucose pyrophosphorylase (Chain a)

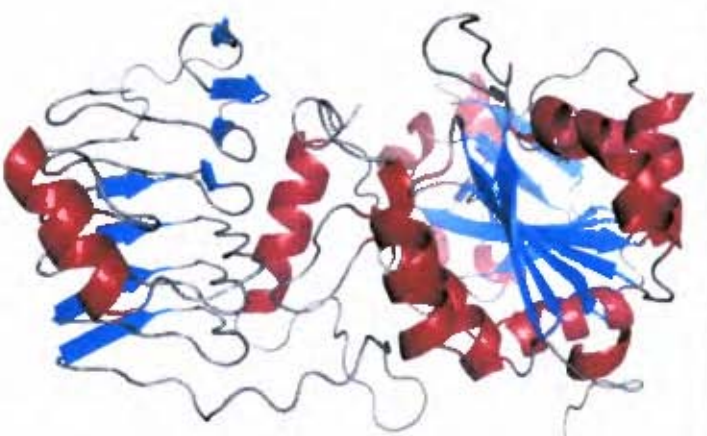

One limitation of this technique is its dependence on solved protein structures and therefore improvements to these results would be expected as crystal structures of proteins which are more closely related to HP-GlcPU are solved.

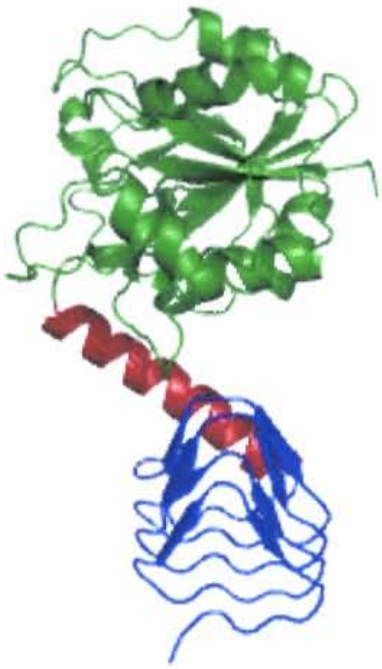

Figure 4.29: Cartoon structure of GlmU from *E.coli* showing the N-domain in green, the C-domain in blue and the helix between the two domains in red.

All three of the matched structures contain a fold consisting of a central mixed β-sheet surrounded by helices, which is similar to the dinucleotide-binding Rossmann fold (Rossmann *et al.*, 1975 in Brown *et al.*, 1999). In the structures of GlmU from *E.coli* and the potato tuber ADP-Glc PPase, this fold forms the N-domain, while the C-domain consists of a left-handed parallel β-helix. The two domains are linked by a long α-helical arm (Figure 4.29) (Brown *et al.*, 1999; Jin *et al.*, 2005). In the ADPGlcNAc PPase structure, the Rossmann-like fold forms a core structure, with a short N- and C-domain on either side of it (Peneff *et al.*, 2001). Brown *et al* (1999) showed that the N-domain of the GlmU is responsible for its uridyltransferase activity, while the C-domain is responsible for its acetyltransferase activity. In the ADP-Glc PPase the N-domain is the catalytic domain (Jin *et al.*, 2005). Although the mixed β-sheet in the GlmU resembles the MTases fold (seven strands, with one strand anti-parallel to the others), the order of the strands is different. In GlmU the β-sheet strand order is 7-5-6-4-1-2-3 (Brown *et al.*, 1999), while in MTases the order is generally 6-7-5-4-1-2-3 (Cheng & Roberts, 2001).

4.11. Comparative Modeling of Hypothetical Protein Containing Glucose-1-phosphate Uridylyltransferase conserved domain (HP- GlcPU) from *N. crassa*

Comparative modeling involves the generation of a 3-dimentional model of a protein (target) from the solved 3-D structures of one or more related protein(s) (template(s)). Modeling consists of three steps. Firstly a template is selected by searching existing databases of solved structures and an optimal alignment is generated. Secondly, restrains are obtained from the template and the alignment is used to identify the equivalent residues in the target. Finally, the model is generated and optimized until it best satisfies the restraints (Sánchez R & Šall A.).

A model of the HP- GlcPU was generated by Mr. EK Murungi using the comparative modeling programme MODELLER (http://salilab.org/modeller/). The target sequence that was selected was Human AGX1, which corresponds to the second highest GenTHREADER match. The model is shown below in Figure 4.30A, while a close-up of the β-sheet organisation of the core shown in Figure 4.30B.

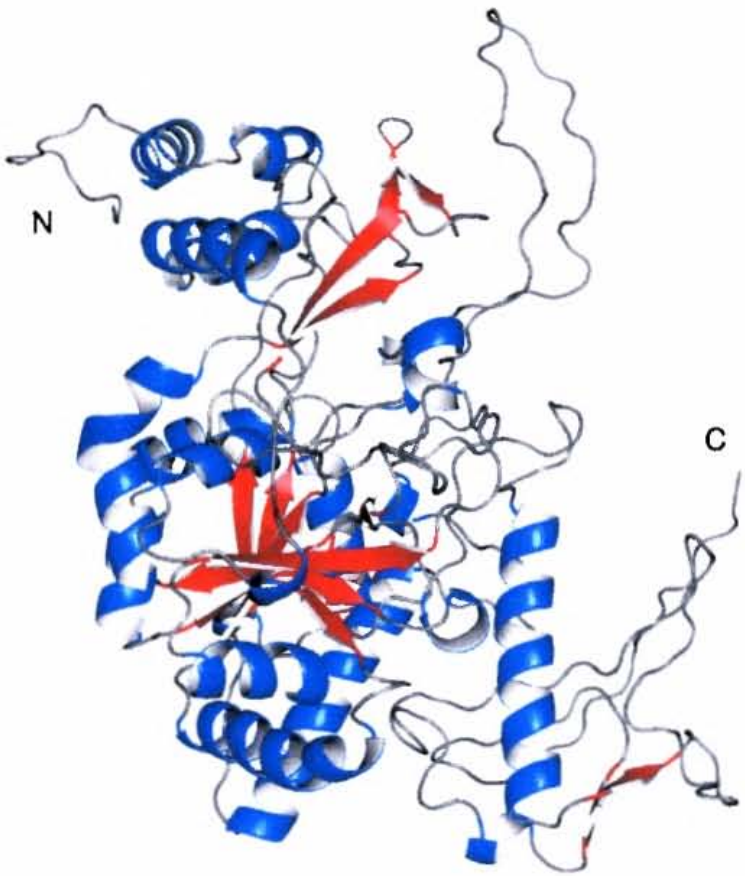

Figure 4.30A: Model of HP-GlcPU. The structure contains a core which consists of an 8-strand, mixed β-sheet surrounded by helices and is similar to the Rossmann fold. The core is flanked by a C-terminal and N-terminal domain.

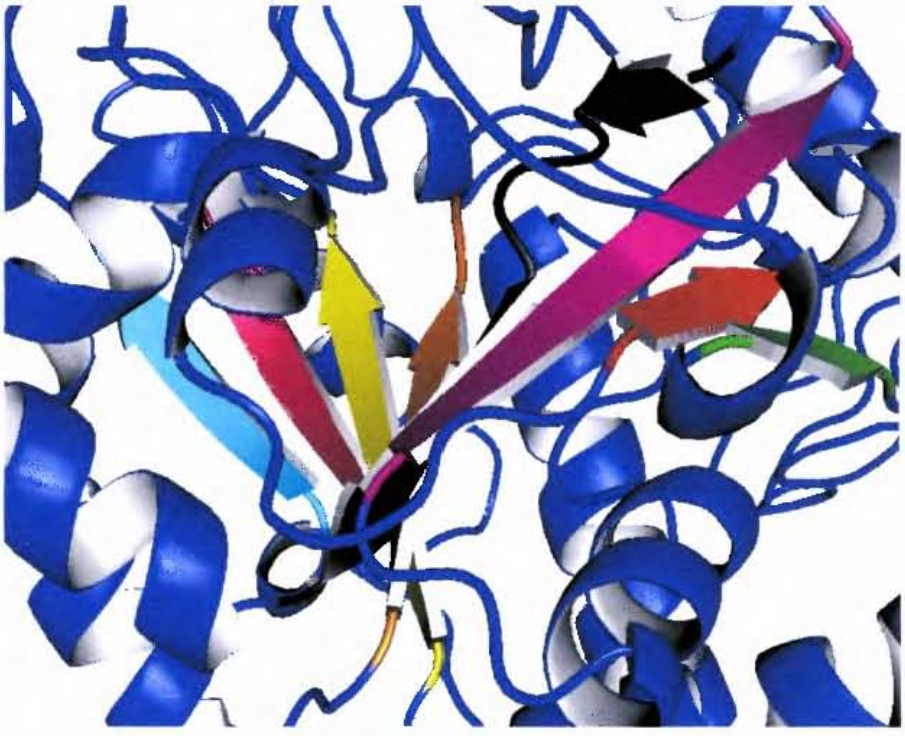

Figure 4.30B: Core structure of the HP-GlcPU model. The core structure consists of eight strand mixed β-sheet in the order 1-12-6-7-5-2-3-4 (from right to left), in which strand 7 is anti-parallel. **β_1 green, β_2 yellow, β_3 pink, β_4 cyan, β_5 orange, β_6 magenta, β_7 black, β_{12} red.**

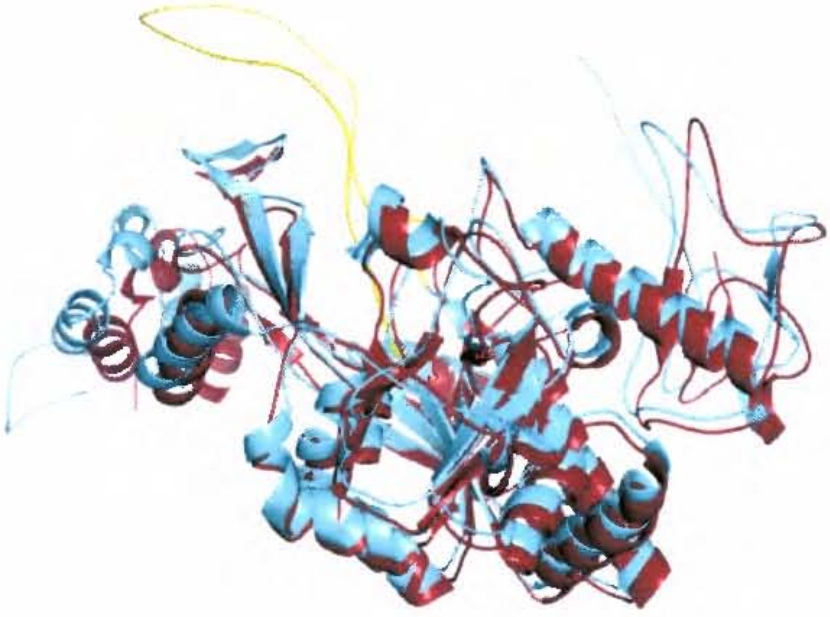

Figure 4.31: Structural alignment of HP-GlcPU model and the template on which it was modelled. The template is shown in red and the model in blue. The loop of the model which deviates from the template is shown in yellow.

The structural alignment of the model of HP- GlcPU and the template, Human AGX1, (Figure 4.31) shows the similarity between the two structures. Both structures contain a core resembling a Rossmann fold, flanked by a C-terminal and N-terminal domain. Deviation from the template is present at the two termini and between amino acids 111 and 155. This region forms a large loop (shown in yellow) in the model and corresponds to a region of very low identity between the two proteins.

Despite the low overall sequence homology between the two proteins, their structures are similar. This demonstrates that in order to generate a similar fold only certain critical residues need to be conserved rather than the entire sequence. Comparative modeling is therefore a powerful tool for the identification of possible methyltransferases, since they possess poor overall sequence homology but a highly conserved MTase fold. The core of the model possesses an eight strand mixed β-sheet with strand 7 being anti-parallel (Figure 4.30). Interestingly strand 7 is situated between strands 5 and 6, which is characteristic of the MTase fold.

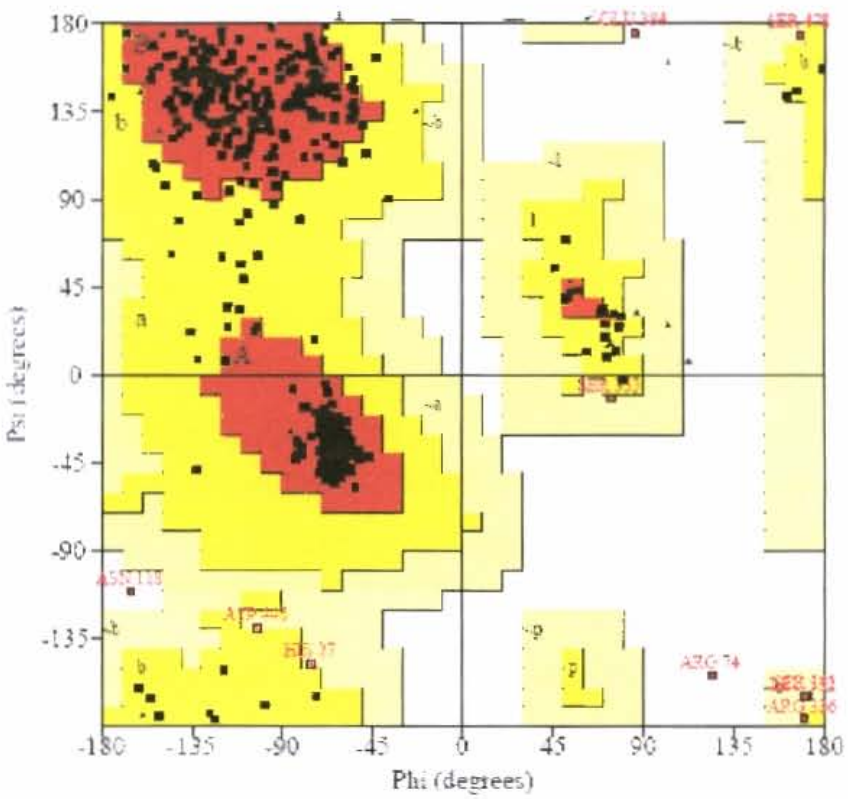

Figure 4.32: Ramachandran Plot of the model of HP-GlcPU.
The plot shows that only three residues are present in the disallowed region.

One of the critical steps in generating a model is in choosing the correct template, which in turn is limited by the available solved structures. Models generated from targets with greater than 50% identity are very accurate, but this accuracy declines greatly as the identity falls below 20% (Ginalski, 2006). Since the template used here has less than 20% identity with HP-GlcPU the accuracy of the model is expected to be poor and therefore caution is required when deriving insights from the model. The model was validated using PROCHECK (Laskowski *et al.,* 1993), which checks the stereochemistry of structures. The result is illustrated in the form of a Ramachandran Plot, which plots the phi and psi angles for each residue in the structure. The Ramachandran plot for the model of HP- GlcPU is shown in Figure 4.32. Despite the poor sequence identity, the Ramachandran Plot indicates that the quality of the model is excellent with 87.2% of the residues in the most favourably allowed regions, 10.7% in the additionally allowed regions, 1.4% in the generously allowed region and only 0.6% in the disallowed region. The three residues which are in the disallowed region are located in the loop regions of the model, which due to the flexibility of these regions may have unusual geometry. Although several proteins which have greater than 50% identity with HP- GlcPU are known, their crystal structures have not been solved. The improvement of this model is therefore dependent these structures being solved.

Although sequence and structural analysis can provide insights about the function of a protein, they are limited by the amount information available for closely related proteins. Improvements to genome annotation methods, increased experimental knowledge and the increasing the number of solved protein structures will lead to the exponential increase in the usefulness of these predictive techniques. The sequence and structural analysis performed using the available data suggests that HP-GlcPU is not a methyltransferase and therefore rules it out as the first enzyme in ergothioneine biosynthesis.

PART B:

Conditions Affecting Ergothioneine Levels in *Mycobacterium smegmatis*

The function of Ergothioneine (ESH) in mycobacteria has never been determined. Biochemical studies have shown that ESH has antioxidant properties and is able to scavenge hydroxyl radicals, superoxide and peroxynitrite. It is therefore postulated that ESH plays a role in protecting mycobacteria against the reactive oxygen intermediates (ROI) and reactive nitrogen intermediates (RNI).

5.1. The Generation of ROI and RNI as a Host Defense against Bacterial Pathogens

A relatively effective host-defense against bacterial pathogens is the production of reactive oxygen intermediates (ROI) and reactive nitrogen intermediates (RNI) by innate immune cells. Although all eukaryotic cells produce ROI and RNI at low levels, macrophages possess two enzymes which generate reactive species in large amounts when they are required. (NADPH)-oxidase catalyses the production of superoxide ($O_2^{\cdot-}$) which in turn leads to the formation of hydrogen peroxide (H_2O_2) and the hydroxyl radical (OH•). The production of NO is catalysed by a family of enzymes called the NO synthases (NOSs), and its formation under physiological conditions can result in the production of other reactive species such as nitrosonium (NO^+), nitroxyl anion (NO^-), and S-nitrosothiols (Stamler *et al.*, 1992). The reaction of superoxide with nitric oxide leads to the formation of peroxynitrite, which is a potent biological oxidant. Therefore, the production of superoxide and nitric oxide results in the formation, both enzymatically and spontaneously, of a range of species which are damaging to cells.

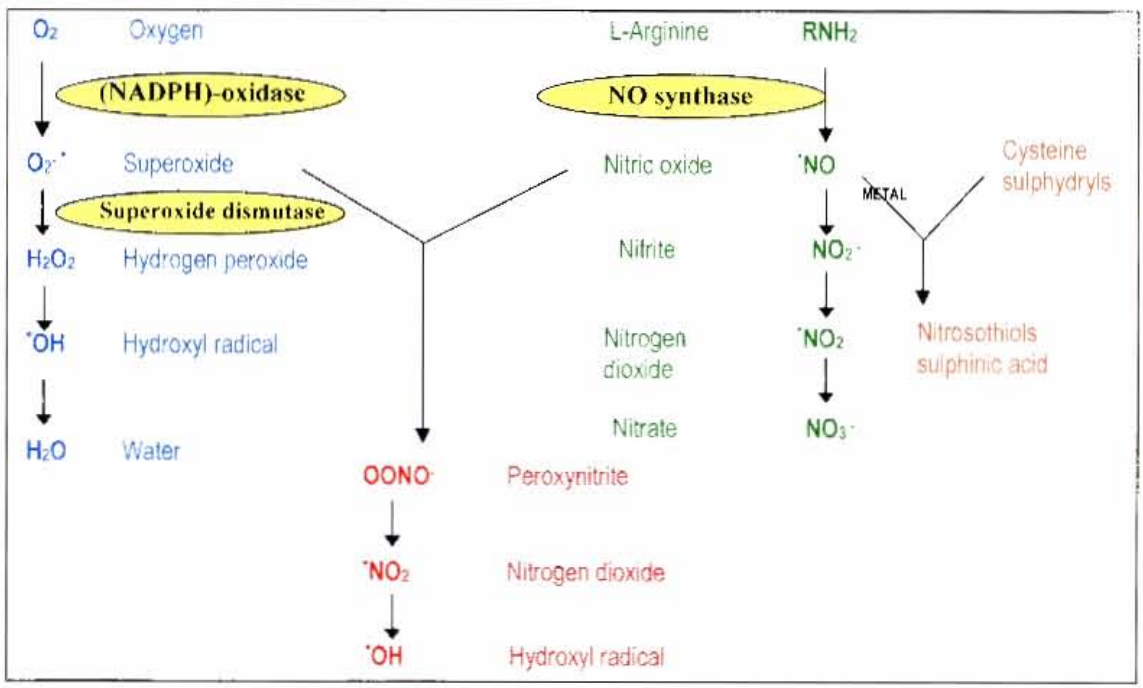

Figure 5.1: Schematic of the ROI and RNI generation pathways. The steps catalysed by the enzymes (NADPH)-oxidase (phox), Nitric oxide synthase (NOS2) and superoxide dismutase (SOD) are indicated. (Modified from Zahrt and Deretic 2002)

5.2. The Role of ROI and RNI in Tuberculosis

Genetic deficiencies in NADPH-oxidase (phox) in humans cause chronic granulomatous disease (CGD), which is associated with recurrent infections. However, the role of NADPH-oxidase in response to *M. tuberculosis* infection is unclear, since tuberculosis was only shown to be a major threat to CGD patients in areas with a high prevalence of TB (Lau *et al.*, 1998). The importance of NADPH-oxidase as part of the innate immune response to TB infection may be undermined by the bacteria's ability to counter the oxidative burst. This hypothesis is supported by the finding in mice, that the MTB KatG catalase-peroxidase has a major role in the pathogenesis of TB only in hosts capable of generating an oxidative burst (Ng *et al.*, 2004).

In the host defense against intracellular microorganisms such as *M. tuberculosis*, the high out-put production of nitric oxide (NO) plays an important role. Although the mechanism(s) by which RNIs kill *M. tuberculosis* is not fully understood, it is thought to be the modification of bacterial DNA, proteins and lipids both on the microbial surface and intracellularly. Rhee *et al.* (2005) showed that RNIs could act to inactivate enzymes through the S-nitrosylation of their active sites. The induction of macrophage apoptosis by NO, may also initiate mycobacterial killing by facilitating the fusion of mycobacterial-containing vacuoles to lysosomes.

In the mouse model of TB, the disruption of NOS2 (NOS2 -/-) is associated with a significantly higher risk of disseminated disease and mortality after infection with *M. tuberculosis* as compared with wild type mice (MacMicking *et al.*, 1997). When activated macrophages from wild-type, phox-deficient and NOS2-deficient mice were infected with *M. tuberculosis*, the wild-type and phox-deficient macrophages were able to control bacterial growth while NOS2-deficent macrophages were not. This correlation however was not as clearly seen in infected mice, since the susceptibility to *M. tuberculosis* was tissue-dependant. Although mice deficient in either RNI or ROI both showed elevated growth of bacilli in their lungs compared to wild-type mice, this increase was delayed in NOS2 KO mice. The inability of mice to produce RNI also resulted in elevated growth of *M. tuberculosis* in the spleen, which was not observed for the mice deficient in ROI (Adams *et al.*, 1997). The production of $gp91^{phox-/-}/NOS2^{-/-}$ double knock-out mice revealed that phox and NOS2 can compensate for each other's deficiency in the prevention of spontaneous infections (Shiloh *et al.*, 1999). Activation of *M. tuberculosis*-infected wild-type macrophages with IFN-γ resulted in the differential expression of 68 *M. tuberculosis* genes, however this expression pattern was obliterated when $NOS2^{-/-}$ macrophages were used (Schnappinger *et al.*, 2003). Most of

these genes were also induced after exposure to NO in liquid culture, suggesting that the change in the *M. tuberculosis* transcriptome after IFN-γ activation is directly caused by NO. Since there is no known correlate to the NOS2 KO in humans, the role of RNI in *M. tuberculosis* infection remains controversial. Collectively studies suggest that NO is likely to play a contributory role in the defense against *M. tuberculosis*. Macrophages from the lungs of TB patients have been shown to express NOS2 in potentially mycobacteriocidal amounts, and could use it to kill *M. tuberculosis* in vitro (Nathan and Shiloh, 2000).

5.3. Resistance Mechanisms of *M. tuberculosis* to ROI and RNI

The genetically regulated response of bacteria to ROI and RNI has been extensively studied in the enteric bacteria *Escherichia coli* (*E. coli*) and *Salmonella typhimurium*. In these organisms two response systems, namely the OxyR and the SoxRS systems, have been identified (Reviewed in Demple, 1999; Pomposiello & Demple, 2001; Zahrt and Deretic, 2002). The OxyR protein is a transcription factor which responds to hydrogen peroxide stress and nitrosothiols. OxyR activated genes include *katG* catalase-peroxidase which removes hydrogen peroxide from the cell and *gorA* (Glutathione reductase), which functions to maintain the redox balance within cells. The SoxRS system responds to superoxide and nitric oxide stress, and the induced genes act collectively to prevent or repair oxidative damage by a number of mechanisms. These include scavenging of oxidants, repairing DNA damage and altering permeability of the bacterial cell.

The study of the genetically regulated response of mycobacteria to ROI has revealed some surprising results. In enteric bacteria, the OxyR response facilitates the development of resistance to lethal doses of hydrogen peroxide as a result of pre-treatment with sub-lethal doses. When similar experiments were performed with mycobacterial species only *M. smegmatis* showed comparable results, while *M. bovis* and *M. avium* did not develop resistance (Sherman *et al.*, 1995). Furthermore, sequence analysis has revealed that the OxyR gene in *M. tuberculosis* contains a number of mutations and is likely to be a pseudo gene. The genome sequence of *M. tuberculosis* also revealed that the SoxRS regulon is absent (Cole *et al.*, 1998). The exposure of *M. bovis* to hydrogen peroxide resulted in the induction of only a single protein (compared to more than 10 in *M. smegmatis*) (Sherman *et al.*, 1995), while in *M. tuberculosis* exposure to menadione and cumene hydroperoxide resulted in the induction of only a few peptides (Garbe *et al.* 1996). This may suggest that pathogenic mycobacteria do not

require the induction of genes to combat oxidative stress or alternatively, that a different regulation system may be present in pathogenic mycobacteria.

Genome expression profiling of *M. tuberculosis* exposed to hypoxic conditions revealed in a significant change in the expression of approximately 100 genes, including the upregulation of 47 genes (Sherman *et al.,* 2001). The exposure of *M. tuberculosis* to low doses of nitric oxide (nanomole range) was found to induce the same subset of genes, and rt-PCR performed on RNA extracted from lung tissue of mice infected with *M. tuberculosis* revealed that five sentinel genes of the group were highly expressed in *M. tuberculosis* during infection (Voskuil *et al.,* 2003). Park *et al.* (2003) demonstrated that in *M. tuberculosis* the hypoxic response is mediated by the *dosRS* two-component system. The same system exists in *M. smegmatis*, in which it was shown to regulate gene expression on entry in stationary phase induced by oxygen limitation (O'Toole *et al.,* 2003). DosR is a transcription factor which binds to a consensus sequence present upstream of most genes induced by hypoxia (Park *et al.,* 2003). In response to hypoxia the two sensor kinases, *dosS* and *dosT*, phosphorylate DosR which increases its affinity for DNA thereby upregulating transcription (Roberts *et al.,* 2004). Interestingly, the *M. tuberculosis dosR* mutant was found to be hypervirulent in immunodeficient and immunocompetent mice, and showed improved survival in IFN-γ activated macrophages (Parish *et al.,* 2003). The majority of the genes induced by the DosRST system are hypothetical proteins, which demonstrates that dormant state in mycobacteria remains poorly understood.

Of the genes up-regulated in *E. coli* by the OxyR response, only two homologues have been identified in mycobacteria, namely *katG* and *ahpC* (Sherman *et al.,* 1995). KatG is a catalase-peroxidase, which is required for the activation of the front-line anti-tubercular drug isoniazid (INH) (Zhang *et al.,* 1992). The most common mechanism of resistance to INH in *M. tuberculosis* is the inactivation of *katG*. AhpC is an alkyl hydroperoxide reductase, which is able to detoxify organic peroxides. Despite the loss of OxyR, AhpC is important during infection since wild-type *M. tuberculosis* survives better in un-stimulated macrophages than the AhpC-mutant. This survival advantage is abrogated after stimulation of the macrophages with IFNγ, suggesting that the role of AhpC may be stage-specific (Master *et al.* 2002). INH-resistant strains of *M. tuberculosis* which lack *katG* over-express AhpC, which appears to compensate for the loss of KatG activity (Sherman *et al.,* 1996). *M. tuberculosis* also has two superoxide-dismutases (SODs), *sodA* and *sodC*, which convert superoxide to molecular oxygen and

hydrogen peroxide. A *sod*C mutant of *M. tuberculosis* was found to have increased sensitivity to exogenous superoxide and the oxidative burst generated by IFN-γ activated macrophages (Piddington *et al.*, 2004).

5.4. The Role of Thiols in Protecting *M. tuberculosis* against ROI and RNI

Various mycothiol-deficient mutants have been used to demonstrate the role of mycothiol in protecting *M. tuberculosis* against ROI and RNI. The *M. tuberculosis* Rv1170 (MshB) mutant produced approximately 20 % of wild-type levels of mycothiol during exponential growth. This decrease in mycothiol production resulted in increased sensitivity to the organic peroxide cumene hydroperoxide (Buchmeier *et al.*, 2003). A *M. tuberculosis* MshD mutant, which produces approximately 1% of mycothiol as compared to the wild-type, showed a moderate increase in sensitivity to hydrogen peroxide (Buchmeier *et al.*, 2006). In *M. tuberculosis Erdman* the MshC (Sareen *et al.*, 2003) and MshA (Buchmeier & Fahey, 2006) were found to be essential, suggesting that MSH is required for growth of this strain under laboratory conditions. In genome-wide screen using transposon mutagenesis, MshD was found to be essential for survival of *M. tuberculosis* within macrophages (Rengarajan *et al.*, 2005).

5.5. Aim

Since no ergothioneine-deficient mutants have as yet been identified, its role in protection against ROI and RNI is not known. Due to its shorter generation time and fewer handing constraints, *M. smegmatis* was chosen as a model for the study of the role of ergothioneine in mycobacteria. The aim in this study was to monitor the levels of ergothioneine under various conditions, including exposure to exogenous ROI and RNI, with the intention of better understanding its function.

CHAPTER 6: MATERIALS & METHODS

6.1. Materials

Chemical/Reagent:	**Supplier:** (see Appendix C for details)
2,3-dimethoxy-1,4-naphthoquinone	Sigma
2'-bromoacetonaphthone	Sigma
H_3BO_3	Merck
NH_4OH	Riedel-de Haën
KCl	BDH
KH_2PO4	Merck
K_2HPO_4	Fluka
NH_4HCO_3	Saarchem
$NaNO_3$	Merck
NaOH	Fluka
NaCl	Fluka
Protein assay reagent	BioRAD
Bovine serum abumin	Roche
Ergothioneine	Pharmatech International
Formic acid	Riedel-de Haën
Glutathione (reduced)	Boeringer Ingelheim
Glycerol	Sigma
HCl	BDH
Middlebrooks 7H9 base	DIFCO
Perchloric Acid	Merck
Tween 80	Sigma
Solvents:	
Acetonitrile (HPLC grade)	Sigma
TFA (HPLC grade)	Sigma
HPLC columns:	
Luna $C_{18(2)}$ (200 x 4.6 mm 5μ)	Phenomenex
Preotein and Peptide C_{18} preparative column (250 x 21.2 mm 10μ)	Vydac
Phenyl hexyl column (200 x 4.6 mm 5μ)	Phenomenex

6.2. Methods

6.2.1. Survival of *M. smegmatis* in the Presence of DMNQ

An exponential phase starter culture of *M. smegmatis* MC^2 was diluted 100-fold into six 25 ml aliquots of Middlebrooks 7H9 media containing 5 % glycerol and 0.05 % Tween 80. 2, 3-dimethoxy-1, 4-naphthoquinone (DMNQ) was added to five of the cultures to give the final concentrations of 5, 10, 20, 50 and 100 μM. The sixth culture was used as a control. The six cultures were incubated at 37°C with shaking (200rpm), and their growth monitored by measuring the absorbance at 600nm after 24 and 48 hours.

6.2.2. Monitoring Thiol Levels in the Presence of DMNQ

Two 100 ml aliquots of Middlebrooks 7H9 media containing 5 % glycerol and 0.05 % Tween 80 were inoculated from a starter culture of *M. smegmatis* MC^2, and grown at 37°C with shaking (200 rpm). Cultures were grown to early exponential phase and DMNQ was then added to one culture at a final concentration of 20 μM. Two 5ml aliquots were removed from each culture at 0, 1, and 3 hrs after the addition of DMNQ. The growth of the cultures were monitored by measuring absorbance at 600nm and the cells were pelletted and frozen for later analysis of the thiols. A standard curve was constructed which related OD_{600} to colony forming units (Appendix A) and used to determine the amount of thiols presents per 10^9 cells.

6.2.3. Monitoring Thiol Levels in the Presence of S-Nitrosoglutathione

The synthesis of nitrosoglutathione was performed as previously described by Vogt RN and Steenkamp DJ. (2003). Briefly, equimolar amounts of glutathione and sodium nitrite were dissolved in 0.1 M HCl and incubated at 23°C for 20min. The solution was prepared on the day of use and was quantified by measuring its absorbance at 335 nm (ε_{335} = 920 $M^{-1}.cm^{-1}$). Growth of *M. smegmatis* in the presence of S-nitrosoglutathione was performed as previously described by Vogt *et al.*(2003). The synthesized nitrosoglutathione was added to an exponential phase culture of *M. smegmatis* MC^2 at a final concentration of 250μM. Two 5ml aliquots were removed from the culture at 0, 1, 3 and 10 hrs after the addition of nitrosoglutathione. The growth of the culture was monitored by measuring total protein and the cells were pelletted and frozen for later analysis of the thiols.

6.2.4. Synthesis of Ergothioneine Disulphide

Ergothioneine disulphide was synthesized via its S-nitroso derivative using a modification of the method described by Amado *et al.* (2001). Ergothioneine was combined with an equimolar amount of sodium nitrite, in the presence of 0.1 M HCl. The reaction was monitored spectrophotometrically between 220nm and 350 nm, using an Ocean Optics USB4000 spectrophotometer. The products of the reaction were separated by HPLC using a Luna 5μ $C_{18\,(2)}$ (250 x 4.60 mm) reverse phase column. The

column was eluted with 0.1 % TFA and the product of the reaction was identified by mass spectrometry.

6.2.5. Determination of the Stability of Ergothioneine Disulphide

Six micromoles of ergothioneine were reacted to form ergothioneine disulphide. The disulphide was isolated using a preparative protein and peptide C_{18} column eluted isocratically with 0.1 % TFA, 5 % CH_3CN. The pH of the solution containing the disulphide was raised to between 8 and 9 using sodium carbonate and incubated at room temperature for 30 min. After incubation the components of the mixture were then separated by HPLC on a luna 5μ $C_{18\ (2)}$ column (250 x 4.60 mm) column eluted with 0.1 % TFA.

6.2.6. Determination of Ergothioneine Levels in Different Phases of Growth

A starter culture of *M. smegmatis* MC^2 was used to inoculate 100 ml of Middlebrooks 7H9 media containing 0.5 % glycerol and 0.05 % Tween 80. The culture was grown at 37°C in a rotary-shaker incubator at a speed of 200rpm. At each time point, two 5ml samples were removed from the culture and the cells were pelletted by centrifugation. The media and cells were frozen separately at -20°C until thiol analysis was performed. Growth was monitored by measuring the absorbance at 600nm and by determining total protein.

6.2.7. Effect of Adding Ergothioneine to the Growth Media

A starter culture of *M. smegmatis* MC^2 was used to inoculate 100 ml of Middlebrooks 7H9 media containing 0.5 % glycerol and 0.05 % Tween 80. The culture was grown at 37°C in a rotary-shaker incubator at a speed of 200rpm. Once the culture had reached early exponential phase, it was split into 10 ml cultures and ergothioneine added at a range of concentrations between 2 and 100 μM. These, along with a control culture to which no ergothioneine had been added, were incubated at 37 °C with shaking. Growth of the cultures was monitored by measuring the absorbance at 600nm.

6.3. Quantitative Methods:

6.3.1. Monitoring of Culture Growth by Total Protein

At each sampling time point, two 1 ml aliquots of the culture was removed to determine total protein as previously described by Meyers *et al.* (1998). Cells were centrifuged twice at 7 300 rpm for 5min. The supernatant was removed and the cells were then washed with 500μl of PBS (pH 7.4). The washed cells were stored at -80°C for later analysis. The frozen cells were resuspended in 500μl of 1M NaOH, and boiled for 10 min. The cell debris was removed by centrifugation at 16 100g for 30min and 100 μl of the supernatant was neutralized with 5M HCl. The BIO-RAD protein assay (Appendix

A) was then used to determine the protein in 50µl of the neutralized extract. A standard curve was constructed using Bovine Serum Albumin standards (Appendix A).

6.3.2. Quantitative Analysis of Thiols in Cells

Thiols from whole-cell extracts were quantified as their 2'-bromoacetonaphthone (BAN) derivatives. Frozen cells pellets were resuspended in a minimum volume of extraction buffer (0.25M perchloric acid, 50% acetonitrile), and disrupted by sonication (20s). The cellular debris was removed by centrifugation at 16 100g for 2min. The pH of the cell-free extract was raised to between 8 and 9 with potassium carbonate, and the resulting precipitate removed by centrifugation. BAN was added to a final concentration of 1mM and the derivatisation reaction allowed to proceed at room temperature for 60min.

The BAN-derivatized thiols were separated by reverse-phase chromatography using a luna 5µ phenyl-hexyl column (250 x 4.60 mm) and detected at 248nm. The column was equilibrated with 90% A (5mM ammonium formate pH 3.0) and 10% B (acetonitrile). After injection of 20µl of the derivatized extract, the percentage B was raised to 20 in 5min. The column was eluted with a linear gradient from 20 to 30% acetonitrile over 20min. The acetonitrile concentration was then raised to 90% over 5min and maintained at this concentration for a further five minutes. The solvent concentrations were then returned to initial conditions over 5 min. A standard curve which correlates peak area to nmoles of derivatized mycothiol was constructed (Appendix A) and used to determine the thiol content of the samples.

6.3.3. Quantitative Analysis of Thiols in Media

The 5 ml media samples were freeze-dried and resuspended in 500µl of 50mM Clark and Lubs buffer (pH 9.5). The acetonitrile concentration was raised to 50 % and the resulting precipitate was removed by centrifugation. BAN was added to a final concentration of 1mM and the reaction allowed to proceed at room temperature for 60 min. The derivatized thiols were analysed as previously described for cell extracts.

CHAPTER 7: RESULTS & DISCUSSION

7.1. The Effect of Oxidative and Nitrosative Stress on Thiol Levels

The synthesis of ergothioneine by a number mycobacterial strains, including *M. smegmatis*, has previously been shown (Genghof & van Damme, 1964; Genghof & van Damme, 1968). Thiols are thought to be important in protecting cells against oxidative and nitrosative stress. The levels of thiols in *M. smegmatis* were therefore monitored in the presence of the superoxide generator 2, 3-dimethoxy-1, 4-naphthoquinone (DMNQ) and the NO releaser s-nitrosoglutathione (GSNO).

7.1.1. DMNQ

DMNQ was chosen as a superoxide generator since previous work with plumbagin showed that a reduction in thiol levels occurred as a result of a reaction with plumbagin directly (Personal communication Prof. D. Steenkamp). Quinones generate oxidative stress in cells by acting as subversive substrates for the flavoenzymes (Figure 7.1). Apart from producing superoxide, these subversive substrates also increase oxidative stress by wasting NADH reducing equivalents and inhibiting disulphide reduction (Krauth-Siegel & Schöneck, 1995). Since superoxide dismutase converts superoxide into hydrogen peroxide, which in turn can form hydroxyl radicals, treatment with DMNQ should provide insight into the general oxidative stress response.

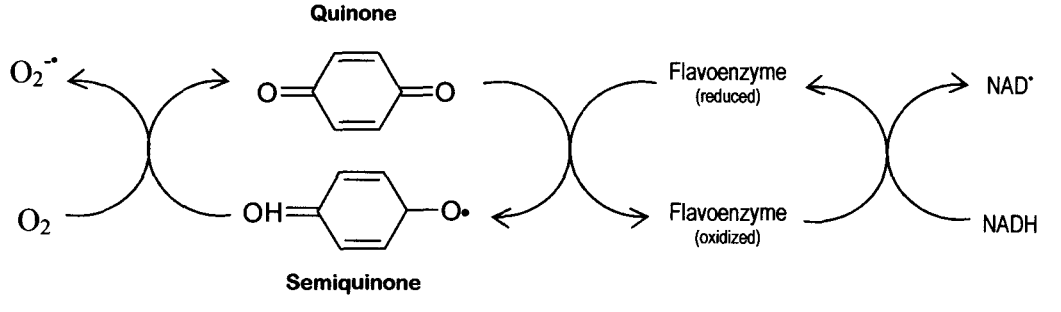

Figure 7.1: Redox cycling. Mechanism by which quinones generate superoxide in cells as a result of their reduction by flavoproteins

In order to determine the appropriate amount of DMNQ to add to cultures, the survival of *M. smegmatis* in the presence of various concentrations of DMNQ was determined. Table 7.1 indicates the level of growth of *M. smegmatis* in the presence of DMNQ as determined by absorbance at 600nm.

Table 7.1: Survival of *M. smegmatis* cultures grown in various concentrations of DMNQ

Concentration (μM)	Absorbance	
	24hrs	48hrs
0	1.392	7.5
5	0.55	5.7
10	0.324	5.8
20	0.333	3.8
50	0.09	1.4
100	0.024	0.059

The growth *M. smegmatis* was inhibited by all concentrations of DMNQ tested. At the concentration of 100 μM DMNQ, *M. smegmatis* reached an absorbance of 0.025 after 24 hrs. This is more than a fifty-fold reduction compared to the control and after 48 hrs of growth the absorbance had only increased to 0.059 (approximately double). Although the culture grown at 50 μM DMNQ also showed very little growth after 24 hrs (OD_{600} ~ 0.09), it had increased more than 10-fold to 1.4 after 48 hrs. A similar trend was observed with 20 μM DMNQ, which increased from 0.333 at 24 hrs to 3.8 after 48 hrs of growth. This suggests that the bacteria are better able to survive in the presence of DMNQ as time progresses. At a concentration of 20 μM DMNQ, *M. smegmatis* grows to approximately 50 % of the density of the control culture. This concentration was chosen to determine the effect of oxidative stress on ergothioneine levels.

Thiol levels in cells exposed to 20μM DMNQ during exponential growth were determined and compared to levels in cells which had not been exposed to DMNQ. The results are shown in Figure 7.2 and no significant difference was observed between thiol levels in the presence and absence of DMNQ.

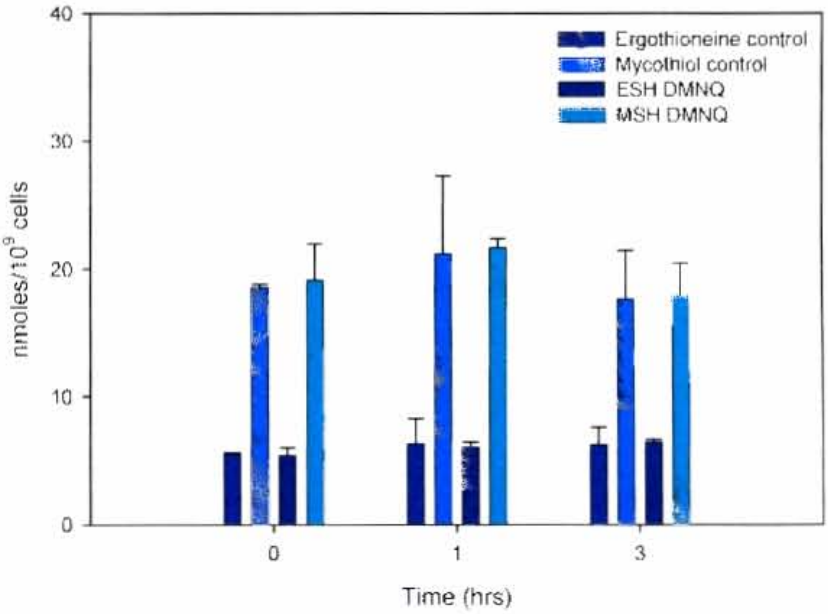

Figure 7.2: Levels of Ergothioneine (ESH) and Mycothiol (MSH) in *M. smegmatis* cells in the presence and absence of 20 μM DMNQ. The levels indicated are averages of two determinations.

In the control cultures, the levels of ergothioneine and mycothiol remain relatively constant during exponential growth as shown at time points 0, 1 and 3 hrs. In the experimental cultures, to which 20 μM of DMNQ was added, the same trend was observed. In a comparison between the mycothiol-dependant response of *M. smegmatis* and *M. bovis* BCG to treatment with diamide and hydrogen peroxide, *M. smegmatis* was shown to be significantly more tolerant to oxidative stress (Ung & Av-Gay, 2006). Exposure of *M. smegmatis* to diamide and hydrogen peroxide resulted in very little change in mycothiol levels and the ratio of oxidized to reduced mycothiol. The authors attributed this to the higher levels of mycothiol present in *M. smegmatis* as compared to *M. bovis* (40 nmole per 10^9 cells compared to 25 nmole per 10^9 cells). However, since the amount of ergothioneine in the present study was found to be 3-fold lower than mycothiol, the stability of the ergothioneine level cannot simply be due to its absolute amount. It is not clear how ergothioneine levels vary between mycobacterial species, since the values reported by Genghof & van Damme (1964) are highly variable. The

two *M. smegmatis* strains tested had 12 and 100 mg of ergothioneine per 100g of cells. For the *M. bovis* strains tested, the levels varied between 5 and 75 mg/100g, while for *M. tuberculosis* the range was between 0 and 50 mg/100g.

7.1.2. S-Nitrosoglutathione (GSNO)

The effect of nitrosative stress on ergothioneine levels was investigated using the nitric oxide donor S-nitrosoglutathione (GSNO). Vogt *et al.* (2003) have shown that *M. smegmatis* has the ability to metabolize S-nitrosoglutathione to glutathione and nitrate. In an *in vitro* study Misiti *et al.* (2001) demonstrated that ergothioneine increases the rate of GSNO decomposition. The effect of exposure of *M. smegmatis* to GSNO on ergothioneine levels was therefore determined. Figure 7.3 shows the growth of *M. smegmatis* in the presence and absence of GSNO as determined by absorbance at 600nm. The growth of cells is inhibited most significantly within the first hour of adding GSNO.

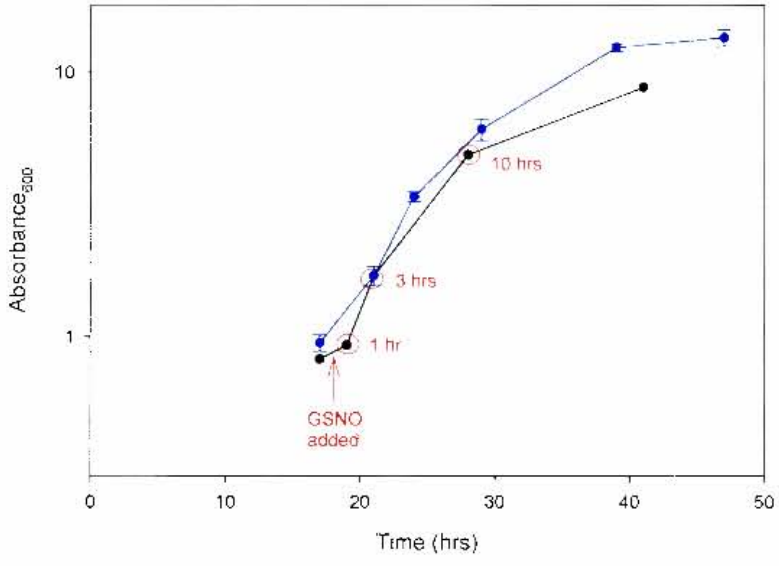

Figure 7.3: Growth of *M. smegmatis* cultures in the presence (black) and absence (blue) of 250 μM GSNO

Figure 7.4 A and B show that after exposure to GSNO, the level of ergothioneine and mycothiol in cells decrease. After 1hr of exposure to GSNO the levels of ergothioneine and mycothiol had decreased to approximately 50 % of the time zero level.

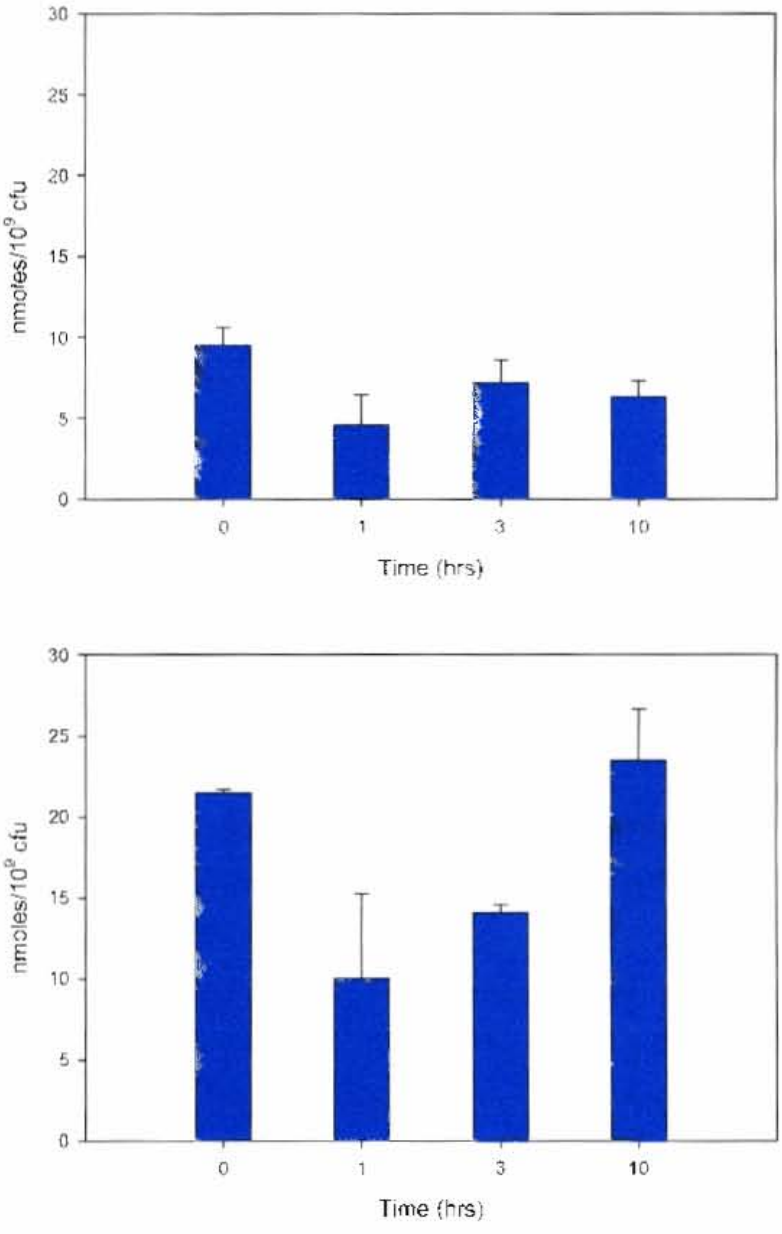

Figure 7.4: Levels of Ergothioneine **(A)** and Mycothiol **(B)** in *M. smegmatis* 1, 3 and 10 hrs after exposure to GSNO. The levels indicated are averages of two determinations.

The reaction of NO with thiols results in the formation of S-nitrosothiols. Vogt *et al.* (2003) demonstrated that *in vitro* the MSNO reductase from *M. smegmatis* converts S-nitrosomycothiol (MSNO) to mycothiol *N*-hydroxysulphenamide, which decomposes to form MSH sulphinic acid. However, *M. smegmatis* metabolises GSNO to form oxidized glutathione and nitrate (Figure 7.5), and MSH sulphinic acid could not be detected in [^{3}H] Inositol labelled cells (Vogt *et al.*2003). The authors suggested that MSNO reductase and HbN interact to form nitrate, however this was not conclusively shown due to the limitations of the *in vitro* system being used. The formation of MSNO could account for the decline in mycothiol levels observed after 1 and 3 hrs of exposure to GSNO. Assuming that MSNO and HbN interact *in vivo*, the mycothiol levels would increase as MSNO is recycled to MSH and nitrate.

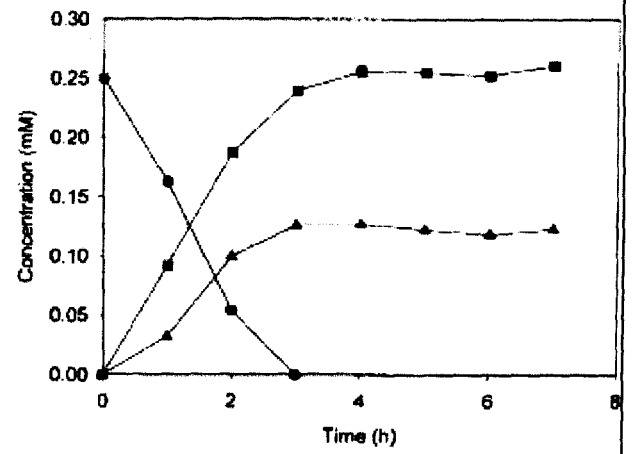

Figure 7.5: Metabolism of GSNO by *M. smegmatis*. GSNO is indicated by circles, nitrate by squares and GSSG by triangles. (from Vogt *et al.* 2003)

7.2. Determination of the Stability of Ergothioneine Disulphide

Misiti *et al.* (2001) reported that the reaction between GSNO and ergothioneine produces glutathione disulphide (GSSG), ergothioneine disulphide (ESSE) and a mixed disulphide (GSSE). If this reaction was occurring *in vivo*, it is possible that the ergothioneine levels indicated in Figure 7.4 are an underestimation. However, Heath and Toennies (1958) reported that ESSE and GSSE are unstable. Therefore the stability of the ergothioneine disulphide was determined under the assay conditions.

Ergothioneine disulphide was synthesized, isolated by HPLC (Figure 7.6) and confirmed by mass spectrometry (Figure 7.7). After exposure to alkaline pH (8-9) for 30 min, the disulphide was chromatographed on HPLC to determine its stability (Figure 7.8). After 30 min at alkaline pH the disulphide had almost completely degraded and an ergothioneine peak had appeared. Since the derivatisation reaction with bromoacetonaphthone is performed at a similar pH for an hour, it is reasonable to assume that the ergothioneine determined in Figure 7.4 would include any ergothioneine present in an oxidized form.

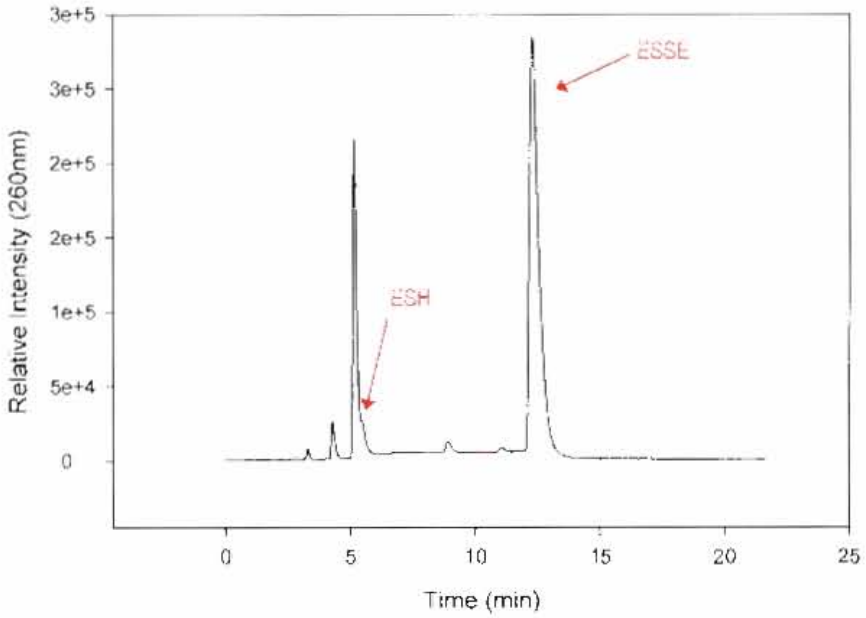

Figure 7.6: Isolation of ergothioneine disulphide by reverse phase HPLC. The disulphide elutes at approximately 12 min.

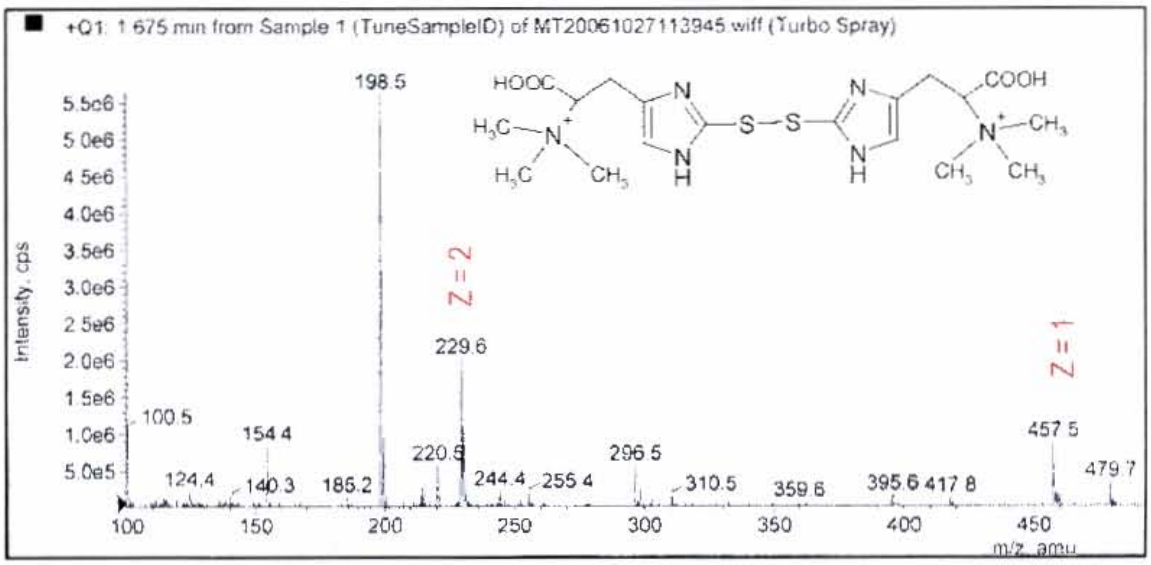

Figure 7.7: Confirmation of the isolated peak as ergothioneine disulphide by mass spectrometry.

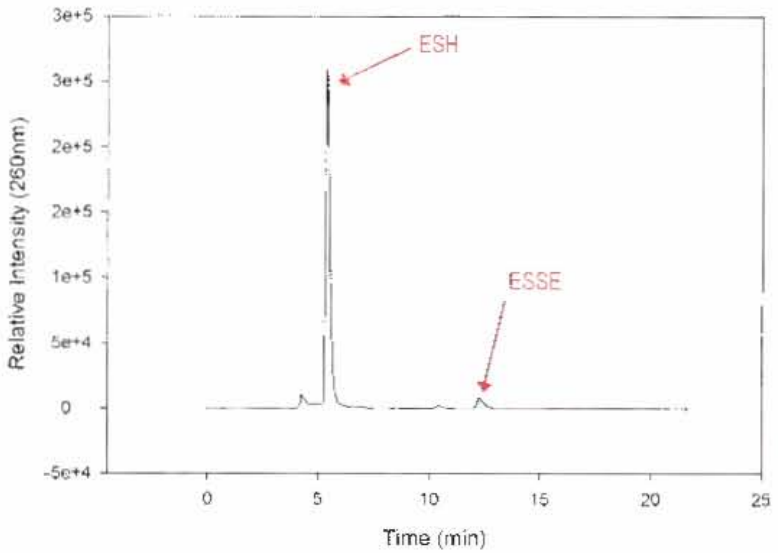

Figure 7.8: The stability of ergothioneine disulphide at alkali pH was determined after 30 min by reverse phase HPLC. Ergothioneine elutes just after 5 min, while the disulphide elutes at approximately 12 min.

It is unclear what drives the decomposition of ESSE, or whether this would occur under physiological conditions. Heath and Toennies (1958) found that only 60-70% of the expected amount of ESH could be recovered from the decomposition of the disulphide, suggesting that it is not a simple reduction. Since ESH has such a high electric potential ($E_o' = 0.06$ V), it is likely that ESSE would be reduced in the presence of thiols such as mycothiol and glutathione. Given the instability of ESSE and GSSE, it is difficult to determine whether ESH drives the decomposition of GSNO *in vivo*. However, the finding by Vogt *et al.* (2003) that GSNO could be accounted for by the formation of equivalent amounts of GSSG and nitrate, suggests that this does not occur.

Genome expression profiling and quantitative rt-PCR have demonstrated that exposure of *M. tuberculosis* to NO induces the DosRS two-component system (Voskuil *et al.*, 2003, Kendall *et al.*2004). It is hypothesized that since *M. tuberculosis* would be exposed to hypoxia and NO in granulomas, that it uses these two signals to induce genes which facilitate the survival in the host (Ohno *et al.*, 2003). Given that mycothiol mutants have an increased sensitivity to oxidative stress (Buchmeier *et al.*, 2003, Buchmeier *et al.* 2006) and that MshD was predicted to be essential for survival within macrophages, it is interesting that none of the mycothiol biosynthetic genes are induced by DosRS (Kendall *et al.*, 2004; Ohno *et al.*, 2003). This however supports the finding in this study that the biosynthesis of neither ergothioneine nor mycothiol is induced in response to ROI and RNI, as their levels do not increase.

7.3. Effect of Growth Phase on Ergothioneine Levels

Ergothioneine levels were determined over a complete growth cycle of *M. smegmatis* and compared to the levels of mycothiol present in the organism. The level of both thiols was also determined in the media. Figure 7.9A shows the level of growth over time, which indicates exponential growth between 20 and 40 hours after which the culture enters stationary phase. The level of ESH and MSH at different phases of growth are shown in Figure 7.9B. Thiol levels were expressed relative to protein due to the inaccuracy of absorbance as a measure of growth in stationary phase.

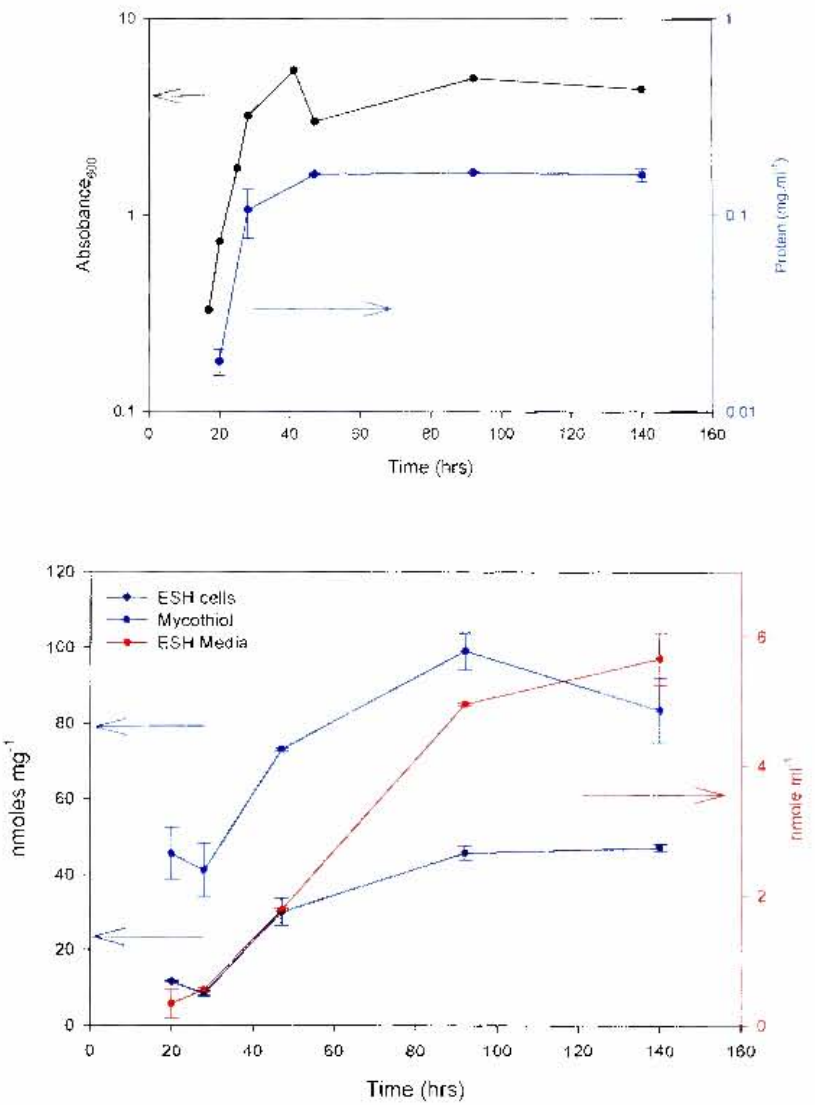

Figure 7.9A: Growth of *M. smegmatis* culture was monitored by Absorbance at 600nm and total protein. **B:** Ergothioneine and mycothiol levels over a complete growth cycle of *M. smegmatis*. Values are an average of two determinations.

MSH was observed to increase from approximately 40 nmole.mg^{-1} protein to 100 nmole.mg^{-1} protein. This is similar to the findings of Buchmeier *et al.* (2003), that MSH in *M. smegmatis* increased 1.6-fold in stationary phase. ESH was detected in both cells and media and was found to increase more dramatically than MSH. ESH in cells increase from approximately 10 nmole.mg^{-1}protein to 40 nmole.mg^{-1} protein, which is a 4-fold increase. In the media ESH increased 19-fold from 0.3 nmole.ml^{-1} to 5.7 nmole.ml^{-1}. Buchmeier *et al.* (2003) showed that MSH production in *M. tuberculosis* is also elevated in stationary phase, and that the increase was greater than for *M. smegmatis*. It is possible that ESH production follows a similar trend in *M. tuberculosis*, but this is yet to be determined. *M. smegmatis* was shown to develop resistance to oxidative stress before entering stationary phase (Smeulders *et al.,* 1999). The increase in MSH and ESH observed as *M. smegmatis* enters stationary phase may contribute to the development of an oxidative stress-resistant phenotype. Buchmeier *et al.* (2003) propose that the elevated levels of MSH in *M. tuberculosis* during stationary phase provide increase protection against stress when growth is slow. This however appears to be contradicted by the finding that *M. smegmatis* is more sensitive to GSNO in stationary phase than exponential phase (Smeulders *et al.,* 2004). The reason for this increased sensitivity is not clear, but the authors suggest it may be due to the increased efficiency of transport of GSNO into cells.

Two models of dormancy, namely stationary phase and oxygen limitation, were studied using genome expression profiling in *M. tuberculosis* (Voskuil *et al.,* 2004). Results showed that a number of the genes regulated by the DosRS system were highly induced under oxygen limiting conditions, while only partial induction of the most highly expressed genes in the DosRS regulon occurred during stationary phase. Interestingly, none of the mycothiol biosynthetic enzymes were induced with either models of dormancy. This suggests that regulation of mycothiol biosynthesis does not occur at the gene expression level, but occurs by another mechanism. While gene expression profiling provides us with vital information about the adaptation of *M. tuberculosis* to various stress conditions, it is clear from this finding that it does not give the complete picture.

7.4. Effect of Adding Ergothioneine to Growth Medium

Quorum sensing is used by bacteria to alter gene expression in response to changes in population density. It involves the production, release and detection of molecules known as autoinducers (Camilli & Bassler, 2006). Two classes of autoinducers have been identified, namely acyl homoserine lactones which are used by Gram-negative bacteria and modified oligopeptides used by Gram-positive bacteria. These groups are however not comprehensive as other molecules have also been identified. Since ESH was found to accumulate in media as the population density in *M. smegmatis* cultures increased, it was investigated as an autoinducer. During stationary phase approximately 6 nmoles.ml^{-1} of ESH was detected in the media. ESH was therefore added to the media at various concentrations during early exponential phase to determine if it would affect bacterial growth. ESH was found to have no effect on growth rate or on the level to which the *M. smegmatis* cultures grew (Figure 7.10). We can therefore conclude that it is not an autoinducer.

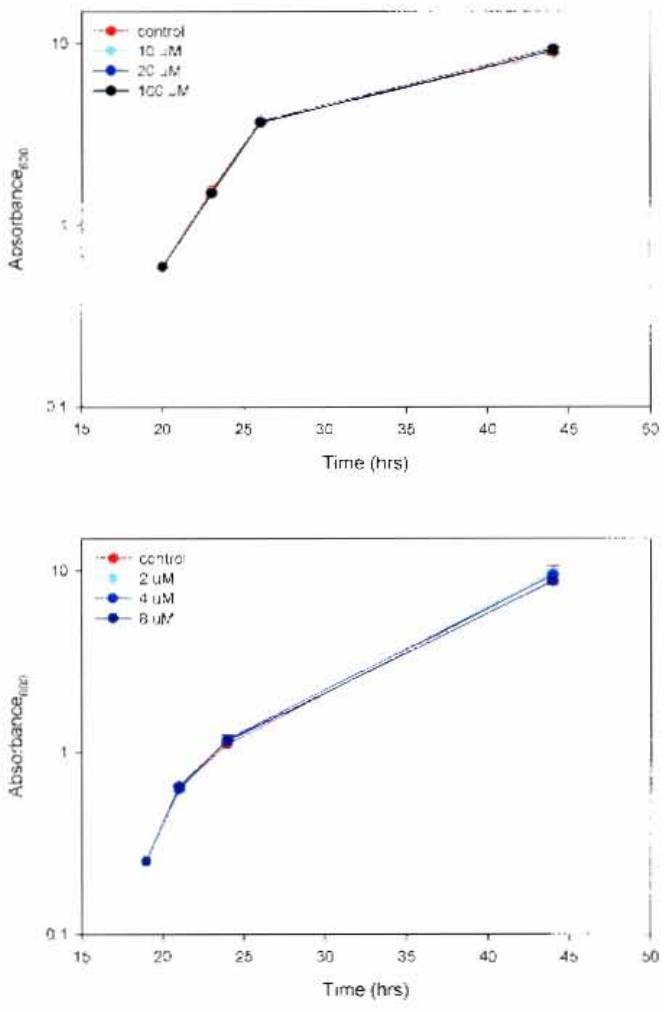

Figure 7.10: Growth of *M. smegmatis* cultures in the presence of various concentrations of ergothioneine.

It is not clear why *M. smegmatis* would release ESH into the media. Since MSH is not released, it would appear to be a specialized function of ESH. The unique chemistry of ESH prevents it auto-oxidising at physiological pH. This may be significant for its role outside of cells, since other thiols require enzymes to maintain them in the reduced form. The export of ESH from *M. smegmatis* is likely to be active process, since human cells which do not express the ESH transporter are impermeable to ESH (Gründermann *et al.,* 2005). It has been reported that pre-treatment of alveolar epithelial cells with ESH inhibits H_2O_2 and TNF-α mediated activation of NF-κβ (Rahman *et al.,* 2003). NF-κβ is activates the transcription of IL-8, which is a cytokine involved in the recruitment and activation of immune cells. Pre-treatment of the cells with ESH also inhibited the increased release of IL-8 in the presence of H_2O_2 and TNF-α. Therefore, the secretion of ESH by *M. tuberculosis* in the host may have an anti-inflammatory function. This is supported by the association which been found between polymorphisms in the ESH transporter and chronic inflammatory diseases (Tokuhiro *et al.,* 2003).

CHAPTER 8: GENERAL DISCUSSION & FUTURE WORK

The recent emergence of drug-resistant strains of tuberculosis which are virtually untreatable has again highlighted the dire need for new anti-tubercular drugs. The two major thiols synthesized by *M. tuberculosis*, mycothiol and ergothioneine, are not synthesized by the human host and consequently their biosynthetic enzymes are attractive drug targets. However, the function of ergothioneine in mycobacteria is unknown and this remains a critical step in validating its biosynthetic enzymes as drug targets. The work in this thesis was aimed at better understanding the function of ergothioneine in mycobacteria by studying its biosynthesis and the conditions affecting its production.

In Part A an attempt was made to purify the α-N, N, N-histidine methyltransferase, the first enzyme in ergothioneine biosynthesis, from *N. crassa*. This would allow the identification of the equivalent gene in mycobacteria, and ultimately facilitate the generation of mutants defective in ergothioneine biosynthesis. However, the purification of the enzyme presented a number of challenges which prevented its purification. Firstly, the number of useful purification methods was limited which made it difficult to remove all other proteins. Secondly, the enzyme was present at very low levels and despite a scaled-up purification which utilized approximately 1kg of frozen mycelium, it could not be visualized at the end of the purification. The further scaling up of the purification presents a number of difficulties including the ability to process a large amount of material in the shortest possible time. Time constraints are therefore a limiting factor when considering the feasibility of the scale-up required to obtain sufficient material for identification of the enzyme.

In Part B *M. smegmatis* was used as a model organism to identify conditions which affect ergothioneine production in mycobacteria. Oxidative and nitrosative stress did not result in the induction of ergothioneine or mycothiol in *M. smegmatis*. For mycothiol this is supported by the finding that its biosynthetic enzymes are not induced in the presence of oxidative and nitrosative stress (Kendall *et. al.*, 2004; Ohno *et. al.*, 2003). Ergothioneine levels were shown to increase dramatically as *M. smegmatis* entered stationary phase and also accumulated in the media. This is similar to the increase observed in mycothiol levels when *M. smegmatis* and

M. tuberculosis enter stationary phase (Buchmeier *et. al.*, 2003). This increase in MSH and ESH may contribute to the development of an oxidative and nitrosative stress-resistant phenotype. Due to its accumulation in the media ergothioneine was investigated as an autoinducer, but was found to have no effect on growth of *M. smegmatis.* It is not understood why *M. smegmatis* releases ergothioneine into the media, but in a pathogen like *M. tuberculosis* it could play an anti-inflammatory role.

Future Work

Synthesis of Improved Affinity Resins

One avenue which could be explored further is the improvement of the DMH-agarose that was synthesized. Changing the resin by altering the spacer length or position of attachment and modifying chromatography conditions may result in a significant improvement in its purification potential. Secondly, the coupling of ergothioneine to alanine via a disulphide linkage (Figure 8.1) could be used to generate a ligand which mimics hercynine. Since the biochemical data suggests that hercynine is the last product to leave the enzyme, this ligand may overcome the problems that were encountered with the other affinity resins.

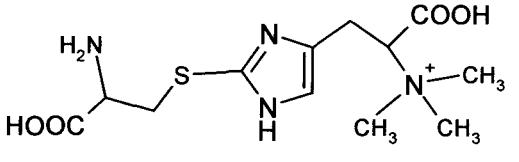

Figure 8.1: Ergothionine coupled to alanine via a disulphide bond

Generation of Ergothioneine Deficient Mutants

An alternate strategy for the identification of the enzymes in the ergothioneine biosynthetic pathway is the generation of ergothioneine deficient mutants using transposon mutagenesis. The presence of the transposon would facilitate the identification of the disrupted gene using PCR or a hybridisation probe. The difficulty associated with this strategy however is the screening for ergothioneine-deficient mutants. Since *M. smegmatis* releases ergothioneine into the media during stationary

phase, the development of a plate-based colorimetric screen to identify ergothioneine-deficient colonies would make this a more feasible approach.

Screening for α-N,N,N-Histidine Methyltransferase Activity

The availability of the annotated genome sequence of *M. tuberculosis* would facilitate the use of a recombinant DNA strategy to identify the gene for the α-N,N,N-histidine methyltransferase. This would involve the expression of potential methyltransferases in an appropriate expression system and assaying for α-N,N,N-histidine methyltransferase activity. Since expression of mycobacterial proteins can be problematic, this approach would rely on the development of a system which is able to over-express a range of functional mycobacterial proteins.

Due to the limitations associated with correctly annotating methyltransferases, it may be necessary to screen a larger number of genes in order to identify the α-N,N,N-histidine methyltransferase. This could be achieved through the generation and screening of an expression library from *M. tuberculosis*. The development of new technologies such as the GATEWAY system (Life Technologies) has made this a more feasible approach by simplifying the cloning process. The major advantage of this system is that once resource clones have been generated by GATEWAY cloning of amplified open reading frames into entry vectors, the genes can easily be transferred into a number of expression systems for functional studies (Rual *et al.* 2004).

The challenge currently facing scientists is the analysis of the large volume of genome-data which has been generated. Traditionally the elucidation of gene or protein function has employed techniques such as the isolation and phenotypic analysis of mutants, *in vitro* analysis of protein function and the generation of mutants by recombinant genetics. In order to meet the challenge of the "post-genomic" era we require the development of high-throughput methods to facilitate the study of several proteins simultaneously. The datasets generated from this high-throughput approach in turn requires bioinformatics tools which will allow the integration of information obtain from various experiments. Although the accurate assignment of gene function remains a daunting task, the promise of the genomic era will not be fully realised without it.

References:

Adams LB, Dinauer MC, Morgenstern DE, Krahenbuhl JL (1997) Comparison of the roles of reactive oxygen and nitrogen intermediates in the host response to *Mycobacterium tuberculosis* using transgenic mice. Tuber Lung Dis. 78(5-6):237-46.

Akanmu D, Cecchini R, Aruoma OI, Halliwell B. (1991) The antioxidant action of ergothionine. Arch Biochem Biophys. 288(1):10-6.

Altschul, Stephen F., Thomas L. Madden, Alejandro A. Schäffer, Jinghui Zhang, Zheng hang, Webb Miller, and David J. Lipman (1997) Gapped BLAST and PSI-BLAST: a new generation of protein database search programs. Nucleic Acids Res. 25:3389-3402.

Amado S, Blakelock L, Holmes AJ, Williams DLH. (2001) Kinetics and mechanism of the formation and reactions of *S*-nitroso derivatives of some heterocyclic thiones. J. Chem. Soc., Perkin Trans. *2*, 441-447

Amberson JB. (1938) The significance of latent forms of tuberculosis. N Engl J Med 219:572-6

Andries K, Verhasselt P, Guillemont J, Gohlmann HW, Neefs JM, Winkler H, Van Gestel J, Timmerman P, Zhu M, Lee E, Williams P, de Chaffoy D, Huitric E, Hoffner S, Cambau E, Truffot-Pernot C, Lounis N, Jarlier V. (2005) A diarylquinoline drug active on the ATP synthase of *Mycobacterium tuberculosis*. Science. 307(5707):223-7.

Andersen P (2001) TB vaccines: progress and problems. Trends Immunol. 22(3):160-8.

Aruoma OI, Whiteman M, England TG, Halliwell B. (1997) Antioxidant action of ergothionine: assessment of its ability to scavenge peroxynitrite. Biochem Biophys Res Commun. 231(2):389-91.

Aruoma OI, Spencer JP, Mahmood N. (1999) Protection against oxidative damage and cell death by the natural antioxidant ergothionine. Food Chem Toxicol. (11):1043-53.

Askari A. Melville DB. (1962) The reaction sequence in ergothionine biosynthesis: hercynine as an intermediate. J Biol Chem. 237:1615-8.

Asmus KD, Bensasson RV, Bernier JL, Houssin R, Land EJ. (1996) One-electron oxidation of ergothionine and analogues investigated by pulse radiolysis: redox reaction involving ergothionine and vitamin C. Biochem J. 315 (Pt 2):625-9.

Banerjee R, Evande R, Kabil O, Ojha S, Taoka S. (2003) Reaction mechanism and regulation of cystathionine beta-synthase. Biochim Biophys Acta. 1647(1-2):30-5.

Bateman A, Birney E, Cerruti L, Durbin R, Etwiller L, Eddy SR, Griffiths-Jones S, Howe KL, Marshall M, Sonnhammer EL. (2002) The Pfam protein families database. Nucleic Acids Res. 30(1):276-80.

Beck F, Yegian D. (1952) A study of the tubercle bacillus in resected pulmonary lesions. Am Rev Tuberc. 66(1):44-51.

Bloom BR, Murray CJ. (1992) Tuberculosis: commentary on a reemergent killer. Science 257:1055-64.

Bork P, Dandekar T, Diaz-Lazcoz Y, Eisenhaber F, Huynen M, Yuan Y.(1998) Predicting function: from genes to genomes and back. J Mol Biol. 283(4):707-25.

Borum PR, Broquist HP (1977) Purification of S-adenosylmethionine: epsilon-N-L-lysine methyltransferase. The first enzyme in carnitine biosynthesis. J Biol Chem. 252(16):5651-5.

Brigelius R, Muckel C, Akerboom TPM, Sies H (1983) Identification and quantitation of glutathione in hepatic protein mixed disulfides and its relationship to glutathione disulfide Biochem Pharmacol 32: 2529-34

Brosch R, Gordon SV, Marmiesse M, Brodin P, Buchrieser C, Eiglmeier K, Garnier T, Gutierrez C, Hewinson G, Kremer K, Parsons LM, Pym AS, Samper S, van Soolingen D, Cole ST. (2002) A new evolutionary scenario for the *Mycobacterium tuberculosis* complex. Proc Natl Acad Sci U S A. 99(6):3684-9.

Brown K, Pompeo F, Dixon S, Mengin-Lecreulx D, Cambillau C, Bourne Y. (1999) Crystal structure of the bifunctional N-acetylglucosamine 1-phosphate uridyltransferase from Escherichia coli: a paradigm for the related pyrophosphorylase superfamily. EMBO J. 18(15):4096-107.

Buchmeier NA, Fahey RC. (2006) The mshA gene encoding the glycosyltransferase of mycothiol biosynthesis is essential in *Mycobacterium tuberculosis* Erdman. FEMS Microbiol Lett. 264(1):74-9.

Buchmeier NA, Newton GL, Fahey RC. (2006) A mycothiol synthase mutant of *Mycobacterium tuberculosis* has an altered thiol-disulfide content and limited tolerance to stress. J Bacteriol. 188(17):6245-52.

Buchmeier NA, Newton GL, Koledin T, Fahey RC. (2003) Association of mycothiol with protection of *Mycobacterium tuberculosis* from toxic oxidants and antibiotics. Mol Microbiol 47(6):1723-32.

Camilli A, Bassler BL. (2006) Bacterial small-molecule signaling pathways. Science. 311(5764):1113-6.

Centers for Disease control and prevention (2006) Emergence of *Mycobacterium tuberculosis* with extensive resistance to second-line drugs--worldwide, 2000-2004. MMWR Morb Mortal Wkly Rep. 55(11):301-5.

Chua J. Deretic V. (2004) *Mycobacterium tuberculosis* reprograms waves of phosphatidylinositol 3-phosphate on phagosomal organelles. J Biol Chem. 279(35):36982-92

Chaudiere J, Ferrari-Iliou R. (1999) Intracellular antioxidants: from chemical to biochemical mechanisms. Food Chem Toxicol. 37(9-10):949-62.

Cheng X, Roberts RJ. (2001) AdoMet-dependent methylation, DNA methyltransferases and base flipping. Nucleic Acids Res. 29(18):3784-95.

Clothia C, Lesk AM. (1986) The relation between the divergence of sequence and structure in proteins. EMBO J. 5(4):823-6.

Colditz GA, Brewer TF, Berkey CS, Wilson ME, Burdick E, Fineberg HV, Mosteller F (1994) Efficacy of BCG vaccine in the prevention of tuberculosis. Meta-analysis of the published literature. JAMA 271(9):698-702.

Cole S.T. Alzari P.M. (2005) Microbiology. TB--a new target, a new drug. Science. 307(5707):214-5.

Cole ST, Brosch R, Parkhill J, Garnier T, Churcher C, Harris D, Gordon SV, Eiglmeier K, Gas S, Barry CE 3rd, Tekaia F, Badcock K, Basham D, Brown D, Chillingworth T, Connor R, Davies R, Devlin K, Feltwell T, Gentles S, Hamlin N, Holroyd S, Hornsby T, Jagels K, Krogh A, McLean J, Moule S, Murphy L, Oliver K, Osborne J, Quail MA, Rajandream MA, Rogers J, Rutter S, Seeger K, Skelton J, Squares R, Squares S, Sulston JE, Taylor K, Whitehead S, Barrell BG. (1998) Deciphering the biology of *Mycobacterium tuberculosis* from the complete genome sequence. Nature 393, 537–544.

Collins KR, Quinones-Mateu ME, Toossi Z, Arts EJ. (2002) Impact of tuberculosis on HIV-1 replication, diversity, and disease progression.AIDS Rev. 4(3):165-76.

Comstock GW, Baum C, Snider DE Jr. (1979) Isoniazid prophylaxis among Alaskan Eskimos: a final report of the bethel isoniazid studies. Am Rev Respir Dis. 119(5):827-30.

de Wit D, Wootton M, Dhillon J, Mitchison D A. (1995) The bacterial DNA content of mouse organs in the Cornell model of dormant tuberculosis Tuber Lung Dis 76(6): 555-62

Deiana M, Rosa A, Casu V, Piga R, Assunta Dessi M, Aruoma OI (2004) L-ergothionine modulates oxidative damage in the kidney and liver of rats in vivo: studies upon the profile of polyunsaturated fatty acids. Clin Nutr. 23(2):183-93.

Demple B. (1999) Radical ideas: genetic responses to oxidative stress. Clin Exp Pharmacol Physiol. 26(1):64-8.

Devos D, Valencia A (2001) Intrinsic errors in genome annotation. Trends Genet. 17(8):429-31.

Dickinson DA, Forman HJ (2002) Cellular glutathione and thiols metabolism. Biochem Pharmacol. 64(5-6):1019-26.

Dutt A.K. Stead W.W. (1999) Chapter 1: Epidemiology and Host Factors in Tuberculosis and Nontuberculosis Mycobacterial infections. 4th Edition. Ed. Schlossberg D. W. B. Saunders Company, Pennsylvania, p3-16.

East African/ British Medical Research Councils Study. (1977) Results of 5 years of a controlled comparison of a 6-month and a standard 18-month regime of chemotherapy for tuberculosis. Am Rev Respir Dis 116: 3-8

East African/ British Medical Research Councils Study. (1972) Controlled clinical trial of short-course (6-month) regimes of chemotherapy for treatment of pulmonary tuberculosis. Lancet 1:1079-85.

Eaton DL, Bammler TK (1999) Concise review of the glutathione S-transferases and their significance to toxicology Toxicol. Sci. 49: 156-164

Eddine AN, Kauffman SH (2005) Improved protection by recombinant BCG. Microbes and Infection 7: 939–946

Fahey R.C. (2001) Novel thiols of prokaryotes. Annu Rev Microbiol. 55:333-56.

Ferrari G, Langen H, Naito M, Pieters J. (1999) A coat protein on phagosomes involved in the intracellular survival of mycobacteria. Cell. 97(4):435-47.

Flynn JL, Chan J. (2001) Tuberculosis: latency and reactivation. Infect Immun. 69(7):4195-201.

Fox W, Ellard GA, Mitchison DA (1999) Studies on the treatment of tuberculosis undertaken by the British Medical Research Council tuberculosis units, 1946-1986, with relevant subsequent publications. Int J Tuberc Lung Dis. 3(10 Suppl 2):S231-79.

Franco-Paredes C, Rouphael N, Del Rio C, Santos-Preciado JI. (2006) Vaccination strategies to prevent tuberculosis in the new millennium: from BCG to new vaccine candidates. Int J Infect Dis. 10(2):93-102.

Fratti R.A. Chua J. Vergne I. Deretic V. (2003) *Mycobacterium tuberculosis* glycosylated phosphatidylinositol causes phagosome maturation arrest PNAS 100: 5437-5442

Galperin MY, Walker DR, Koonin EV (1998) Analogous enzymes: independent inventions in enzyme evolution. Genome Res. 8(8):779-90.

Garay AS (1956) Role of ergothioneine and catalase in infection by ergot fungus (Claviceps purpurea Tul.). Nature. 177(4498):91-2.

Garbe TR, Hibler NS, Deretic V. (1996) Response of Mycobacterium tuberculosis to reactive oxygen and nitrogen intermediates. Mol Med. 2(1):134-42.

Genghof DS van Damme O (1964) Biosynthesis of Ergothionine and Hercynine by Mycobacteria. J Bacteriol. 87:852-62.

Genghof DS. Van Damme O (1968) Biosynthesis of ergothioneine from endogenous hercynine in *Mycobacterium smegmatis*. J Bacteriol. 95(2):340-4.

Genghof DS (1970) Biosynthesis of ergothionine and hercynine by fungi and Actinomycetales. J Bacteriol. 103(2):475-8.

Ginalski K. (2006) Comparative modeling for protein structure prediction. Curr Opin Struct Biol. 16(2):172-7.

Gomez JE, McKinney JD. (2004) M. tuberculosis persistence, latency, and drug tolerance. Tuberculosis 84(1-2):29-44.

Grode L, Seiler P, Baumann S, Hess J, Brinkmann V, Nasser Eddine A, Mann P, Goosmann C, Bandermann S, Smith D, Bancroft GJ, Reyrat JM, van Soolingen D, Raupach B, Kaufmann SH. (2005) Increased vaccine efficacy against tuberculosis of recombinant *Mycobacterium bovis* bacille Calmette-Guerin mutants that secrete listeriolysin. J Clin Invest. 115(9):2472-9.

Gründemann D, Harlfinger S, Golz S, Geerts A, Lazar A, Berkels R, Jung N, Rubbert A, Schomig E. (2005) Discovery of the ergothioneine transporter. Proc Natl Acad Sci USA. 102(14):5256-61.

Hand CE, Honek JF. (2005) Biological chemistry of naturally occurring thiols of microbial and marine origin. J Nat Prod. 68(2):293-308.

Hanlon D.P. (1971) Interaction of ergothionine with metal ions and metalloenzymes. J Med Chem. 14(11):1084-7.

Heath H, Wildy J. (1957) Biosynthesis of ergothioneine. Nature. 179(4552):196-7.

Heath H, Toennies G. (1958) The preparation and properties of ergothioneine disulphide. Biochem J. 68(2):204-10.

Hernandez-Pando R, Jeyanathan M, Mengistu G, Aguilar D, Orozco H, Harboe M, Rook GA, Bjune G. (2000) Persistence of DNA from *Mycobacterium tuberculosis* in superficially normal lung tissue during latent infection. Lancet. 356(9248):2133-8.

Hobby Gl, Auerbach O, Lenert TF, Small MJ, Comer JV. (1954) The late emergence of *M. tuberculosis* in liquid cultures of pulmonary lesions resected from humans. Am Rev Tuberc. 70(2):191-218.

Holmgren A, Johansson C, Berndt C, Lonn ME, Hudemann C, Lillig CH. (2005) Thiol redox control via thioredoxin and glutaredoxin systems. Biochem Soc Trans. 33(Pt 6):1375-7.

Hu Y. Coates A.R. Mitchison D.A. (2003) Sterilizing activities of fluoroquinolones against rifampin-tolerant populations of *Mycobacterium tuberculosis*. Antimicrob Agents Chemother. 47(2):653-7.

Huygen K. (2003) On the use of DNA vaccines for the prophylaxis of mycobacterial diseases. Infect Immun. 71(4):1613-21.

Ingrosso D, Fowler AV, Bleibaum J, Clarke S. (1989) Sequence of the D-aspartyl/L-isoaspartyl protein methyltransferase from human erythrocytes. Common sequence motifs for protein, DNA, RNA, and small molecule S-adenosylmethionine-dependent methyltransferases. J Biol Chem. 264(33):20131-9.

Ishikawa Y, Israel SE, Melville DB. (1974) Participation of an intermediate sulfoxide in the enzymatic thiolation of the imidazole ring of hercynine to form ergothionine. J Biol Chem. 249(14):4420-7.

Ishikawa Y, Melville DB. (1970) The enzymatic alpha-N-methylation of histidine. J Biol Chem. 45(22):5967-73.

Jawarhar M.S. (2004) Current trends in chemotherapy of tuberculosis. Indian J Med Res. 120(4):398-417.

Jin X, Ballicora MA, Preiss J, Geiger JH (2005) Crystal structure of potato tuber ADP-glucose pyrophosphorylase. EMBO J. 24(4):694-704.

Jones DT. (1999) GenTHREADER: an efficient and reliable protein fold recognition method for genomic sequences. J Mol Biol. 287(4):797-815.

Kagan RM, Clarke S. (1994) Widespread occurrence of three sequence motifs in diverse S-adenosylmethionine-dependent methyltransferases suggests a common structure for these enzymes. Arch Biochem Biophys. 310(2):417-27.

Kanoun S, Amourache L, Krishnan S, Vijayalakshmi MA. (1986) New support for the large-scale purification of proteins. J Chromatogr. 376:259-67.

Katz JE, Dlakic M, Clarke S. (2003) Automated identification of putative methyltransferases from genomic open reading frames. Mol Cell Proteomics. 2(8):525-40.

Keller JP, Smith PM, Benach J, Christendat D, deTitta GT, Hunt JF. (2002) The crystal structure of MT0146/CbiT suggests that the putative precorrin-8w decarboxylase is a methyltransferase. Structure. 10(11):1475-87

Kendall SL, Movahedzadeh F, Rison SC, Wernisch L, Parish T, Duncan K, Betts JC, Stoker NG. (2004) The *Mycobacterium tuberculosis* dosRS two-component system is induced by multiple stresses. Tuberculosis 84(3-4):247-55.

Koledin T Newton G.L. Fahey R.C. (2002), Identification of the mycothiol synthase gene (mshD) encoding the acetyltransferase producing mycothiol in actinomycetes, Arch. Micro. 178: 331-337.7

Krauth-Siegel RL, Schöneck R. (1995) Flavoprotein structure and mechanism. 5. Trypanothione reductase and lipoamide dehydrogenase as targets for a structure-based drug design. FASEB J. 9(12):1138-46.

Laemmli UK. (1970) Cleavage of Structural Proteins during the Assembly of the Head of Bacteriophage T4, Nature, 227: 680-685

Lancet editorial (2006) XDR-TB--a global threat. Lancet. 368(9540):964.

Laskowski, R., McArthur, M., Moss, D., and Thornton, J. (1993) PROCHECK: A program to check the stereochemical quality of protein structures. J. Appl. Cryst. 26: 283–298.

Lau YL, Chan GC, Ha SY, Hui YF, Yuen KY. (1998) The role of phagocytic respiratory burst in host defense against *Mycobacterium tuberculosis*. Clin Infect Dis. 26(1):226-7.

Lauster R, Trautner TA, Noyer-Weidner M.(1989) Cytosine-specific type II DNA methyltransferases. A conserved enzyme core with variable target-recognizing domains. J Mol Biol. 206(2):305-12.

Lawn SD. (2004) AIDS in Africa: the impact of coinfections on the pathogenesis of HIV-1 infection. J Infect. 48(1):1-12.

Ma B, Zhang K, Hendrie C, Liang C, Li M, Doherty-Kirby A, Lajoie G. (2003) PEAKS: powerful software for peptide *de novo* sequencing by tandem mass spectrometry. Rapid Commun Mass Spectrom. 17(20):2337-42.

MacMicking JD, North RJ, LaCourse R, Mudgett JS, Shah SK, Nathan CF. (1997) Identification of nitric oxide synthase as a protective locus against tuberculosis. Proc Natl Acad Sci U S A. 94(10):5243-8.

Mack JP, Slaytor MB. (1978) Affinity chromatography of an S-adenosylmethionine-dependent methyltransferase using immobilized S-adenosylhomocysteine. Purification of the indolethylamine N-methyltransferases of phalaris tuberosa. J Chromatogr. 157:153-9.

Manjunatha UH, Boshoff H, Dowd CS, Zhang L, Albert TJ, Norton JE, Daniels L, Dick T, Pang SS, Barry CE 3rd (2006) Identification of a nitroimidazo-oxazine-specific protein involved in PA-824 resistance in *Mycobacterium tuberculosis.* Proc Natl Acad Sci U S A. 103(2):431-6.

Master SS, Springer B, Sander P, Boettger EC, Deretic V, Timmins GS. (2002) Oxidative stress response genes in Mycobacterium tuberculosis: role of ahpC in resistance to peroxynitrite and stage-specific survival in macrophages. Microbiology. 148(Pt 10):3139-44.

Mayo RE, Stanford JL. (2000) Double-blind placebo-controlled trial of *Mycobacterium vaccae* immunotherapy for tuberculosis in KwaZulu, South Africa, 1991-97. Trans R Soc Trop Med Hyg. 94(5):563-8.

McCormack AL, Schieltz DM, Goode B, Yang S, Barnes G, Drubin D, Yates JR 3rd. (1997) Direct analysis and identification of proteins in mixtures by LC/MS/MS and database searching at the low-femtomole level. Anal Chem. 69(4):767-76.

McCune RM, Feldmann FM, McDermott W. (1966a) Microbial persistence. II. Characteristics of the sterile state of tubercle bacilli. J Exp Med. 123(3):469-86.

McCune RM, Feldmann FM, Lambert HP, McDermott W. (1966b) Microbial persistence. I. The capacity of tubercle bacilli to survive sterilization in mouse tissues. J Exp Med. 123(3):445-68.

McCune RM Jr, Mcdermott W, Tompsett R. (1956) The fate of *Mycobacterium tuberculosis* in mouse tissues as determined by the microbial enumeration technique. II. The conversion of tuberculous infection to the latent state by the administration of pyrazinamide and a companion drug. J Exp Med. 104(5):763-802.

McGuffin LJ, Jones DT (2003) Improvement of the GenTHREADER method for genomic fold recognition. Bioinformatics. 19(7):874-81.

McShane H, Pathan AA, Sander CR, Keating SM, Gilbert SC, Huygen K, Fletcher HA, Hill AV. (2004) Recombinant modified vaccinia virus Ankara expressing antigen 85A boosts BCG-primed and naturally acquired antimycobacterial immunity in humans. Nat Med. 10(11):1240-4. Erratum in: Nat Med. 2004 Dec;10(12):1397.

Medlar EM, Bernstein S, Steward DM. (1952) A bacteriologic study of resected tuberculous lesions. Am Rev Tuberc. 66(1):36-43.

Melville DB, Eich S, Ludwig ML. (1957) The biosynthesis of ergothionine. J Biol Chem. 224(2):871-7

Melville DB, Ludwig ML, Inamine E, Rachele JR. (1959) Transmethylation in the biosynthesis of ergothionelne. J Biol Chem. 234(5):1195-8.

Metcalf C. (1991) Chapter 1:A history of tuberculosis in A Century of Tuberculosis: South African Perspectives, Ed. Coovadia HM. & Benatar S.R. Oxford University Press, Cape Town, p1-41.

Meyers PR, Bourn WR, Steyn LM, van Helden PD, Beyers AD, Brown GD. (1998) Novel method for rapid measurement of growth of mycobacteria in detergent-free media. J Clin Microbiol. 36(9):2752-4.

Misiti F. Castagnola M, Zuppi C. Giardina B, Messana I, (2001) Role of ergothionine on S-nitrosoglutathione catabolism. Biochem. J. 356, 799-804.

Mitchison D.A. (1979) Basic mechanisms of chemotherapy. Chest. 76(6 Suppl):771-81.

Moncaster JA, Walsh DT, Gentleman SM, Jen LS, Aruoma OI. (2002) Ergothionine treatment protects neurons against N-methyl-D-aspartate excitotoxicity in an in vivo rat retinal model. Neurosci Lett. 328(1): 55-9.

Mosli Waldhauser SS, Gillies FM, Crozier A, Baumann TW. (1997) Separation of the N-7 methyltransferase, the key enzyme in caffeine biosynthesis. Phytochemistry. 45(7):1407-14.

Nachega and Chaisson (2003) Tuberculosis Drug Resistance: A Global Threat Clinical Infectious Diseases 36(Suppl 1):S24–30

Nagano N, Orengo CA, Thornton JM (2002) One fold with many functions: the evolutionary relationships between TIM barrel families based on their sequences, structures and functions. J Mol Biol. 321(5):741-65.

Nathan C, Shiloh MU. (2000) Reactive oxygen and nitrogen intermediates in the relationship between mammalian hosts and microbial pathogens. Proc Natl Acad Sci U S A. 97(16):8841-8.

Newton G.L. Koledin T. Gorovitz B Rawat M. Fahey R.C. Av-Gay Y, (2003) The Glycosyltransferase Gene Encoding the Enzyme Catalyzing the First Step of Mycothiol Biosynthesis (mshA), J. Bac. 185(11), 3476-3479.

Newton G.L. Av-Gay Y. Fahey R.C. (2000a) N-Acetyl-1-D-myo-Inosityl-2-Amino-2-Deoxy-α-D-Glucopyranoside Deacetylase (MshB) is a key Enzyme in Mycothiol Biosynthesis, Journal of Bacteriology, 182 (24), 6958-6963.

Newton GL, Av-Gay Y, Fahey RC. (2000b) A novel mycothiol-dependent detoxification pathway in mycobacteria involving mycothiol S-conjugate amidase. Biochemistry. 39(35):10739-46

Newton GL, Unson MD, Anderberg SJ, Aguilera JA, Oh NN, delCardayre SB, Av-Gay Y, Fahey RC. (1999) Characterization of *Mycobacterium smegmatis* mutants defective in 1-d-myo-inosityl-2-amino-2-deoxy-alpha-d-glucopyranoside and mycothiol biosynthesis. Biochem Biophys Res Commun. 255(2):239-44.

Newton GL, Arnold K, Price MS, Sherrill C, Delcardayre SB, Aharonowitz Y, Cohen G, Davies J, Fahey RC, Davis C (1996) Distribution of thiols in microorganisms: mycothiol is a major thiol in most actinomycetes. J Bacteriol. 178(7):1990-5.

Ng VH, Cox JS, Sousa AO, MacMicking JD, McKinney JD. (2004) Role of KatG catalase-peroxidase in mycobacterial pathogenesis: countering the phagocyte oxidative burst. Mol Microbiol. 52(5):1291-302.

Niewmierzcha A. Clarke S. (1999) S-Adenosylmethionine-dependent methylation in Saccharomyces cerevisiae. Identification of a novel protein arginine methyltransferase. J Biol Chem. 274(2):814-24.

Obayashi K, Kurihara K, Okano Y, Masaki H, Yarosh DB (2005) L-Ergothionine scavenges superoxide and singlet oxygen and suppresses TNF-alpha and MMP-1 expression in UV-irradiated human dermal fibroblasts. J Cosmet Sci. 56(1):17-27.

Ofran Y, Punta M, Schneider R, Rost B. (2005) Beyond annotation transfer by homology: novel protein-function prediction methods to assist drug discovery. Drug Discov Today. 10(21):1475-82.

Ohno H, Zhu G, Mohan VP, Chu D, Kohno S, Jacobs WR Jr, Chan J. (2003) The effects of reactive nitrogen intermediates on gene expression in *Mycobacterium tuberculosis*. Cell Microbiol. 5(9):637-48.

Orme IM. (2005) Current progress in tuberculosis vaccine development.Vaccine. 23(17-18): 2105-8.

O'Toole R, Smeulders MJ, Blokpoel MC, Kay EJ, Lougheed K, Williams HD. (2003) A two-component regulator of universal stress protein expression and adaptation to oxygen starvation in *Mycobacterium smegmatis*. J Bacteriol. 185(5):1543-54.

Park HD, Guinn KM, Harrell MI, Liao R, Voskuil MI, Tompa M, Schoolnik GK, Sherman DR. (2003) Rv3133c/dosR is a transcription factor that mediates the hypoxic response of *Mycobacterium tuberculosis*. Mol Microbiol 48(3):833-43.

Parish T, Smith DA, Kendall S, Casali N, Bancroft GJ, Stoker NG. (2003) Deletion of two-component regulatory systems increases the virulence of *Mycobacterium tuberculosis*. Infect Immun. 71(3):1134-40.

Parrish NM, Dick JD, Bishai WR. (1998) Mechanisms of latency in *Mycobacterium tuberculosis*. Trends Microbiol. 6(3):107-12.

Patel MP, Blanchard JS. (2001) *Mycobacterium tuberculosis* mycothione reductase: pH dependence of the kinetic parameters and kinetic isotope effects. Biochemistry. 40(17):5119-26.

Peneff C, Ferrari P, Charrier V, Taburet Y, Monnier C, Zamboni V, Winter J, Harnois M, Fassy F, Bourne Y. (2001) Crystal structures of two human pyrophosphorylase isoforms in complexes with UDPGlc(Gal)NAc: role of the alternatively spliced insert in the enzyme oligomeric assembly and active site architecture. EMBO J. 20(22):6191-202.

Piddington DL, Fang FC, Laessig T, Cooper AM, Orme IM, Buchmeier NA. (2001) Cu, Zn superoxide dismutase of *Mycobacterium tuberculosis* contributes to survival in activated macrophages that are generating an oxidative burst. Infect Immun. 69(8):4980-7.

Pomposiello PJ, Demple B. (2001) Redox-operated genetic switches: the SoxR and OxyR transcription factors. Trends Biotechnol. 19(3):109-14.

Ponting CP. (2001) Issues in predicting protein function from sequence. Brief Bioinform. 2(1): 19-29.

Posfai J, Bhagwat AS, Posfai G, Roberts RJ. (1989) Predictive motifs derived from cytosine methyltransferases. Nucleic Acids Res. 17(7):2421-35.

Raja A (2004) Immunology of tuberculosis. Indian J Med Res. 120(4):213-32.

Rahman I, Gilmour PS, Jimenez LA, Biswas SK, Antonicelli F, Aruoma OI. (2003) Ergothioneine inhibits oxidative stress- and TNF-alpha-induced NF-kappa B activation and interleukin-8 release in alveolar epithelial cells. Biochem Biophys Res Commun. 302(4):860-4.

Rakwal R, Agrawal GK, Yonekura M, Kodama O. (2000) Naringenin 7-O-methyltransferase involved in the biosynthesis of the flavanone phytoalexin sakuranetin from rice (Oryza sativa L.). Plant Sci. 155(2):213-221.

Rawat M. NewtonG.L. Ko M.L. Martinez G.J. Fahey R.C. Av-Gay Y. (2002) Mycothiol-deficient *Mycobacterium smegmatis* are hypersensitive to alkylating agents, free radicals and antibiotics. Antimicrobial agents & Chemotherapy 46(11), 3348-3355.

Reinhold VN, Ishikawa Y, Melville DB. (1970) Conversion of histidine to hercynine by Neurospora crassa. J Bacteriol. 101(3):881-4.

Rengarajan, J., B. R. Bloom, and E. J. Rubin. (2005) Genome-wide requirements for *Mycobacterium tuberculosis* adaptation and survival in macrophages. Proc. Natl. Acad. Sci. USA 102:8327-8332

Rhee KY, Erdjument-Bromage H, Tempst P, Nathan CF. (2005) S-nitroso proteome of *Mycobacterium tuberculosis*: Enzymes of intermediary metabolism and antioxidant defense, Proc Natl Acad Sci U S A.102(2):467-72.

Roberts DM, Liao RP, Wisedchaisri G, Hol WG, Sherman DR. (2004) Two sensor kinases contribute to the hypoxic response of *Mycobacterium tuberculosis*. J Biol Chem. 279(22):23082-7.

Romano J.D. Michaelis S. (2001) Topological and mutational analysis of Saccharomyces cerevisiae Ste14p, founding member of the isoprenylcysteine carboxyl methyltransferase family. Mol Biol Cell. 12(7):1957-71.

Roure M, Bouillant ML. (1986) Development and application of a bioassay to study the effects of nutrients, pH and active substances on *Sordaria macrospora* fruiting. Can J. Microbiol. 32: 930-36.

Rual JF, Hill DE, Vidal M. (2004) ORFeome projects: gateway between genomics and omics. Curr Opin Chem Biol. 8(1):20-5.

Sánchez R, Šali A. Comparative Protein Structure Modelling in Methods in Molecular Biology vol 143: Protein Structure Prediction: Methods and Protocols. Humana Press Inc. Totowa, NJ p 97- 129

Sareen D. Newton G.L. Fahey R.C. Buchmeier N.A. (2003) Mycothiol Is Essential for Growth of *Mycobacterium tuberculosis* Erdman, J. Bac. 185(22), 6736-6740.

Sareen D. Steffek M. Newton G.L. Fahey R.C. (2002) ATP-Dependent L-Cysteine:1D-myo-Inosityl 2-Amino-2-deoxy-R-D-glucopyranoside Ligase, Mycothiol Biosynthesis Enzyme MshC, Is Related to Class I Cysteinyl-tRNA Synthetases, Biochem. 41(22), 6885-6890.

Scanga CA, Mohan VP, Joseph H, Yu K, Chan J, Flynn JL. (1999) Reactivation of latent tuberculosis: variations on the Cornell murine model. Infect Immun. 67(9):4531-8.

Schnappinger D, Ehrt S, Voskuil MI, Liu Y, Mangan JA, Monahan IM, Dolganov G, Efron B, Butcher PD, Nathan C, Schoolnik GK. (2003) Transcriptional Adaptation of Mycobacterium tuberculosis within Macrophages: Insights into the Phagosomal Environment. J Exp Med. 198(5):693-704.

Scopes RK (1994) Protein purification: Principles and practice. Springer-Verlag, New York, Inc. p211

Sehgal D, Vijay IK. (1994) A method for the high efficiency of water-soluble carbodiimide-mediated amidation. Anal Biochem. 218(1):87-91.

Sherman DR, Voskuil M, Schnappinger D, Liao R, Harrell MI, Schoolnik GK. (2001) Regulation of the *Mycobacterium tuberculosis* hypoxic response gene encoding alpha -crystallin. Proc Natl Acad Sci U S A. 98(13):7534-9.

Sherman DR, Mdluli K, Hickey MJ, Arain TM, Morris SL, Barry CE 3rd, Stover CK. (1996) Compensatory ahpC gene expression in isoniazid-resistant *Mycobacterium tuberculosis*. Science. 272(5268):1641-3.

Sherman DR, Sabo PJ, Hickey MJ, Arain TM, Mahairas GG, Yuan Y, Barry CE 3rd, Stover CK. (1995) Disparate responses to oxidative stress in saprophytic and pathogenic mycobacteria. Proc Natl Acad Sci U S A. 92(14):6625-9.

Shevchenko A, Wilm M, Vorm O, Mann M. (1996) Mass spectrometric sequencing of proteins silver-stained polyacrylamide gels. Anal Chem. 68(5):850-8.

Shoen CM, DeStefano MS, Cynamon MH (2000) Durable cure for tuberculosis: rifalazil in combination with isoniazid in a murine model of *Mycobacterium tuberculosis* infection. Clin Infect Dis. 30 Suppl 3:S288-90.

Sigrist CJ, Cerutti L, Hulo N, Gattiker A, Falquet L, Pagni M, Bairoch A, Bucher P. (2002) PROSITE: a documented database using patterns and profiles as motif descriptors. Brief Bioinform. 3(3):265-74.

Smeulders MJ, Keer J, Gray KM, Williams HD. (2004) S-Nitrosoglutathione cytotoxicity to *Mycobacterium smegmatis* and its use to isolate stationary phase survival mutants. FEMS Microbiol Lett 239(2):221-8.

Smeulders MJ, Keer J, Speight RA, Williams HD. (1999) Adaptation of *Mycobacterium smegmatis* to stationary phase. J Bacteriol. 181(1):270-83.

Sohaskey CD, Wayne LG (2003) Role of narK2X and narGHJI in hypoxic upregulation of nitrate reduction by *Mycobacterium tuberculosis*. J Bacteriol. 185(24):7247-56.

Sonnenberg P, Murray J, Glynn JR, Shearer S, Kambashi B, Godfrey-Faussett P. (2001) HIV-1 and recurrence, relapse, and reinfection of tuberculosis after cure: a cohort study in South African mineworkers. Lancet. 358(9294):1687-93.

Stamler JS, Singel DJ, Loscalzo J. (1992) Biochemistry of nitric oxide and its redox-activated forms. Science. 258(5090):1898-902.
Stewart GR, Robertson BD, Young DB. (2003) Tuberculosis: a problem with persistence. Nat Rev Microbiol. 1(2):97-105.

Stothard P, Wishart DS. (2006) Automated bacterial genome analysis and annotation. Curr Opin Microbiol. (5):505-10

Stover CK, Warrener P, VanDevanter DR, Sherman DR, Arain TM, Langhorne MH, Anderson SW, Towell JA, Yuan Y, McMurray DN, Kreiswirth BN, Barry CE, Baker WR (2000) A small-molecule nitroimidazopyran drug candidate for the treatment of tuberculosis. Nature. 405(6789):962-6.

Tokuhiro S, Yamada R, Chang X, Suzuki A, Kochi Y, Sawada T, Suzuki M, Nagasaki M, Ohtsuki M, Ono M, Furukawa H, Nagashima M, Yoshino S, Mabuchi A, Sekine A, Saito S, Takahashi A, Tsunoda T, Nakamura Y, Yamamoto K. (2003) An intronic SNP in a RUNX1 binding site of SLC22A4, encoding an organic cation transporter, is associated with rheumatoid arthritis. Nat Genet. 35(4):341-8.

Tovar J. Ruiz-Herrera J. (1986) Purification and properties of glucose-1-phosphate uridylyltransferase from *Neurospora crassa* Exp. Mycol. 11: 36-48.

Ung KS, Av-Gay Y. (2006) Mycothiol-dependent mycobacterial response to oxidative stress. FEBS Lett. 580(11):2712-6.

van den Broeke LT, Beyersbergen van Henegouwen GM. (1993) Thiols as potential UV radiation protectors: an in vitro study. J Photochem Photobiol B. 17(3):279-86.

van Rie A, Warren R, Richardson M, Victor TC, Gie RP, Enarson DA, Beyers N, van Helden PD. (1999) Exogenous reinfection as a cause of recurrent tuberculosis after curative treatment. N Engl J Med. 341(16): 1174-9.

Velkov V. Lawen A. (2003) Mapping and molecular modeling of S-adenosyl-L-methionine binding sites in N-methyltransferase domains of the multifunctional polypeptide cyclosporin synthetase. J Biol Chem. 278(2):1137-48.

Vogt RN, Steenkamp DJ, Zheng R, Blanchard JS. (2003) The metabolism of nitrosothiols in the Mycobacteria: identification and characterization of S-nitrosomycothiol reductase. Biochem J. 374(Pt 3):657-66.

Vogt RN, Steenkamp DJ. (2003) The metabolism of S-nitrosothiols in the trypanosomatids: the role of ovothiol A and trypanothione. Biochem J. 371(Pt 1):49-59.

von Reyn CF, Vuola JM. (2002) New vaccines for the prevention of tuberculosis. Clin Infect Dis. 35(4):465-74.

Voskuil MI, Visconti KC, Schoolnik GK. (2004) *Mycobacterium tuberculosis* gene expression during adaptation to stationary phase and low-oxygen dormancy. Tuberculosis (Edinb). 84(3-4): 218-27.

Voskuil MI, Schnappinger D, Visconti KC, Harrell MI, Dolganov GM, Sherman DR, Schoolnik GK. (2003) Inhibition of respiration by nitric oxide induces a *Mycobacterium tuberculosis* dormancy program. J Exp Med. 198(5):705-13.

Vukmirovic OG, Tilghman SM. (2000) Exploring genome space. Nature. 405(6788):820-2.

Walburger A, Koul A, Ferrari G, Nguyen L, Prescianotto-Baschong C, Huygen K, Klebl B, Thompson C, Bacher G, Pieters J. (2004) Protein kinase G from pathogenic mycobacteria promotes survival within macrophages. Science. 304(5678):1800-4.

Wang H, Boisvert D, Kim KK, Kim R, Kim SH. (2000) Crystal structure of a fibrillarin homologue from Methanococcus jannaschii, a hyperthermophile, at 1.6 A resolution. EMBO J. 19(3):317-23.

Wang W, Ballatori N. (1998) Endogenous glutathione conjugates: occurrence and biological functions. Pharmacol Rev. 50(3):335-56.

Walker V, Selby G, Wacogne I. (2006) Does neonatal BCG vaccination protect against tuberculous meningitis? Arch Dis Child. 91(9):789-91.

Wayne LG, Hayes LG. (1998) Nitrate reduction as a marker for hypoxic shiftdown of *Mycobacterium tuberculosis*. Tuber Lung Dis. 79(2):127-32.

Wayne LG, Hayes LG. (1996) An in vitro model for sequential study of shiftdown of *Mycobacterium tuberculosis* through two stages of nonreplicating persistence. Infect Immun. 64(6):2062-9.

Wayne LG, Sramek HA. (1994) Metronidazole is bactericidal to dormant cells of *Mycobacterium tuberculosis*. Antimicrob Agents Chemother. 38(9):2054-8.

Wayne LG, Lin KY. (1982) Glyoxylate metabolism and adaptation of *Mycobacterium tuberculosis* to survival under anaerobic conditions. Infect Immun. 37(3):1042-9.

Wayne LG (1976) Dynamics of submerged growth of *Mycobacterium tuberculosis* under aerobic and microaerophilic conditions. Am Rev Respir Dis. 114(4):807-11.

Whisstock JC, Lesk AM. (2003) Prediction of protein function from protein sequence and structure. Q Rev Biophys. 36(3):307-40.

Wu G, Williams HD, Zamanian M, Gibson F, Poole RK. (1992) Isolation and characterization of Escherichia coli mutants affected in aerobic respiration: the cloning and nucleotide sequence of ubiG. Identification of an S-adenosylmethionine-binding motif in protein, RNA, and small-molecule methyltransferases. J Gen Microbiol. 138(10):2101-12.

Wu SL, Amato H, Biringer R, Choudhary G, Shieh P, Hancock WS. (2002) Targeted proteomics of low-level proteins in human plasma by LC/MSn: using human growth hormone as a model system. J Proteome Res. 1(5):459-65.

Yeates T.O. (2002) Structures of SET domain proteins: protein lysine methyltransferases make their mark.Cell. 111(1):5-7.

Zahrt TC, Deretic V. (2002) Reactive nitrogen and oxygen intermediates and bacterial defenses: unusual adaptations in *Mycobacterium tuberculosis*. Antioxid Redox Signal. 4(1):141-59.

Zhang Y, Heym B, Allen B, Young D, Cole S. (1992) The catalase-peroxidase gene and isoniazid resistance of *Mycobacterium tuberculosis*. Nature. 358(6387):591-3

Zimmerman MR. (1979) Pulmonary and osseous tuberculosis in an Egyptian mummy. Bull N Y Acad Med. 55(6):604-8

Internet References:

Fourie B. The burden of tuberculosis in South Africa, MRC National Tuberculosis Research Programme, South Africa, http://www.sahealthinfo.org/tb/tbburden.htm

UNAIDS AIDS epidemic update. December 2005 http://www.unaids.org/ Accessed April 2006

Tuberculosis and AIDS: UNAIDS point of view. October 1997 UNAIDS best practice collection http://www.unaids.org Accessed January 2005

Appendix A: Standard Curves

Part A:
Area vs. Total S-adenosyl-L-methioneine

- Various amounts of [^{3}H]-S-adenosyl-L-methioneine (SAM) were chromatographed on HLPC using the method for separating assay components (Section 3.2.2.) and the radioactivity of the eluent measured using a β-ram flow-thru scintillation counter (Insus Systems Inc.).
- The area of the resultant ^{3}H peak was then related to Total SAM by means of its Specific Activity in the assay and a standard curve constructed.

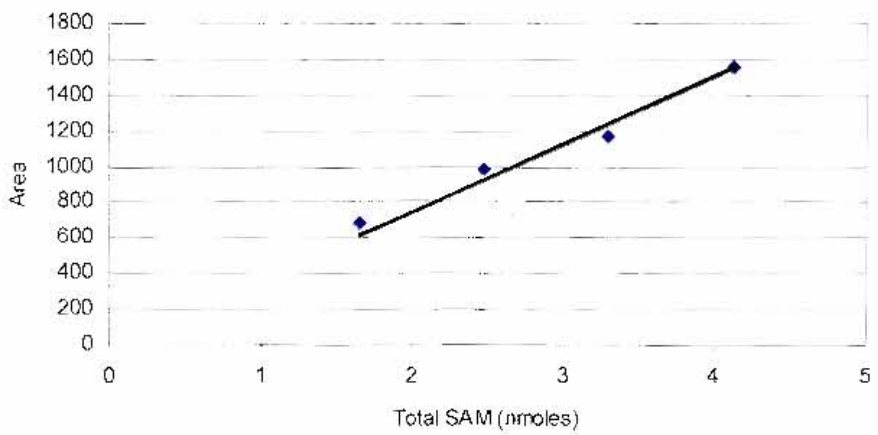

Equation: Area = 375.5 (nmoles of SAM/product)

cpm vs. Total S-adenosyl-L-methioneine

- Various amounts of [^{3}H]-S-adenosyl-L-methioneine were counted using a liquid scintillation counter (Packard) with the counting window set between 0 and 18.6 keV.
- The cpm of each standard was then related to Total SAM by means of its Specific Activity in the assay and a standard curve constructed.

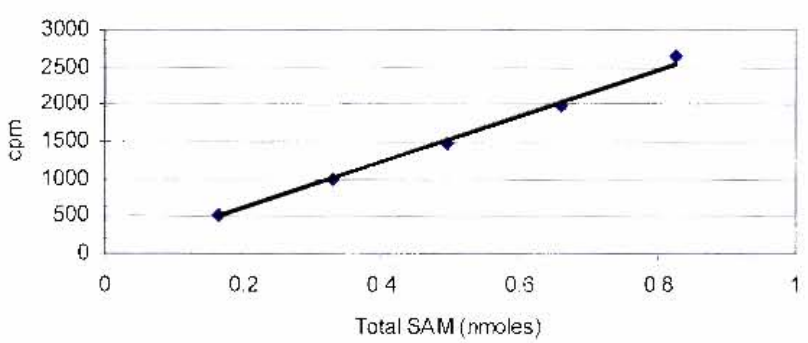

Equation: cpm = 3094.7 (nmoles of SAM/product)

Part B:
Colony Forming Units* vs. Absorbance @ 600nm

- 10-fold dilution was performed for absorbance measurements above 1.
- *M. smegmatis* was cultured on Middlebrooks 7H9 plates containing 5% glycerol, and incubated ay 37^{0}C for 3 days.

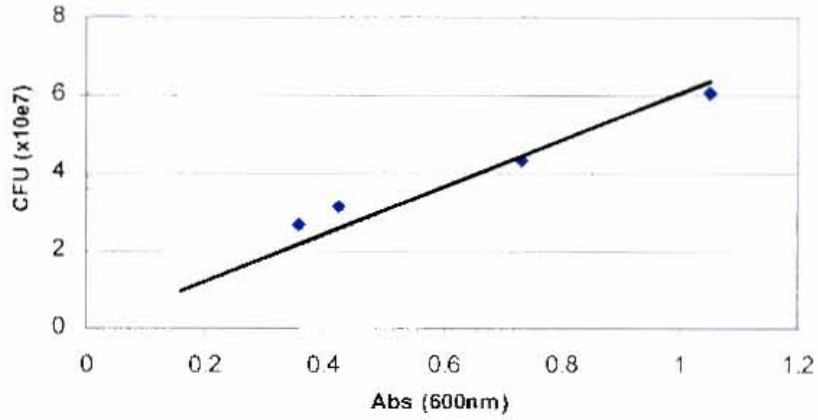

Equation: CFU = (Abs_{600}) x $6.045x10^7$

Peak Area vs. nmoles of ESH-BAN

- Various amounts of ESH-BAN were chromatographed on HPLC using the protocol for the separation thiols in cell extracts (Section 6.8.2.).
- The area of the Absorbance (248nm) peak was determined for each standard using the Delta for Windows 5.0 software.

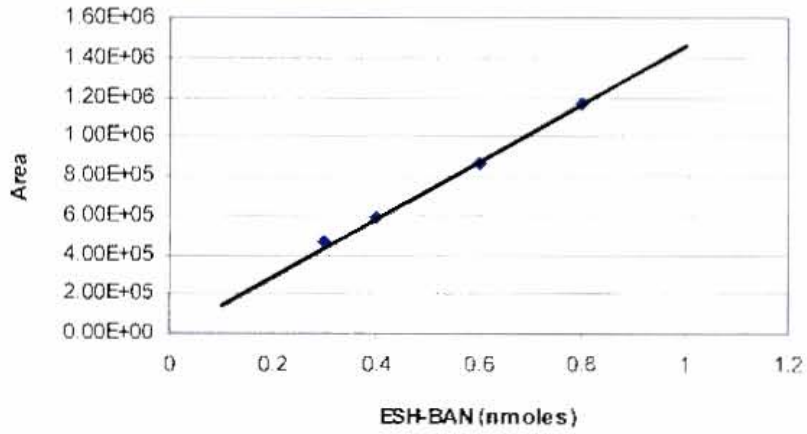

Equation: Area = (nmoles of ESH-BAN) x $1.458x10^6$

Absorbance @ 595nm vs. Amount of Protein (BSA)
Standard curve for BIORAD protein assay

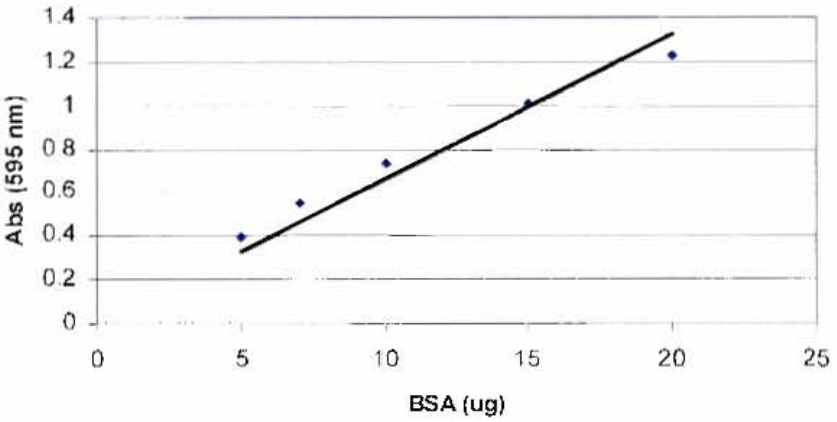

Equation: $Absorbance_{595} = BSA\ (ug) \times 0.0662$

Appendix B:

Complex media for Neurospora agar plates:

Yeast extract	0.5%
Malt Extract	0.5%
Casein hydrolysed	0.5%
Agar	2.0%

Fries Medium:

Per 1L:

Ammonium tartrate	5g
Ammonium nitrate	1g
KH_2PO_4	1g
$MgSO_4.7H_20$	0.5g
$CaCl_2$	0.1g
NaCl	0.1g
Biotin (5% w/v)	0.1ml
Trace element solution	0.1ml
Sucrose	20g

Trace element solution: (mg/L medium) Zn: 2.0, Fe: 0.2, Cu: 0.1, Mn: 0.02, B: 0.01 Mo: 0.02

Clark and Lubs Buffers:

- Prepare 50ml solution containing 0.1 M KCl and 0.1 M H_3BO_3
- Add appropriate volume of 0.1 M NaOH:

pH 8.0	3.9 ml
pH 9.0	20.8 ml
pH 9.5	34.6 ml

- Make up to 100 ml

Protein determination using BIO-RAD protein assay

- Sample diluted appropriately in 800µl of water
- Assay blank was prepared with 800 µl of either water or buffer
- Added 200 µl of Dye Reagent Concentrate to each sample
- Incubation at room temperature for 5min
- Absorbance measured for samples and blank at 595nm
- Protein concentration was determined by the equation: [protein] = Abs_{595} x C
- C is determined experimentally using a Bovine Serum albumin standard curve (Appendix A)

Trichloroacetic acid Precipitation of proteins:

- 10ug of Insulin added as a carrier protein to each sample
- TCA added to a final concentration of 10%
- Incubate on ice for 1hr
- Centrifuge at 16 000g for 4min at 4°C
- Wash pellets with 300 µl of cold acetone (-20°C)
- Air dry pellets
- Re-suspend in 80 µl of Sample Treatment buffer for SDS PAGE

Protein Molecular Weight Markers:

The Electrophoresis Calibration Kit (Pharmacia) used contained the following protein standards:

Phosphorylase b	94 000 Da
Bovine Serum Albumin	67 000
Ovalbumin	43 000
Carbonic Anhydrase	30 000
Soybean Trypsin Inhibitor	20 100
α-Lactalbumin	14 400

The Protein Molecular weight Marker (Fermentas) contains the following protein standards

β-galactosidase	116 000 Da
Bovine Serum Albumin	66 200
Ovalbumin	45 000
Lactate dehydrogenase	35 000
Restriction Endonuclease Bsp981	25 000
β-lactoglobulin	18 400
lysozyme	14 400

Appendix C:

Beckman Coulter Inc.
4300 N. Harbor Boulevard
P.O. Box 3100
Fullerton, CA 92834-3100 USA
www.beckmancoulter.com

BDH Laboratory Suppliers
Poole, Dorset
England BH15 1TD

BioRAD Laboratories
1000 Alfred Nobel Drive
Hercules, CA 94547
www.bio-rad.com

Biospec Products
POB 788
Bartlesville
OK 74005
www.biospec.com

BioTechnology Institute
University of Minnesota
1479 Gortner Avenue
St. Paul, MN55108
http://cbs.umn.edu/bti/

Boehringer Ingelheim
Dept. Fine Chemicals
Binger Straße 173
D-55216 Ingelheim
Germany
www.boehringer-ingelheim.com/finechem

Fermentas International Inc.
830 Harrington Court
Burlington
Ontario L7N 3N4
www.fermantas.com

Grace Vydac
17434 Mojave Street
Hesperia, CA 92345 USA
www.vydac.com

Invitrogen Ltd.
3 Fountain Drive
Inchinnan Business Park
Paisley, UK
PA4 9RF
www.invitrogen.com

KIMIX
P.O. Box 93
7475 Eppindust
South Africa
www.chemicalsupplier.co.za

Merck
Frankfurter StraBe 250
D-6100 Darmstadt 1
www.merck.co.za

Oxoid Limited
Wade Road, Basingstoke
Hampshire RG24 8PW
United Kingdom
www.oxoid.com

Perkin-Elmer
940 Winter Street
Waltham
Massachusetts 02451 USA
www.perkinelmer.com

PhamaTech International
21 Just Rd. Fairfield
New Jersey 07004 USA
www.oriondevel.com/pharmatech/index.aspx

Phenomenex
2320 W. 205th Street
Torrance
California 90501 USA
www.phenomenex.com

Research Organics Inc.
4353 East 49th Street
Cleveland, OH. 44125
http://resorg.com/body.cfm

Roche Ltd.
Group Headquarters
Grenzacherstrasse 124
CH-4070 Basel
Switzerland
www.roche.com

Sigma-Aldrich / Fluka / Riedel-de Haën
Box 14508, St. Louis
Missouri 63178, USA
www.sigma-aldrich.com

The Nest Group Inc.
45 Valley Road
Southborough
MA 01772-1323
www.nestgrp.com

Waters Corporation
34 Maple Street
Milford Massachusetts
01757 USA
www.waters.com

Whatman
info@whatman.com
www.whatman.com